Development and application of needle trap devices (NTD)

by

Saba Asl-Hariri

A thesis
presented to the University of Waterloo
in fulfillment of the
thesis requirement for the degree of
Doctor of Philosophy
in
Chemistry

Waterloo, Ontario, Canada, 2015

AUTHOR'S DECLARATION

This thesis consists of material all of which I authored or co-authored: see Statement of Contributions included in the thesis. This is a true copy of the thesis, including any required final revisions, as accepted by examiners.

I understand that my thesis may be made electronically available to the public.

Statement of Contributions

I hereby declare that I am the sole author of this thesis. Materials in Chapter 2 have been already published. All of the work reported within this chapter has been performed solely by the author. Professor Janusz Pawliszyn as the co-author was supervised the project, and he was an inventor of the needle trap device. German A. Gomez-Rios as the co-author presented a section through the paper, which is not reported in this thesis. Peter Dawes as the co-author introduced the concept of extended tip needle trap and provided some comments on manuscript. Emanuela Gionfriddo contributed in the practical part of work.

Abstract

Recently, there has been increasing interest in environmental analysis among the scientific community. Monitoring of organic and inorganic environmental pollutants and investigations into their potential to adversely affect human health has prompted the development of new methodologies for environmental analysis. Generally, the analytical procedure is comprised of several steps, such as sample collection, sample preparation, analysis, and data processing. Sample preparation is a critical step in the development of new methodologies, and considered the main source of uncertainty in the analysis of environmental samples. In this context, several sample preparation techniques have been recently developed and optimized with aims to miniaturize extraction, automate procedures, and reduce or circumvent solvent consumption. The currently presented research focused on further development and novel applications of two sample preparation methods, solid phase microextraction (SPME) and needle trap devices (NT).

Solid phase microextraction (SPME) combines sampling, sample preparation, and sample introduction in one step. Analytical sampling by SPME has been employed in a variety of environmental applications. To quantify target analyte content, different calibration approaches can be performed based on the application process. This method is an equilibrium-based sample preparation technique that due to its currently presented configuration provides only information related to free molecules in gas phase.

Conversely, the needle trap device, which contains a sorbent packed inside a needle, is an exhaustive, solventless, one-step sample preparation technique that can be easily calibrated. In addition, this approach eliminates errors associated with sample transportation and storage, which can consequently result in more accurate and precise

analytical data. This technique is also useful for a wide variety of applications, including sample preparation of compounds with different chemical and physical properties, as well as varying volatilities. Furthermore, NT is a valuable sample preparation technique that, based on its geometry, allows it to act as a filter for collection of particles. The initial part of this research focused on new developments in the geometry of needle trap devices. Subsequently, particular attention was dedicated to the principles of collection efficiency as well as particle trapping mechanisms for filtration of particulate matter and aerosols by NTs. Finally, this thesis presents a joint application of NT and SPME for determination of target analytes in gaseous and particulate phases.

The first part of this thesis provides a thorough evaluation of new prototypes of the extended tip needle trap device (NT), and a summary of their application towards *in vivo* sampling of biological emissions, as well as active/passive on-site sampling of indoor air. To increase desorption efficiency, the newly proposed NT device was constructed with a side hole above the sorbent and an extended tip that fits inside the restriction of the narrow neck liner. The commercial prototype needles were packed with divinylbenzene particles and evaluated in terms of robustness after multiple uses, as well as extracted amounts of volatile organic compounds (VOCs). Successively, needles were packed in-lab with synthesized highly cross-linked PDMS as a frit to immobilize carboxen (Car) particles. The performance of needles packed with PDMS and Car were then compared in regards to different flow rates. For passive sampling, the needles were packed with Car particles embedded in PDMS in order to simplify calculations in passive mode. Good performance was obtained using the NT devices as spot samplers, as well as passive samplers under controlled conditions in the laboratory. Commercial modified prototypes

of NT were used to study biogenic emissions of pine trees. The new lab-made NT was then applied in the analysis of indoor air in a polymer synthesis laboratory in both active and passive approaches.

Additionally, this thesis presents work conducted on the development and evaluation of an appropriate frit for NT devices. In order to investigate the feasibility of the NT device for analysis of nanometer-sized particles in high efficiency, three different filters, nanofibrous filter, porous membrane, and granular filter, were used to entrap dioctyl phthalate particles of diameters ranging between 10-200 nm. Subsequently, a series of experiments were carried out to estimate and compare the collection efficiency and pressure drop of the above mentioned filters. The effect of face velocity, fiber thickness, and fiber-packing density on filtration efficiency was also evaluated for each filter. The data showed that the efficiency curves for different filters demonstrated a lower efficiency for particle of sizes ranging between 40 to 60 nm, and at a face velocity of 17 cm/s. Calculated theoretical values based on the filtration model showed good agreement with the experimental data. This study demonstrated that use of the nanofibrous filter led to a significant improvement in the filtration efficiency of the NT device. Nevertheless, the proposed porous membrane was chosen as an appropriate filter instead for subsequent studies due to its relative simplicity of packing through the needle trap devices and high reproducibility in regards to packing procedure in comparison to the nanofribrous filter, which has high efficiency and poor reproducibility.

Finally, needle-trap (NT) devices were applied in conjunction with solid phase microextraction (SPME) towards the measurement of free and particle-bound fragrances derived from personal care products. In order to simulate in-use exposure scenarios, the

experiments were conducted in a specially constructed 0.1 m^3 chamber configured to simulate in-use conditions in a bathroom. The perfumed body spray was introduced to the chamber in three second bursts to mimic typical consumer use. The produced aerosol was then continuously monitored using a scanning mobility particle sizer (SMPS) to determine the number and size of particles; characterization of the aerosol size distribution is an important factor when considering risk assessment, as particles <7μm are considered respirable and those of size <20 μm inhalable. Needle trap devices using a range of packing materials were evaluated for measurement of total concentrations of target analytes, while free concentrations of the fragrance present in the aerosol spray were determined concurrently by SPME based on the external calibration method. The results showed similar concentration trends with the same sampling devices over different days.

Acknowledgment

I would like to express my gratitude to my supervisor, Professor Janusz Pawliszyn, for providing me the opportunity to work on his research group. Thanks for his valuable ideas, support and encouragement.

I would like to thank my advisory committee members, Dr. Jean Duhamel, Dr. Kam Tong Leung and Daniel Thomas for their valuable advice during my studies and throughout preparation of my thesis.

I would like to especially thank my external examiner Dr. Jose Almirall, and my internal examiner Dr. Xianshe Feng for their critical evaluation of my thesis and their helpful advice.

I would like to express my thanks to all my collaborators, co-workers and friends for their support and friendship during my work, especially to Mr. Mike Pleasant from Unilever Inc. (London, UK), Dr. Emanuela Gionfriddo, Mr. German A. Gomez-Rios, Mr. Dietmar Hein, Dr. Fatemeh Mirnaghi, and Dr. Fatemeh Mousavi.

I would like to express my appreciation and admiration to my beloved parents Prichehr Geranmayeh and Bozorg Asl Hariri, my sister Mahsa Asl Hariri for their endless support and ongoing love.

Dedication

I dedicated this thesis to my adoring parents and my beloved sister for their unconditional love, understanding and support.

Table of contents

List of Figures

List of tables

List of abbreviations and Symbols

α	Packing density of the sorbent bed
A	Cross-sectional area of needle
BTEX	Benzene, Toluene, Ethyl benzene, Xylene
BTV	Breakthrough volume
BVOCs	Biogenic Volatile Organic Compounds
Car	Carboxen
C_o	Concentration of analyte in the sample
C_s	Concentration of analyte at the surface of the sorbent
D	Diffusion coefficient
d_p	Diameter of the sorbent particle
d_s	Sample particle size
DVB	Divinylbenzene
Σ	Single fibre efficiency
E	Collection efficiency
FID	Flame Ionization Detector
GC	Gas Chromatography
GC/MS	Gas Chromatograph/ Mass Spectrometry
K_{es}	Distribution constant of the analytes between extraction phase and sample matrix
L	Length of the packed sorbent bed
LOD	Limit of Detection
LOQ	Limit of Quantification
NT	Needle Trap
NTD	Needle Trap Device
N_{in}	Number of particles entering the filter
N_{out}	Number of particles leaving the filter
Δp or Δn	Pressure drop
PAHs	Polycyclic aromatic hydrocarbons
PDMS	Polydimethylsiloxane

ppb	Parts per billion
ppt	Parts per trillion
Q	Volumetric flow rate
Re	Reynolds number
SMPS	Scanning Mobility Particle Sizer
SPME	Solid Phase Microextraction
SPE	Solid Phase Extraction
t_R	Retention time
t	Sampling time
TWA	Time Weighted Average
TEX	Toluene, Ethyl benzene, Xylene
u	Face velocity
V_s	Sample volume
V_f	Volume of the extraction phase
VOCs	Volatile Organic Compounds
μ	Viscosity of the fluid

Chapter 1 : Introduction

1.1. Atmospheric analysis

Over the past few decades, atmospheric pollutant levels have increased significantly due to human activities.[1,2] Research indicates that in addition to their impact on human health, pollutants can heavily impact ecological and environmental systems as well.[3,4] Consequently, determination and analysis of pollutants have become an increasingly important area of research within the scientific community, and reliable analytical techniques are needed for assessment studies of risk and toxicological potential.[5] In air analysis of pollutants, typical studies mainly focus on indoor air quality, public and occupational health, photochemical smog, global climate change, and genesis of atmospheric acidity.[6,7,8,9]

Generally, air samples consist of complex matrices with low levels of target analytes and the presence of several interferences.[10] As such, a sample preparation step is usually necessary to extract target analytes from complex matrices. As sample preparation is one of the main sources of uncertainty in air sample analysis,[11] it is important that a given sample preparation procedure can adequately eliminate interfering compounds from the matrix. It should be noted that the common accurate sample preparation methods are time consuming. To this purpose, there is increasing scientific interest in the development of accurate, cost-effective, rapid, and environmentally friendly sample preparation techniques.[12,13] Commercially available procedures, which employ stainless steel containers or nylon bags, have been used for determination of trace gaseous contaminants and aerosols in air.[14] However, these approaches require long sample preparation times,

multiple steps, different adsorbents with high breakthrough volumes, and a large amount of solvents. To address these concerns, sample preparation techniques such as Solid Phase Microextraction (SPME)[15] and Needle Trap Devices (NTDs)[16] have been developed and optimized for analysis of pollutants in air samples in order to provide solventless techniques, to automate systems, for convenient introduction to analytical instruments, and to integrate extraction steps.[17] Combining these sample preparation technologies allows for quantitative analysis of gaseous and particulate-bound compounds in atmospheric samples.[18] Applications of NTD and SPME towards organic volatile compounds (VOCs),[19] breath analysis,[20] and biogenic emissions have been described in the literature.[21]

In this section, the fundamentals, procedures, and applications of two sample preparation methods, solid phase microextraction and needle trap devices, are described. New developments in the geometry of needle trap and its mode of desorption are also discussed. Particular attention is dedicated to the principles of filtration efficiency and particle trapping mechanisms for determination of particulate matter and aerosols by NTs.

1.2. Solid Phase Microextraction (SPME)

SPME was developed in 1989 by Pawliszyn and coworkers to address some of the deficiencies of conventional sampling techniques by providing an efficient method capable of facilitating sampling and sample preparation.[15] SPME is a solvent-free technique that combines sampling, isolation, and concentration. Due to its simplicity of use, short sampling times, elimination of matrix interferences, reusability of fibers, and

availability of a wide variety of commercial fibers,[22] SPME has been widely employed in a variety of applications, such as environmental[23] and food analysis,[24] as well as pharmaceutical applications. [25]

In this technique, a fused-silica fiber coated with a small amount of extraction phase, for example liquid polydimethylsiloxane (PDMS), or solid Carboxene (Car) and divinylbenzene (DVB), is exposed to the sample matrix. Upon exposure, the analytes partition between the extraction phase and matrix to reach equilibrium. Quantification is then accomplished by determining the amount of analyte extracted under equilibrium conditions. At equilibrium conditions, Equation 1.1 describes the amount of analyte extracted by SPME:[15]

$$n = \frac{K_{fs} V_f V_s C_0}{K_{fs} V_f + V_s} \tag{1.1}$$

where n is the number of moles extracted by the sorbent, K_{fs} is the distribution coefficient of the analyte between the fiber coating and the sample matrix, V_f is the volume of the fiber coating, V_s is the sample volume, and C_0 is the initial concentration of target analyte found in the sample.

In comparison with traditional methods such as liquid-liquid extraction (LLE), solid phase extraction (SPE), and Soxhlet extraction, SPME is a non-exhaustive technique, as it only removes a small amount of analyte from the sample matrix. As such, SPME requires appropriate calibration methods for quantitative analysis. Accordingly, SPME calibration methods have been developed based on the mass transfer of analytes in multiphase systems. Several methods, such as diffusion-based calibration, kinetic

calibration, exhaustive extraction, and external calibration, have been described in the literature.[15]

The most commonly applied method, external calibration,[15] can be used when a partitioning equilibrium between the sample matrix and the extraction phase is reached. This method includes preparation of different levels of standards that are used to establish a relationship between instrument response and target standard concentrations. The amount of unknown analyte can then be calculated from an equation obtained from the calibration curve. As well, the same sampling procedure can be applied towards the analytes of interest as used for standard extraction conditions. In such cases, the method does not require that convection or agitation remain constant. However, in cases where extraction times are too long, other calibration methods are recommended.

1.3. Needle Trap Device (NTD)

The use of a syringe needle packed with Tenax was first documented in the 1970s to sample airborne volatile organic compounds (VOCs).[16] In 1996, a similar approach was developed for determination of gaseous trace organic compounds in urban air and industrial atmospheres using needles packed with charcoal and silica gel.[26] However, the proposed design suffered from a major drawback due to the need for a modified inlet system for the GC instrument, which was required due to the large size of the used needles and the need of a dedicated carrier gas purge line.

The first practical and successful application of NT suitable for automation and on-site analysis was introduced by Pawliszyn's research group in 2001.[27] An NT device containing a 23 gauge stainless steel needle measuring 40 mm in length and containing 5

mm of quartz wool packing was used to trap particulate matter. Air samples were then drawn through the NT. Next, the NT was placed directly into the injector of the GC, followed by injection of clean air into the injector, which aided introduction of thermally desorbed analytes to the column. In 2005, Pawliszyn and co-workers proposed two new designs of NT that afford more efficient extraction and a superior packing sorbents[19]. One type of NT called Shinwa, shown in Fig. 1.1**,** was designed with small side hole in its sealed conical tip in which sorbents are filled segmentally from the tip with PDMS, DVB, and Car. Quartz wool is packed between the tip and side hole. Sampling is performed by drawing air through the NT via attachment of a syringe pump or gas-tight syringe. In this configuration, desorption is accomplished by applying inert gas, as thermal expansion can facilitate the desorption process. The second type of NT uses a configuration where the NT is packed with Car near the blunt tip of the NT and with the side hole positioned above the sorbent, as illustrated in Fig. 1.2. In this design**,** desorption is performed by directly injecting the blunt tip of the NT into the GC injector equipped with a narrow neck liner. As can be seen in Fig. 1.3, the restriction of the liner seals the blunt tip NT. Subsequently, the carrier gas enters from the side hole and passes through the sorbent to assist the transfer of analytes into the column. The side hole NT desorption approach has been shown to boast a higher efficiency compared to previous NT designs and desorption methods.[28] Recently, a new prototype of NT with an extended tip (as shown in Fig. 1.4) was introduced by Pawliszyn's research group to improve the desorption efficiency of the blunt-tip NT. In this new prototype, the shape and diameter of the tip was modified to increase the efficiency of the sealing with restriction of the narrow neck liner.[29]

Figure 1.1. Schematic illustration of Shinwa needle trap

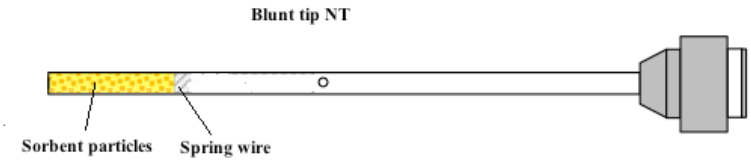

Figure 1.2. Schematic design of blunt tip needle trap with side hole

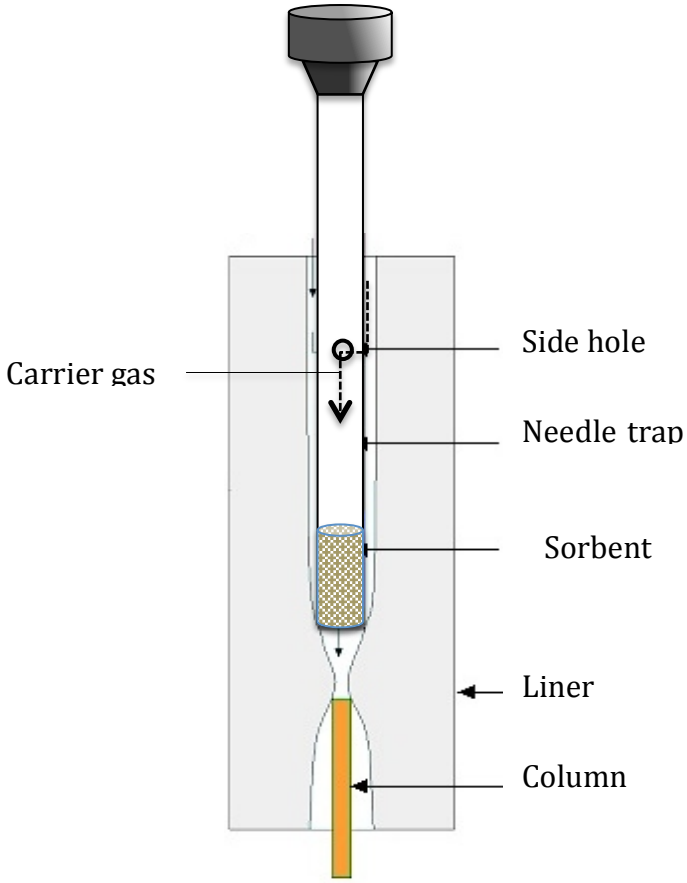

Figure 1.3. Schematic illustration of narrow neck liner design and blunt tip needle trap during desorption process

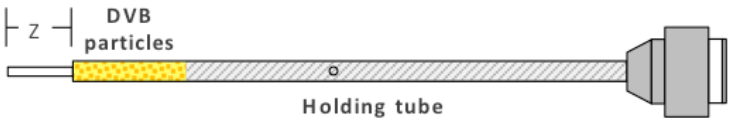

Figure 1.4. Schematic design of extended tip needle trap with side hole and holding tube for immobilization of sorbent particles

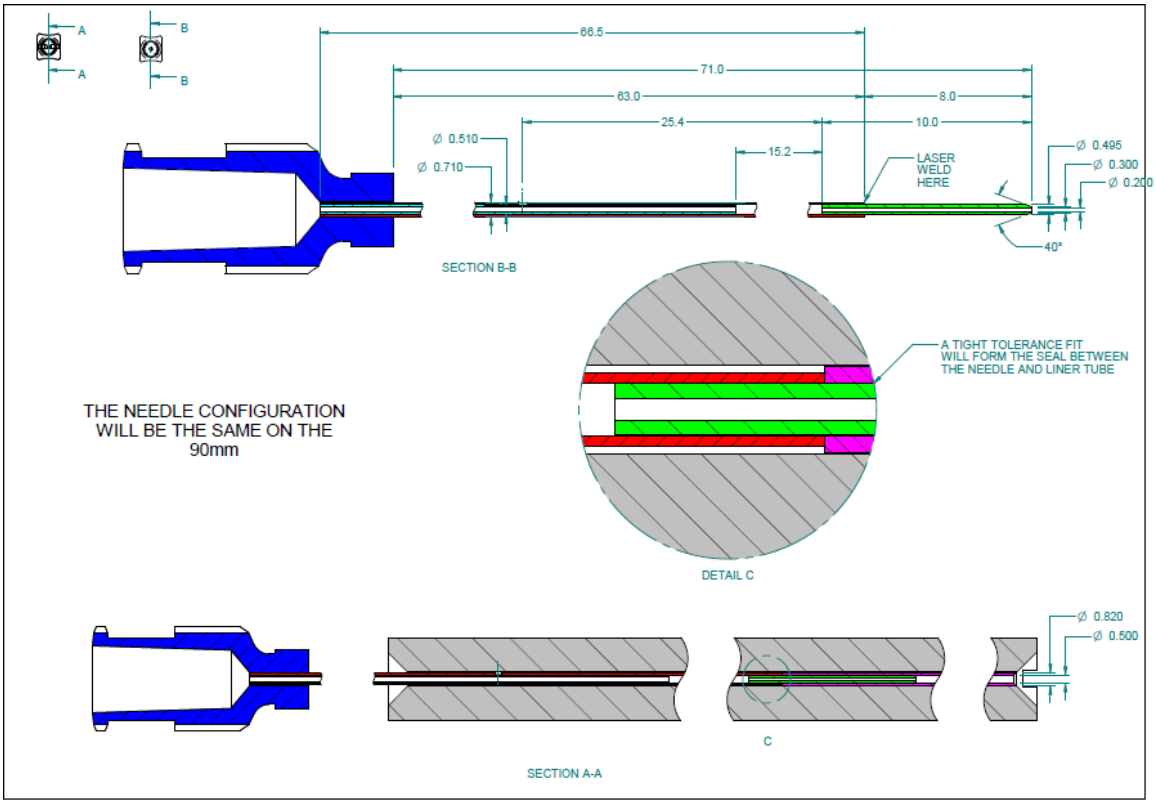

Figure 1.5. Schematic illustration of NT and matching narrow neck liner

Various studies to date have been conducted with aims to increase the desorption efficiency of the NT devices; in these, several desorption methods have been examined, including air-assisted desoption,[27] thermal expansion,[30] inert gas-assisted desorption,[16] water vapour assisted desorption,[31] and diversion of carrier gas flow through[19] the side hole of the NTs. In air-assisted desorption, clean air is drawn through the syringe and expelled when the NT is injected into the GC. Conversely, in the thermal expansion technique, the NT is inserted into the injector, and desorption occurs based on the injector temperature profile. In related work, thermal expansion studies conducted by Wang et al. demonstrated that carry over effects dependent on exposure of the sorbent to the heated zone.[19] Moreover, the design of the injector set-up as well as the geometry of the NT

were concluded to be critical parameters in determining optimal desorption conditions. In work related to inert gas-assisted desorption, several authors have demonstrated that thermal desorption may be successfully obtained with the use of an inert gas injection through the NT device. The limitations of this technique include the introduction of oxygen through the sorbent bed due to penetration of air into the inert gas syringe, and insufficient gas amounts for desorption of analytes. Studies performed by Warren et al. and Zhan et al.[32,29] demonstrated that in order to achieve complete desorption (non-carry over), an aid-gas should be directed through the needle trap packing, either through carrier gas or gas-tight assistance desorption.[32] Thus, if a good seal is created between the outer surface of the needle and the inner surface of the liner, the carrier gas is exclusively driven through the side-hole of the needle, passing through sorbent, then finally migrating alongside the extracted analytes by the needle tip. The sealing system on the first side-hole NTs relied entirely on the tapered shape of the needle's tip. However, inefficient desorption of analytes and carryover issues revealed the weakness of this design.

The efficient needle/liner prototype described a metal/metal seal between the tip of the needle and the bore of the metal liner. In this design, as shown in Fig. 1.5 and Fig. 1.6, the outside diameter of the needle tip (O.D. 0.495 mm) fits precisely on the bottom section of the GC-liner, which has a smaller diameter (I.D. 0.500 mm) than the upper part of the liner. A conical guiding system allows for smooth insertion of the needle tip into the smaller section of the liner.[32,29] Since this design guarantees a better seal with the narrow neck liner, the carrier gas is forced to only pass through the sorbent bed, as seen in Fig. 1.6. In addition, metal liners were proven to be more efficient in transferring heat evenly throughout the full length of the packing.

Figure 1.6. Schematic illustration of extended tip needle trap with designed narrow neck liner

Several groups have worked on the development of sorbent-packed needles or similar devices.[33] Some of the sorbents that have been used for the analysis of volatile organic compounds (VOCs) include carboxen (Car), divinylbenzene (DVB), Porapak Q™ , and Carbopack X.[34,16] Several factors, such as pore size and shape, surface area, and particle size can affect the ability of the analyte to access and interact with the surface of the adsorbent.[35] Moreover, because of the special shape of the needle, sorbents used for NT must have suitable physical characteristics in regards to size, hardness, and shape (spherical), as well as adequate mechanical and thermal stability. Generally, the design of the NT geometry must guarantee several factors: exhaustive extraction (active sampling), negligible breakthrough during sampling, and efficient desorption.[36]

The breakthrough volume of NT, which corresponds to the capacity of NT, is related to the length and density of packing, the concentration of the analyte of interest, and the

affinity of the analyte to the sorbent.[35] In addition, the breakthrough volume is inversely proportional to the sampling rate. However, while the sampling rate and the concentration of target analyte are constant, the breakthrough volume of NT is proportional to the sampling volume. As such, the volume of air that passes through the NT device, namely the sampling volume, should be accurately measured; in other words, it is important to select an appropriate sampling volume and sampling flow rate due to the breakthrough volume. Different types of sorbent and packing lengths have specific breakthrough volumes depending on the properties of the analytes of interest and the surface area of the sorbent particles. Due to the limited surface area, the sorbent can be easily saturated at high concentrations and/or large sample volumes. However, several factors, such its simple operation, rapid analysis, and elimination of dilution or sample preparation steps, in addition to its relative low cost, make the NT method a valuable alternative for environmental sampling.[37] Moreover, the NT can be easily calibrated by controlling the sampled volume (v) and determining the amount extracted (n) in an analytical instrument, as shown in Equation 1.2.

$$n = C_0 V \tag{1.2}$$

Furthermore, NT is able to act as a passive sampler. While active sampling can be performed by drawing air samples through the sorbent bed of NT using a pump or gas-tight syringe, this manual sampling method is not always a reliable method, in particular for higher volumes of sampling. On the other hand, passive sampling can be achieved by diffusion of samples over a period of time of interest.[38] The basic principle of the passive

sampler relies on diffusion to move the analytes from the matrix exposed to the tip of the needle to the extraction phase (Fig. 1.7). During this process, the linear concentration profile exists in a defined distance (Z) between the small opening of the needle, the characterized surface area (A), and the position of the extraction phase. The amount of loaded analyte (n), during the sampling time (t), can be determined by Fick's first law of diffusion:[15]

$$dn = -A\,D\,.\frac{dc}{dx}\,.dt = -A\,D.\frac{\Delta c\,(t)}{Z}\,.dt \qquad (1.3)$$

and D is diffusion coefficient of the gas phase. After integration of Equation (1.3);

$$n = D\,.\frac{A}{Z}\int C(t)dt \qquad (1.4)$$

In passive sampling, the extraction phase should be a zero sink for all target analytes. Moreover, the concentration of samples in the bulk of the matrix and at the face of the opening should be equal, and the amount of analyte collected should be proportional to different concentrations of analytes at the face of the needle.[39] Finally, the Equation (1.4) could be simplified and rewritten

$$C = \frac{n\,Z}{A\,D\,t} \qquad (1.5)$$

- Sampling time (t)
- Distance (Z) diffusion path
- Characterized surface area (A)
- The amount of loaded analyte (n)
- Diffusion coefficient in gas phase (D)

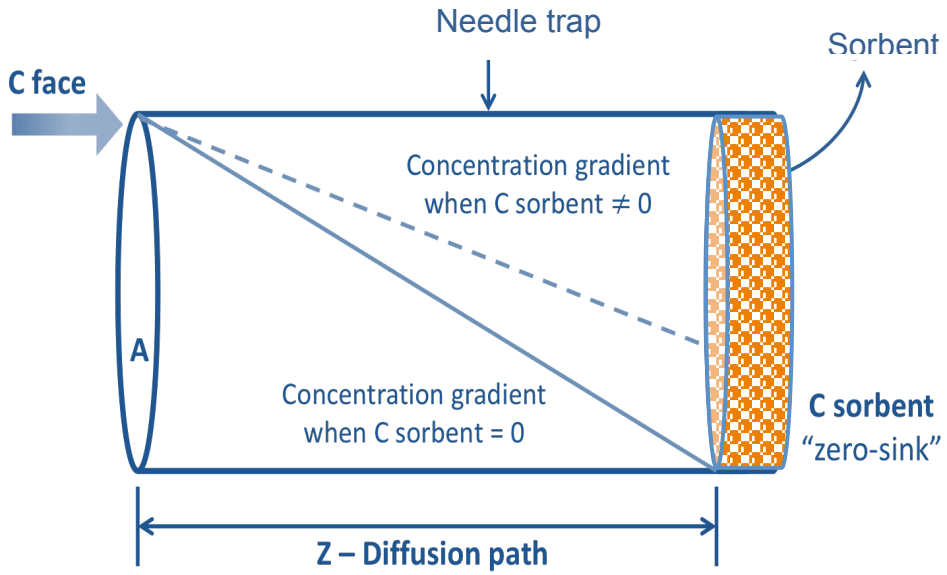

Figure 1.7. Concentration gradient of an analyte produced between the opening of the needle and the position of the sorbent Z. Z: diffusion path; $C_{sorbent}$: concentration near the sorbent interface; C_{face}: time dependent concentration of the analyte at the needle opening; A: area of the cross-section of the diffusion barrier

Numerous applications of NT-based techniques have been reported in the literature. With the development of needle trap theory, several sorbent materials and desorption methods have been proposed to extend the applications of NT. Needle trap techniques have been widely used for the analysis of VOCs,[40] biogenic volatile organic compounds (BVOCs),[17] and breath,[41] as well as for determination of free and total concentrations of target analytes.[42]

Early applications of NTs were focused on extraction of VOCs in air samples. In 2003, Berezkin et al. packed needles with Tenax to analyze benzene and toluene from tobacco smoke.[43] Subsequently, the same research group proved that NT was comparable to SPME in simplicity and flexibility.[44,31] Later, Pawliszyn and co-workers proposed a NT packed with three sorbents, DVB, Car, and PDMS, for extraction of a wide range of volatile compounds.[19] Additional work conducted by Pawliszyn's research group showed that the detection limit for extraction of BTEX with multi-bed NT was below 0.1 ng/mL.[35] In addition, experimental results proved that the detection limit of NT was comparable to techniques such as purge and trap. Concurrently, Jinno's group packed NT devices with co-polymer particles to determine specific organic compounds in gas phase.[45] Moreover, several applications have been introduced for NT, such as analysis of formic and acetic acid,[46] determination of poly-aromatic hydrocarbons (PAHs),[47] and analysis of emitted biogenic compounds from trees.[21]

In addition to the above mentioned applications, the use of NT for trace gas analysis in breath has been widely documented in the literature. In 2005, Jinno and co-workers investigated acetone in breath.[48] Successively, an alveolar sampling method using NT was developed by Miekisch and co-workers.[49] The same group introduced the application of NT in GC × GC characterization of breath samples. Currently, different research groups have reported the use of NT technology towards the determination of various compounds in breath, such as acetone, isoprene, and cancer biomarkers.[20,50–52]

One of the most interesting applications of the NT method is its combination with SPME to determine free and particulate-bound analyte concentrations. Koziel[27] et al. and Niri[18] et al. have demonstrated that NT can act both as a filter and as an extraction phase.

Therefore, it is possible for NT to extract free molecules and particulate-bound analytes simultaneously.

Koziel et al. packed NT with 5 mm quartz wool to investigate the amounts of triamcinolone acetonide in breath samples, as well as quantities of polycyclic aromatic hydrocarbons (PAHs) in diesel exhaust.[27] Niri et al. reported successful qualitative analysis of free and total concentrations of allethrin in mosquito coil smoke.[18] Both groups reported high extraction efficiencies for NT for semi-volatile compounds. This can be related to the higher distribution coefficient of semi-volatile compounds between gaseous and particulate phases compared with the low distribution coefficient of volatile compounds. While volatile compounds tend to release as gaseous compounds, which can then easily diffuse to the boundary layer of the SPME fiber, the diffusion of particles through the boundary layer is much lower. A comprehensive study was performed by Li et al. on the validation of NT and SPME devices for sampling aerosols: using theoretical calculations and experimental data, the authors demonstrated that NT is capable of extracting both gaseous and particulate analytes, while SPME can only extract the gaseous molecules. Theoretical calculations were validated experimentally through determination of PAHs found in smoke emitted from barbecues and cigarettes.[42]

1.4. Basic principles of filtration

Particles smaller than 100 nm in size are classified either as nanoparticles or ultrafine particles. Traditionally, ultrafine particles are particulate matter of nanoscale size that are formed due to chemical reactions and released into the atmosphere, such as diesel exhaust, industrial fumes, and photochemical smog, while nanoparticles have been defined as nanometer-sized particles that are commercially produced for industrial and

medical applications. Although the electrical, optical, and chemical properties of nanoparticles can provide a wide range of useful applications, these particles have been formed to potentially increase risks to human health and the environment.[53]

Inhalation exposure to nanoparticles, which can take place at home, the workplace, and ambient air, can potentially increase health concerns; the deposition of nanoparticles in the respiratory system has been shown to contribute to a higher incidence of asthma, infection, chronic obstructive pulmonary disease, and lung cancer.[54,55,56]

In determination of nanoparticles, filtration is the most commonly used method of aerosol collection. The two major types of filters employed in aerosol sampling are fibrous and membrane filters. Fibrous filters are comprised of a mat of fine fibers organized in such a way that most are perpendicular to the aerosol flow.[57] In comparison, membrane filters consist of high solid fractions and a complex pore structure, leading to high efficiency and a greater resistance to flow.[58,59,60]

Factors such as such filter structure, particle properties, and operational parameters can affect the filtration process. Research into the relationships between efficiency and particle size and between face velocity and efficiency can help to find the optimized condition for the highest aerosol filtration.[61,62]

1.4.1. Evaluation performance of a filter

In order to compare and contrast the performance of different filters, a parameter which defines filtration performance is first required. Quality factor (Q_f) a parameter for assessment of filter performance,[57] can be defined as:

$$Q_f = \frac{-\ln p}{\Delta n} \tag{1.6}$$

where Δn is the pressure drop and p is the penetration.

The resistance airflow across a filter is called a pressure drop. In 1973, Davies defined pressure drop as: [63]

$$\Delta p = \frac{\eta\ t\ U_0 f(\alpha)}{d_f^2} \tag{1.7}$$

where η is the viscosity of air, t is the thickness of the filter, U_0 is the face velocity ($U_0 = \frac{Q}{A}$), Q is volumetric flow, A is the surface area of filter, α is the solidity or packing density of filter, and d_f^2 is the diameter of the filter.

Penetration refers to the fraction of particles that exit the filter or penetrate the filter. [57]

$$P = \frac{N}{N_0} = 1 - E \tag{1.8}$$

E refers to the collection efficiency, which is described as the fraction of entering particles retained by the filter. Equation 1.7 shows the macroscopic properties of filter efficiency:[57]

$$E = \frac{N_0 - N}{N_0} \tag{1.9}$$

where N_0 and N are the particle concentrations at the inlet and outlet of the filter, respectively. Collection efficiency can be also defined in terms of particle mass concentrations. For high efficiencies, the penetration is a clearer indicator of efficiency as

small changes in collection efficiency are associated with large changes in penetration. For example, when *E* increases from 90 to 99%, *P* drops from 1 to 10 %.

In summary, filtration performance can be assessed by collection efficiency and pressure drop. A good filter is expected to show high collection efficiency and low pressure drop.

1.4.2. Single fiber efficiency

In comprehensive investigations into the microscopic properties of filters, the theory of single fiber efficiency for analysis of the fibrous filtration process has been developed and documented by Brown,[64] Hinds,[57] and Lee and co-workers.[65] To the best of this author's knowledge, significantly fewer studies on membrane filters have been published in comparison to fibrous filters. While a few number of authors have recommended the capillary[61] tube model to predict the particle collection properties of the Nulecpore membrane filter,[66] the fibrous filter has been shown to yield a more accurate prediction for solvent-cast membranes. In addition, the results from the proposed model presented a good agreement between the effective fiber diameter in the model and the diameter of fiber-like structures in the membrane.[67]

In theory, NT is able to act as a filter to trap particles. The ability of NT to collect the particles can be explained by filtration theory, which is based on the concept of single fiber efficiency. Therefore, the efficiency of an NT device can be estimated by integration of single fiber efficiency of whole sorbent length *L*; a simplified equation is expressed below. The equation relates the macroscopic properties of filter efficiency to the microscopic properties of single-fiber efficiency.[57]

$$E = 1 - \left(\frac{4\,\alpha\,E_{\Sigma}L}{\pi\,d_f}\right) \tag{1.10}$$

where α refers to the solidity or packing density of the sorbent bed, d_f is the fiber diameter or sorbent particle diameter, and E_Σ is the collection efficiency of the single sorbent, which is determined by deposition mechanisms.

The particles may be deposited on the fiber by simultaneous actions of several mechanisms, including interception, diffusion (Brownian motion), inertial impaction, and gravitational settling.[57] These mechanisms, illustrated in Fig. 1.8, are known as mechanical capture mechanisms. Inertial impaction occurs when a given particle, by its inertia, is unable to adjust its direction and deviate from the original gas streamline. Capture by interception occurs when a particle that follows the gas stream has insufficient inertia to depart from the original gas stream. Such particles will deposit as they come within a one-particle radius of the fiber surface. Collection of particles by interception is related to the ratio of the particle diameter to the sorbent diameter as well as the packing density. Diffusion is caused by a Brownian motion that is sufficiently strong to move the particles from the gas stream to the fiber. Typically, this mechanism is only significant for particles smaller than a few tenths of a micrometer. Contribution of gravitational settling is negligible compared to these three mechanisms, only for nanoparticles.

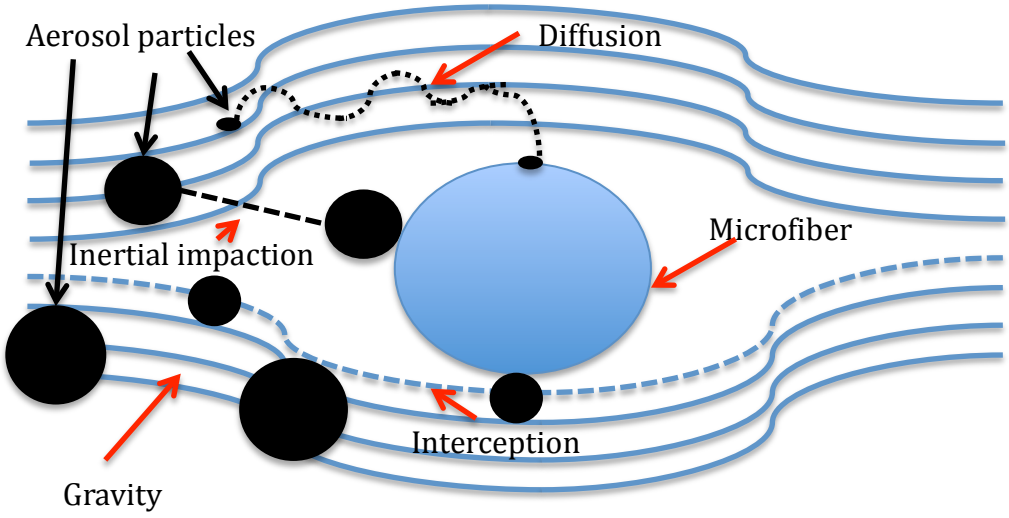

Figure 1.8. Mechanical particle collection mechanisms

Total filtration efficiency can then be understood to be the sum of efficiencies by individual filtration mechanisms. Consequently, the overall single fiber efficiency can be written as:

$$E_{\Sigma} = E_{Int} + E_{Diff} + E_{Imp} + E_{Grv} + E_{Diff+Int} \tag{1.11}$$

Here, the single fiber efficiency that occurs due to interception, as determined by Wang et al. is expressed as:[68]

$$E_{Int} = \frac{(1-\alpha)R^2}{Ku(1+R)} \tag{1.12}$$

Likewise, single fiber efficiency due to impaction is determined from the following equation:[68]

$$E_{Imp} = \frac{1}{(2\,Ku)^2}[(29.6 - 28\alpha^{0.62})R^2 - 27.5R^{2.8}]Stk \tag{1.13}$$

Single fiber efficiency of diffusion is expressed as: [68]

$$E_{Diff} = 2\,Pe^{-(2/3)} \tag{1.14}$$

To estimate the overall single-sorbent collection efficiency, specifically for smaller size particles, it is essential that the interception of diffusing particles is accounted for, which can be written as:[68]

$$E_{Diff+Int} = \frac{1.24\,(R)^{2/3}}{(Ku\,Pe)^{1/2}} \tag{1.15}$$

Gravitational settling is described by the dimensionless term G_{Grv}:[57]

$$E_{Grv} = \frac{V_g/U}{1+V_g/U} \tag{1.16}$$

Where U is the face velocity; Ku is a hydrodynamics factor,

$Ku = -0.5\ln\alpha - 0.75 - 0.25\alpha^2 + \alpha$; Pe is the Peclet number, $Pe = \frac{Ud_f}{D}$, where D is a particle diffusion coefficient; R is the ratio of particle diameter to fiber diameter $R=d_f/d_p$; Stk is the Stokes number; and V_g is the settling velocity.

1.5. Thesis objectives

The research objectives of this thesis included (i) performance evaluation of a new prototype of needle traps; (ii) improvement of the NT packing procedure for active and passive sampling mode; (iii) development and optimization of a frit for NT to enhance the filtration efficiency of the device towards determinations of nanometer-sized

particles; and (iv) development of a sampling method for quantitative analysis of free and particulate-bound analytes in gas and particle phases.

To address the limitations of previous designs of NT in terms of desorption and sampling, the main focus of second chapter centered in the evaluation of a new extended tip NT packed with DVB particles, a new prototype that includes modifications that allow for the use of Car particles as sorbent as well as the use of the NT device for passive sampling. In addition, this thesis also contains a reassessment of the extended tip designs as well as their application to on-site analysis in active and passive sampling modes.

Moreover, while NT has already been previously shown to be able to act as a particle collecting filter, its collection efficiency towards particles in the nanometer range had not to date been studied. Consequently, the aim of third chapter also involved the development and comparison of various frits for NT devices that were applied in an investigation of the feasibility of the NT device in the capture of particles smaller than 200 nm size in high efficiency, as well as an optimization of the parameters under which such determinations can be accomplished.

Chapter four of the thesis was to accomplish simultaneous analysis of free and particulate-bound target analytes in breathing zones. For this purpose, SPME and NT were both applied towards the determination of free and total released fragrances from body sprays in breathing zones. The performance of SPME and NT were also evaluated in terms of extraction efficiency and reproducibility.

Chapter 2 : Evaluation, development and application of extended tip NT

Preamble

This chapter has been published as a paper: Saba Asl-Hariri, German A. Gomez-Rios, Emanuela Gionfriddo, Peter Dawes, Janusz Pawliszyn, Development of Needle Trap Technology for On-Site Determinations: Active and Passive Sampling, *J. Anal. Chem,* 2014, 86 (12), pp 5889-5897. The materials of the current chapter are reprinted from this publication with the permission of American chemical society (Copyright ACS publication 2014).

2.1. Introduction

Recently, there has been increasing interest in air analysis among environmental scientists. Ideally, air samples should be analyzed on-site to avoid losing sample integrity[15]. In cases where on-site analysis is not possible, simple sampling/sample preparation techniques for field applications are required.[69,70] Sampler devices for field sampling should be simple and reliable, since sampling sites are generally located far from the laboratory. Consequently, the device should also comprise easy method deployment, one which allows operators with limited knowledge of the extraction mechanisms to easily operate the sampler. Moreover, the production of the device should be uncomplicated and inexpensive.[71,72] Additionally, during sample transportation and storage, any contamination, decomposition, and/or loss of the analytes should be negligible.[72,73] Finally, the device should be sensitive to the substances under study, unaffected by interfering matrix components, and not require in-laboratory sample pre-

treatment[71,73]. Solid phase microextraction (SPME) and needle trap (NT) devices have been shown to be suitable techniques to address these concerns[20,33,74].

A NT is an extraction device that contains a sorbent packed inside of a needle, as shown in Fig.2.1. The NT method combines sampling, sample preparation, and sample introduction as SPME does. However, NT, as an active sampler, is an exhaustive technique that allows particle trapping.

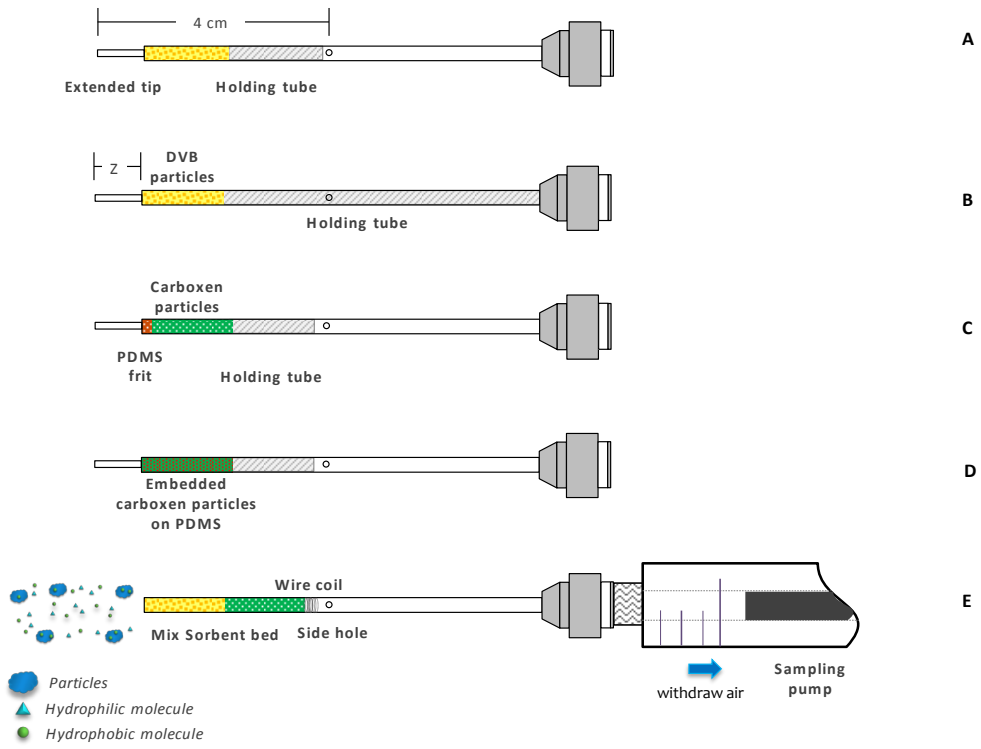

Figure 2.1. Schematic of the modified needle traps. A. Initial prototype packed with DVB particles; B. Modified prototype packed with DVB particles; C. New extended tip needle trap packed with PDMS frit and Car particles for active sampling; D. New extended tip needle trap packed with Car particles embedded on PDMS for passive sampling and E. Sampling with conventional blunt tip NT

Several factors, such as pore size and shape, surface area, and particle size can affect the ability of the analyte to access and interact with the surface of the adsorbent. Therefore,

these parameters must be assessed and controlled when designing new needle trap devices [32,75]. Moreover, because of the special shape of the needle, sorbents used for NT must have the appropriate physical characteristics in size, hardness, and shape (spherical), as well as adequate mechanical and thermal stability[32,33].

This chapter presents an evaluation of new prototypes of extended tip needle trap devices (NT) packed with DVB particles, including modifications to allow the use of Car particles, a reassessment of the new designs, and their application to *in vivo* sampling of biological emissions, and active/passive on-site sampling of indoor air.

2.2. Experimental section

2.2.1. Materials and reagents

HPLC grade methanol was obtained from Caledon laboratories LTD (Georgetown, ON, Canada). Benzene, toluene, xylene, limonene, α-pinene, β-pinene, and decane were purchased from Sigma-Aldrich (Mississauga, ON, Canada). Helium of ultra-high purity was supplied by Praxair (Kitchener, ON, Canada). Gas tight syringes (1 and 5 mL) were purchased from Hamilton Company (Reno, NE, USA). All the preparations were carried out in a ventilated fume hood. Car particles (surface area: 1200 m^2/g) of 60/80 mesh were purchased from Sigma-Aldrich (Bellefonte, PA, USA). DVB particles (surface area: 582 m^2/g) of 60/80 mesh were purchased from Ohio Valley (Marietta, OH, USA). The 3.5 inch long 22-gauge blunt needles (I.D. 0.41 mm, O.D. 0.71 mm) were purchased from Dynamedical Corporation (London, ON, Canada). Stainless steel wires (O.D. 100 μm) were purchased from Small Parts (Lexington, KY, US). Extended tip needle traps were provided by SGE Analytical Science (Victoria, Australia). The 5 min epoxy glue was

purchased from Henkel Canada (Mississauga, Ontario, Canada). The ADM 1000 flow-meter was purchased from Agilent Technologies (Mississauga, ON, Canada)

2.2.2. Instrumentation

An Agilent 6890 gas chromatograph coupled to a 5973 MSD quadrupole mass spectrometer (Agilent Technologies, Mississauga, ON, Canada) was used in this study. For the analysis of biogenic emissions, the chromatographic separations were performed using a SLBTM-5MB (30 m x 0.25 mm x 0.25 μm) fused silica column from Sigma–Aldrich, with helium as the carrier gas at a flow rate of 1.5 mL min^{-1}. The oven temperature was initially held at 50 ºC, gradually increased to 60 ºC at a rate of 1 ºC min^{-1}, then increased to 280 ºC at a rate of 30 ºC min^{-1}, finally held for 0.67 min. The chromatographic separations for indoor air analysis were performed using aRxi®-624Sil MS (30 m x 0.32 mm x 1.80 μm) column from Restek with helium as the carrier gas at a flow rate of 1.5 mL min^{-1}. The oven temperature was initially held at 40 ºC for 2 min, gradually increased to 55 ºC at a rate of 3 ºC min^{-1}, then increased to 250 ºC at a rate of 20 ºC min^{-1}, and finally held for 3.25 min. During the analysis, the transfer line, MS Quad and MS source were set at 280 ºC, 150 ºC and 230 ºC, respectively, with the MS operated in electron ionization mode. Full scan mode (40–250 m/z) was used for all compounds, and quantitation was done using extracted ion chromatograms. The ion m/z 93 was used for quantitative analysis of α-pinene, β-pinene and limonene, while the ion m/z 91 was used for quantitative analysis of toluene. Chromatographic peak identification was made by library matching using the 2002 NIST MS Library (V.2.0 NIST MS Search software) at a flow rate of 1.5 mL min^{-1}. The oven temperature was initially held at 50

ºC, gradually increased to 60 ºC at a rate of 1 ºC min^{-1}, then increased to 280 ºC at a rate of 30 ºC min^{-1}, finally held for 0.67 min. The chromatographic separations for indoor air analysis were performed using aRxi®-624Sil MS (30 m x 0.32 mm x 1.80 μm) column from Restek with helium as the carrier gas at a flow rate of 1.5 mL min^{-1}. The oven temperature was initially held at 40 ºC for 2 min, gradually increased to 55 ºC at a rate of 3 ºC min^{-1}, then increased to 250 ºC at a rate of 20 ºC min^{-1}, and finally held for 3.25 min. During the analysis, the transfer line, MS Quad and MS source were set at 280 ºC, 150 ºC and 230 ºC, respectively, with the MS operated in electron ionization mode. Full scan mode (40–250 m/z) was used for all compounds, and quantification was done using extracted ion chromatograms. The ion m/z 93 was used for quantitative analysis of α-pinene, β-pinene and limonene, while the ion m/z 91 was used for quantitative analysis of toluene. Chromatographic peak identification was made by library matching using the 2002 NIST MS Library (V.2.0 NIST MS Search software). in electron ionization mode. Full scan mode (40–250 m/z) was used for all compounds, and quantification was done using extracted ion chromatograms. The ion m/z 93 was used for quantitative analysis of α-pinene, β-pinene and limonene, while the ion m/z 91 was used for quantitative analysis of toluene. Chromatographic peak identification was made by library matching using the 2002 NIST MS Library (V.2.0 NIST MS Search software).

2.2.3. Preparation of the custom made needle traps at UW

A PDMS pre-polymer was added to the curing agent using a ratio of (10:1). The prepared 1% SDS solution was added to a mixture of PDMS and curing agent (with a ratio of 1:2) and stirred for 15 min to make a homogenized mixture. Glass capillaries with the same inner diameter as NTs were tilled with a homogenized prepared mixture. The

polymerization was allowed to proceed at 80 ºC for 1 hour [76]. After the PDMS mixture was cured, the polymerized PDMS was heated at 120 ºC for 3 hours in order to evaporate water and remove impurities. Both the amount of water added to the mixture and the temperature of polymerization have an effect on the porosity of synthesized PDMS; since temperature is the most effective parameter in obtaining open pores. The temperature was increased to 20 ºC higher than the boiling point of water in order to obtain maximum porosity. To prepare the NT with Car embedded in PDMS, 5 μm Car particles were added to a mixture consisting of the previously described ratios of PDMS pre-polymer, curing agent, and 1% SDS solution, and stirred for 10 min. Next, glass capillaries were tilled with the mixture and heated at 80 ^{0}C for 1 hour. After curing, the oven temperature was increased to 120 ºC, and the mixture containing polymerized Car embedded in PDMS was heated for 3 hours to remove the impurities.

2.2.4. Standard Gas Mixture and permeation tubes

Permeation tubes for the analytes under study were made by encapsulating pure analyte inside a 100 mm long (1/4 in.) Teflon™ tubing capped with 20 mm long solid Teflon™ plugs and (1/4) in Swagelok caps. Emission rates for each permeation tube were verified by periodic monitoring of weight loss of individual analyte tubes. A standard gas generator (model 491 MB, Kin-Tech Laboratories, La Marque, TX, USA) was used to generate standard gases with desired concentrations. The permeation tubes made in our laboratory were placed inside a glass chamber, held in a temperature-controlled oven and swept with a controllable constant flow of compressed air. Different concentrations of the analytes were obtained by adjusting both the permeation chamber temperature and the airflow rate.

2.2.5. Sampling chamber

For the analysis of VOCs and semi-VOCs, a sampling chamber, designed by Koziel et al. [77], was installed downstream from the standard gas generators. This sampling chamber facilitated a steady-state mass flow of all the standards. The sampling chamber consisted of a custom made 1.5 L glass bulb with several sampling ports that were plugged with Thermogreen LB-2 predrilled septa. Omega 120 W heating tape was wrapped around the glass bulb to control the temperature inside the bulb. An Omega K-type thermocouple was attached to the outside surface of the glass bulb in order to control its internal temperature. Both heating tape and thermocouple were connected to an electronic heat control device constructed by the Electronic Science Shop at the University of Waterloo (UW). Air temperatures in the vicinity of the SPME fibers were maintained within ±1.2% of the adjusted temperature. Standard gas flow rates ranged from 50 to 3000 mL/min, resulting in mean air velocities similar to those encountered in indoor air environments. Standard gas generators and sampling chambers were validated using a multi-bed needle trap.

For the extraction of BVOCs emitted by live pine trees, a glass chamber designed by Zini et al. was used [78]. It consisted of a Pyrex glass cylinder (120 mm wide, Ø = 60 mm), where pine needles from a pine tree could be inserted through a hole in one of its ends. After the introduction of the small branch, this hole could be sealed using Teflon tape. A round glass lid secured by clamps closed the other end of the chamber. This lid had several 5-mm holes sealed by Thermogreen LB-2 predrilled septa (Supelco), into which a NT could be introduced to sample the air inside. All glass parts of the container were silanized prior to their use. In order to prevent the presence of artifacts and contamination

from previous analyses, the container was cleaned with methanol and dried with a constant nitrogen flow in a fume hood between samplings.

2.2.6. Sampling procedures

For indoor air sampling and verification of concentrations in the exposure chamber, the NTD was connected to the sampling pump while a volume of the gaseous sample was pumped from the gas standard generator through the needle, at a flow rate of 5 mL/min. After sampling, the NTD was wrapped with aluminum foil and stored in a plastic bag on dry ice. Before injection, the NTD was removed from dry ice and left to reach room temperature. Next, the cap of the tip was removed and then introduced into a GC injector for desorption. Sampling with the NTDs was conducted using a bi-directional syringe pump purchased from Kloehn (Las Vegas, NE, USA).

2.2.7. On-site and in situ sampling of pine trees

A pine tree branch was sealed in the glass sampling chamber and air inside the chamber was extracted for 1 min using a NT packed with DVB. This procedure was performed every 3 hours between 8 am and 8 pm. Blank analyses of the NTs and glass chamber were run before the start of each sampling. After sampling, NTs were sealed with Teflon caps and kept under dry ice while transported to the laboratory[70]. Time elapsed between sampling and analysis never exceeded two hours; under these conditions the loss of extracted analytes is expected to be insignificant, as proven by Chen *et al* [70].

2.3. Results and discussions

2.3.1. Evaluation and application of a new extended tip NT packed with DVB particles

2.3.1.1. Initial assessment of the extended tip NTs

Based on previous findings reported by Warren *et al*. and Zhan *et al*.[29,32], SGE manufactured a NT prototype to be evaluated by our group. This new NT consists of a 22 gauge stainless steel needle with a side-hole 4 cm from the tip, and a sliding-fit tip inserted into the tip of the needle. As previously described [29,32], the outer diameter of the tube is approximately 500 μm, and it fits tightly inside the restriction of the narrow neck liner (section 1.3) providing a dual seal system [29,34]. The inner diameter of the tube is 200 μm, enough to retain sorbent particles, and 1 cm in length. The first prototype evaluated (5 NTs in total) was packed with 2 cm of DVB particles (60/80 mesh) and a small tubing (480 μm) of lesser inner diameter inserted at the back of the packing to hold the particles in place. Numerous parameters were considered in order to have a comprehensive assessment in our study, including a) physical inspection of the NTs before and after usage; b) reproducibility of intra- and inter-NT flow rates reproducibility; c) determination of residual manufacturing of contaminants or sorbent deterioration after multiple uses (chromatographic blank of the NTs), and d) comparison of the amount of analyte collected when performing extractions at different flow rates.

One of the main drawbacks of the initial prototype was the easiness of blocking during sampling and desorption, which was perceived as a diminishing or complete depletion of instrumental signal corresponding to a known concentration. This observation was verified by measuring the NT flow resistance before and after injection. A careful

inspection under the microscope, as seen in Fig. 2.2**,** revealed key aspects of blocking: septum pieces from the GC injector or sampling chamber accumulated in the extended tip, as well as small Teflon fragments, coming from the slider, agglomerated at the side hole. In order to verify the cause of NT blocking, a side-hole of the same size was made on a commercial needle, and the surface surrounding the NT side-hole was not smoothed with sand paper. Hereafter, a Teflon slider was passed several times over the side-hole, simulating the sealing process, and a significant accumulation of Teflon was observed in Fig. 2.3. Therefore, smoothing and blunting of the side-hole and extended tip, respectively, were suggested to the manufacturer in order to improve the reusability of the NTs. In addition to blocking issues, the needle body showed poor robustness to mechanical stress during the injection step. Thus, some of the needles may bend/break during the desorption step, a critical issue if autosamplers are to be used to increase the throughput of the analysis. To overcome this issue, improvements on the welding of the tube to the needle hub, as well as the insertion of a particle holding tube of a smaller diameter inside the NTs, were also recommended to the manufacturer.

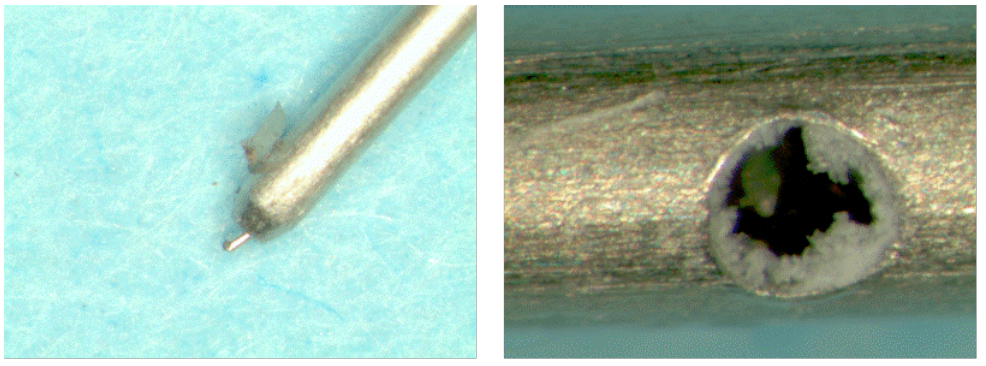

Figure 2.2. Septum and Teflon accumulation after multiple injections

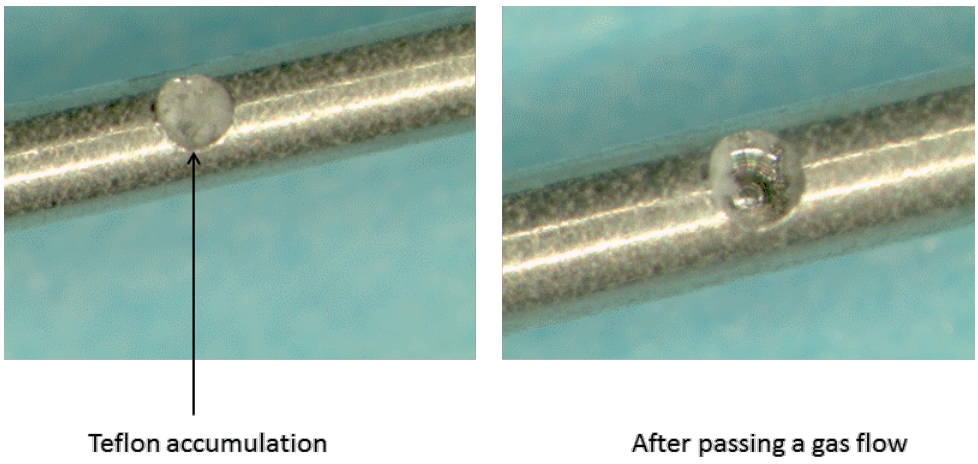

Figure 2.3. Teflon accumulation in a no-polish in-house drilled NT.

2.3.1.2. Evaluation of modified extended tip NTs

In order to evaluate potential differences in the collection capability of the improved prototype at different sampling rates of the improved prototype, extraction of a fixed concentration from the gas generator-sampling chamber was carried out at 5 and 10 mL/min. In order to reduce the contaminating effect of nuisance variables, and statistically evaluate the results obtained only according to the factor of interest, namely the response in terms of mass extracted of the different NTs, extractions were performed using a randomized block design. As can be seen in Table 2.1 and Fig. 2.4, no statistical differences in the amount extracted for the probe analytes was found at a 95% level of confidence when sampling at rates up to 5mL/min. Conversely, sampling at higher flow rates such as 10 mL/min, found in Table 2.2 and Fig. 2.5, provided statistical differences in the amount of probes extracted among the different NTs tested, and lower amounts of analyte extracted per each needle trap. This can be explained by differences on the

packing characteristics of each NT. For example, NTs that provide reproducible adsorption capacity at different flow rates have packing, which is compact enough to evade channeling phenomena. In contrast, for NTs that show a significant reduction in the amount of probes collected at higher flow rates, the packing of the particles is not compacted enough, implying that an increase of the sampling flow rate promotes channeling effects, consequently reducing the amount of probes adsorbed.

Table 2.1. Statistical comparison of 9 commercial needle traps packed with 2 cm of DVB particles. F_{NT} is the F-ratio for the different treatments evaluated (different needle traps) and F_{crit} is the critical value of F for 27 experiments at a 95% level of confidence. RSD is the relative standard deviation for the inter-needle trap repeatability of 9 NTs (n=3) at 5 mL/min.

Compounds	F_{NT}	F_{crit}	RSD
Xylene	1.4		6.0
Decane	0.7	2.5	4.9
Limonene	1.0		6.3

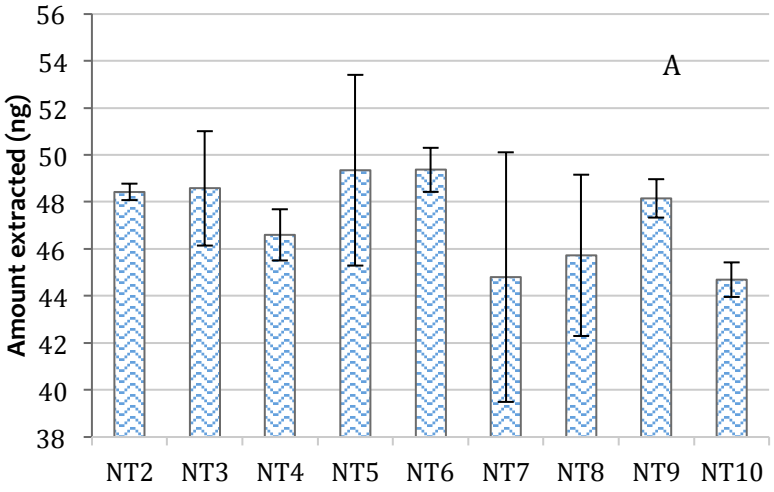

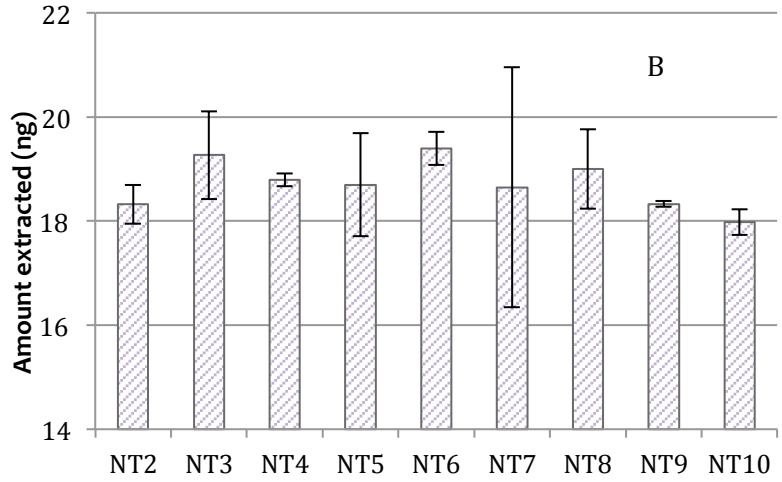

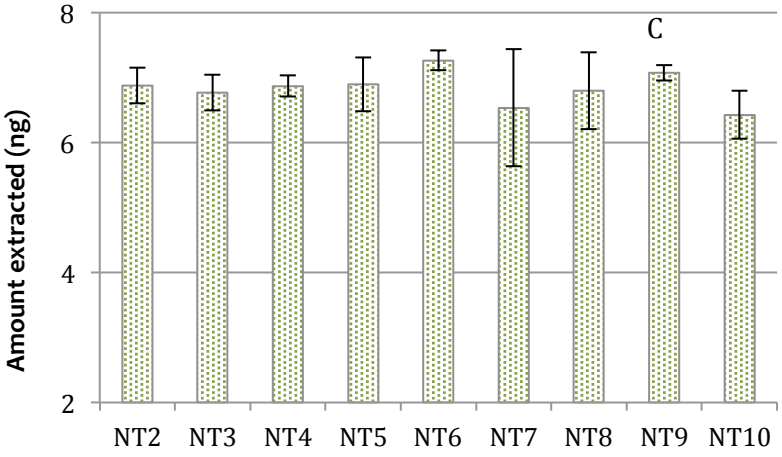

Figure 2.4.(A-C) Comparison of the amount of xylene, decane and limonene extracted by 9 commercial NTs packed with DVB particles. Sample volume was 20 mL at a sampling rate of 5 mL/min.

As a summary, the modified prototype developed by SGE has shown to be statistically reproducible among the 9 different NTs evaluated as far as the sampling is performed at sampling rates lower than 5 mL/min. Additionally, it was found that after approximately 10 injections the pre-punch septum should be replaced in order to avoid pieces of septum

going inside the restriction of the liner. It is also recommended that the liner be checked every 20 injections with a gas duster and a small wire passing through the restriction to remove small pieces of septum remaining from previous injections. It is highly recommended to the users to not tighten the septum too much, otherwise blocking of the restricted liner can lead towards high RSD values. Consequently, in the future, the use of septum-less injection ports to prevent possible septum coring will be evaluated. Finally, it was observed that after 5 injections, the Teflon slider (Fig. 2.6) fails to properly seal the side-hole of the needle trap. This could be related to the intrinsic properties of Teflon, which expands after being exposed at 260 ºC for several injections. Consequently, if the Teflon slider is not replaced, leaks may occur during the sampling, leading to a smaller amount of analytes being adsorbed onto the DVB particles. Lastly, it was found that the hole in the slider should not be bigger than 0.7 mm.

Table 2.2. Statistical comparison of 9 commercial needle traps packed with 2 cm of DVB particles. $F_{NT}$is the F-ratio for the different treatments evaluated (different needle traps) and F_{crit} is the critical value of F for 27 experiments at a 95% level of confidence. RSD is the relative standard deviation for the inter-needle trap repeatability of 9 NTs (n=3) at 10 mL/min.

Compounds	**F_{NT}**	**F_{crit}**	**RSD**
Xylene	4.0		5.4
Decane	4.3	2.5	5.7
Limonene	4.0		5.2

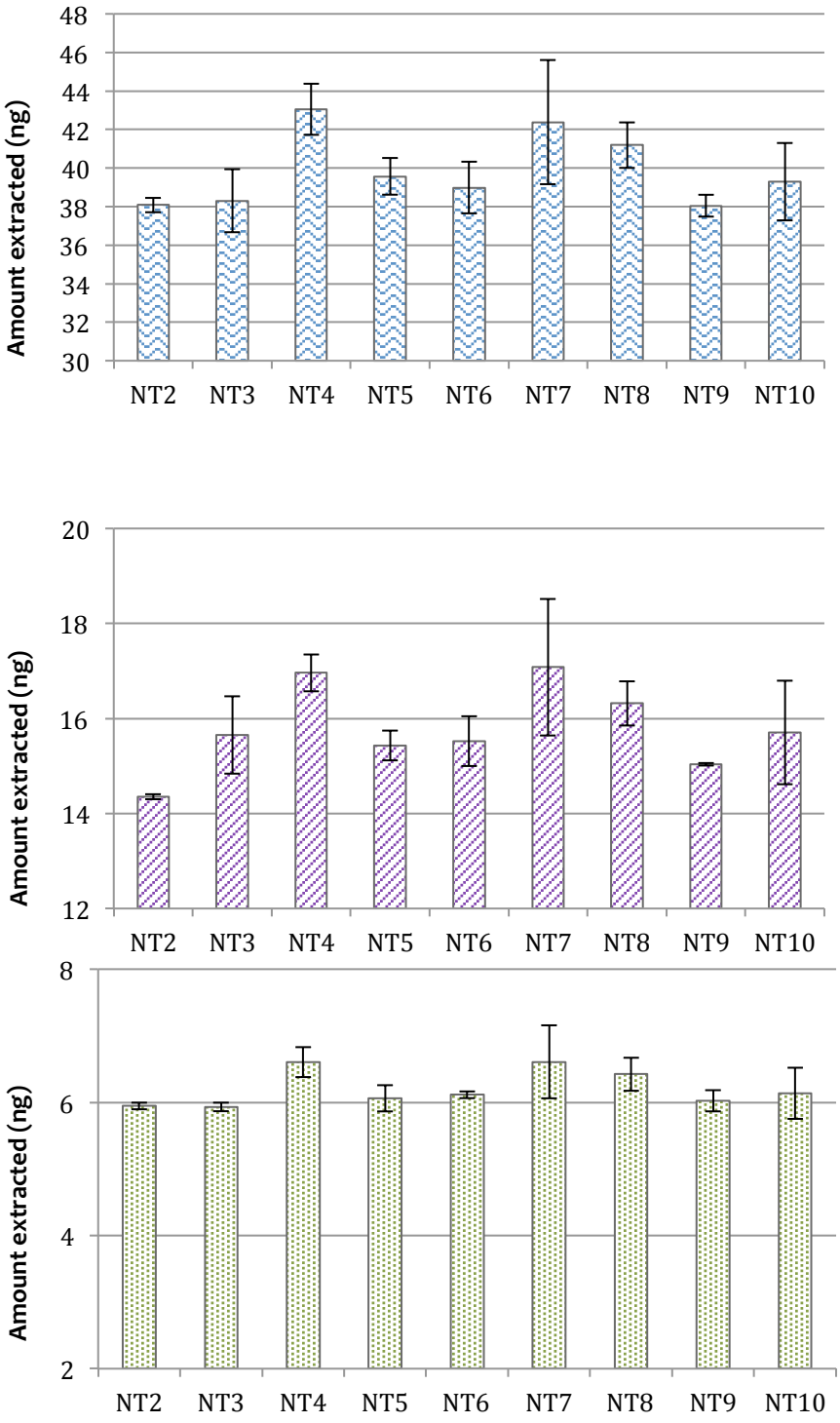

Figure 2.5.Comparison of the amount of xylene, decane and limonene extracted by 9 commercial NTs packed with DVB particles. Sample volume was 20 mL at a sampling rate of 10 mL/min.

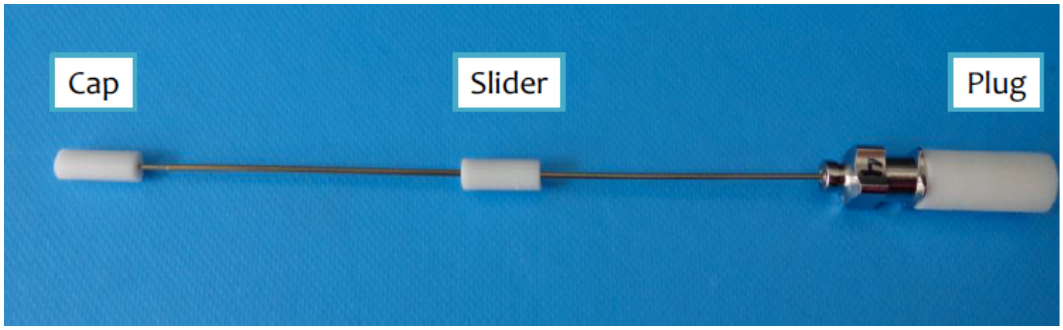

Figure 2.6. Description of a SGE needle trap properly sealed and capped (add here description of the slider)

2.3.1.3. Application of NTs packed with DVB particles towards in situ sampling of plants

Volatile and semi-volatile compounds produced by plants are collectively known as biogenic volatile organic compounds (BVOC)[78]. They comprise a wide variety of organic substances, such as alcohols, terpenes, alkanes and esters. Owing to the fact that BVOCs are responsible for multiple interactions between plants and other organisms, and also play a key role in atmospheric chemistry, their identification, characterization and quantification are of great relevance[78].

Generally, *in situ* research is best suited to observe real conditions when compared to *in vitro* research[78]. As biological systems are very complex and readily react to any perturbation in the surrounding environment, *in situ* research can provide more accurate results than *in vitro* studies [79,80]. An ideal *in situ* sampling technique should be solvent-free, portable, and offer integration of the sampling, sample preparation and analysis steps. With NT, both *in situ* sampling and sample preparation are accomplished by placing the needle in the area surrounding the system under study[80]. Consequently, the plant tissue being analyzed is only minimally disturbed. *In situ* analysis using SPME and

NT is gaining ground in metabolomics studies[81] due to its unique characteristics: on-site sampling, easy extraction, and analysis of whole extracted amounts.[82] Until now, numerous applications for the analysis of BVOCs have been developed with SPME and NT[15]. For instance, circadian BVOC emission profiles and phytoremediation properties of plants were explored by Reyes-Garcés *et al*., Zini *et al*. and Sheehan *et al*., respectively[21,78,83]. However, just as observed in air quality studies, only a handful of these studies have included the use of multiple devices.

In real applications, numerous fibers/NTs are required in order to obtain a better spectrum of the emissions being studied[78]. For that reason, the application of multiple NTs used in the identification and quantification of BVOCs emitted by a pine tree is also presented in this chapter. The selection of NT packed with DVB was based on previous studies conducted in BVOCs analysis[78]. The BVOCs emission profiles of a pine tree branch were evaluated in a timespan of 12 hours during the second week of July, 2013. Three major compounds found at any time of the day were selected for quantitation: limonene, α-pinene and β-pinene. Table 2.3 presents the concentrations determined for each compound every 3 hours, starting from 8 am to 8 pm. Error bars represent the standard deviation of the mean calculated with three independent NTs packed with DVB.

In summary, 18 compounds were completely identified by their linear retention indices and comparison of mass spectra with those found in the NIST database and literature. The concentration of the target analytes showed a similar trend over the duration of the experiment: the highest concentrations for the target compounds were obtained at 2 pm with 0.75, 2.87 and 11.63 ng/mL for β-pinene, limonene and α-pinene, respectively. All the concentrations were in the range of hundreds of nanograms per liter, which are within

the typical range for forest atmospheric environments. Good inter-NT repeatability for 3 NTs was found, with RSD values between 2 to 10 % in all the cases. The circadian variations observed in the concentrations of the target analytes can be a reflex from the variations of temperature and illumination conditions during the sampling cycle. Similar trends have been previously reported for isoprene in the analysis of *Eucalyptus citriodora,* and eucalyptol in the analysis of *Brugmansia suaveolens* flowers[78,80]

Table 2.3. Evaluation of the concentration of α-pinene, β-pinene and limonene emitted at different hours by a pine tree at University of Waterloo. Spot sampling using three NT packed with 2 cm DVB (V= 5mL, Avg. T=26.1ºC)

Time	**α-pinene (ng/mL)**			**β-pinene (ng/mL)**			**Limonene (ng/mL)**		
	NT_1	NT_2	NT_3	NT_1	NT_2	NT_3	NT_1	NT_2	NT_3
8 am	6.6	6.4	6.2	0.3	0.3	0.2	1.8	1.7	1.4
11 am	7.5	7.4	7.7	0.5	0.4	0.6	2.2	2.4	2.3
2 pm	12	11.5	11.4	0.6	0.7	0.8	3.0	2.7	2.9
5 pm	6.7	7.1	6.5	0.5	0.3	0.5	2.1	2.0	1.9
8 pm	3.6	4.2	4.3	0.3	0.2	0.3	1.4	1.2	1.3

2.3.2. Development, evaluationand application of extended tip NT packed with Car particles

2.3.2.1. Development and evaluation of PDMS frit-Car needle traps towards active sampling

The main limitation of the modified extended tip-NTs packed with bare carboxen, compared to DVB, is that the particles do not “stick- together” due to their spherical shape and surface properties, eventually blocking the sliding-fit tubing. As a result, the

flow is completely restricted and no analytes are collected by the NT (data not presented). With the objective of broadening the applicability of the new extended tip-needles, our laboratory manufactured a novel type of NT that allows the use of carboxen as a packing material. The new NT consists of a small PDMS frit (2 mm thickness) that is fitted prior to the carboxen particles being added, as shown in Fig. 2.1.

In total, 6 needles were packed with 2 mm of PDMS frit and 2 cm Car particles (60-80 mesh). For each of the NTs, 2 h (300 ºC) conditioning was carried out, and for all of them, a blank was performed in order to evaluate possible residual contamination. Extractions from the gas-generator chamber were performed at a 5 mL/min sampling flow rate. All the experiments were randomized for different needles and performed in triplicate. As shown in Table 2.4**,** the relative standard deviation for the intra-needle trap repeatability of the 6 needle traps is satisfactory, since values were lower than 8% in all cases for the two analytes evaluated (toluene and ethylbenzene). Similarly, NTs proved to be statistically similar for both compounds, and inter-needle trap RSDs lower than 5.3% were obtained.

Table 2.4. Intra-needle trap repeatability expressed as RSD (%) for each needle trap (n=3) using a 5 mL/min sampling volume, and statistical comparisons of 6 in-house needle traps packed with 2 mm of synthesized PDMS and 2 cm of Car particles. F_{NT} is the F-ratio for the different treatments evaluated (different needle traps) and F_{crit} is the critical value of F for 18 experiments at a 95% level of confidence. RSD* is the relative standard deviation (%) for the inter-needle trap repeatability of 6 NTs (n=3) using a sampling volume of 5 mL/min.

Compound	Intra-needle trap						Inter-needle trap		
	NT_1	NT_2	NT_3	NT_4	NT_5	NT_6	F_{NT}	F_{crit}	RSD*
Toluene (RSD %)	0.9	4.8	2.8	5.2	4.5	4.9	2.8	3.6	3.3
Ethylbenzene (RSD%)	1.8	3.8	3.2	7.8	6.4	0.4	1.5		5.3

In order to evaluate the effect of the sampling rate on the amount of analyte extracted, one of the needle traps was selected to sample at flow rates of 2, 5, and 10 mL/min. As can be seen in Fig. 2.7, results indicate that a slightly higher amount of ethyl benzene was extracted at the lowest tested flow rate, while the same trend was not observed for toluene. However, as presented on Table 2.5, at a 95% level of confidence, no statistically significant difference was observed among the three different flows evaluated. It is important to highlight that variations in the packing of NTs may cause channeling through the bed, which can significantly decrease the amount of analyte extracted at higher flow rates. Such phenomena seems to be more prone in less volatile compounds, but further experiments using analytes with a broader range of vapour pressures are required to validate this observation.

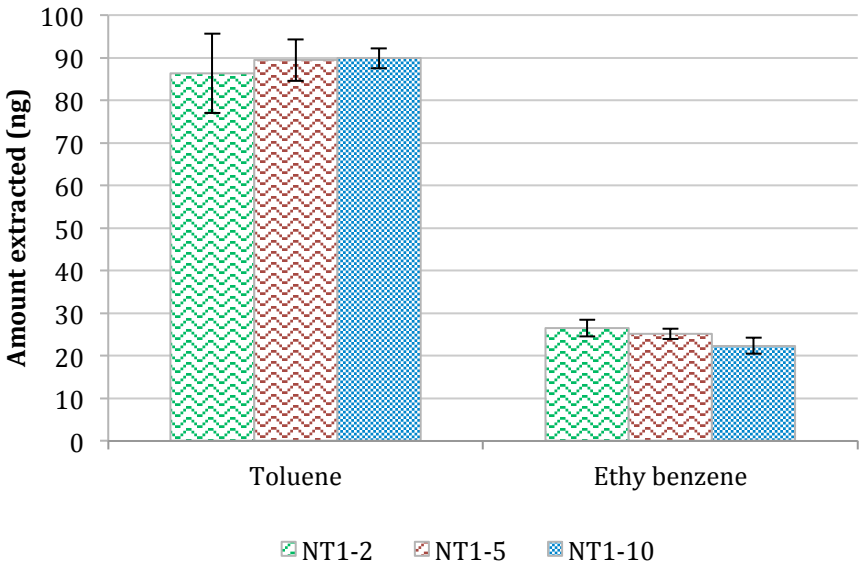

Figure 2.7. Comparison of the amount of extracted by NT1 at different flow rates. Experiments were performed the same day (n=3) at 2, 5 and 10 mL/min.

Table 2.5. Statistical comparison of 3 commercial needle traps packed with 2 mm synthesized porous PDMS and 2 cm of Car particles at different flow rates. $F_{NT}$is the F-ratio for the different treatments evaluated (different needle traps) and F_{crit} is the critical value of F for 9 experiments at a 95% level of confidence. RSD is the relative standard deviation for the inter-needle trap repeatability of 1 NTs (n=3) at 2, 5, and 10 mL/min.

Compounds	F_{NT}	F_{crit}
Toluene	3.0	5.1
Ethyl benzene	2.0	

2.3.3. Development and evaluation of needle traps packed with Car particles embedded in PDMS for passive sampling

Indoor air quality is a vital issue in occupational health. Factors such as ventilation system deficiencies, microbiological contamination, and off-gassing from building materials can cause poor indoor air quality[15]. Since an average person in a developed country spends up to 90% of their time indoors, there has been a growing concern over the past decades in regards to indoor pollutants, including the type of methods currently being used in their analysis[15,40,72]. SPME and NTs have become attractive techniques for indoor air sampling due to their accuracy, cost, simplicity and speed[15,33]. In addition, both microextraction techniques can be indistinctively used for either active or passive sampling[15,32,33,83].

The basic principle of passive sampling is the free circulation of analyte molecules from the sampled medium to the sampling device as a result of the difference in chemical potential between them[72]. Passive sampling can be performed using NTs if a strong sorbent is packed at a defined distance Z from the needle opening of a fixed area A; thus, a diminutive tube-type diffusive sampler is created [33]. As shown in Fig.1.7 in Chapter 1, during the process of diffusion, there exists a linear concentration gradient across Z.

Therefore, by using Fick's law of diffusion, it is possible to determine the amount of analyte loaded on the sorbent, *n*, during the sampling time, *t*[23,84]. The equations that describe the analyte uptake on the NT were summarized in Table 2.6 and have been explained in detail in the literature [15,72,73,85]. In addition, three main conjectures should be achieved during passive sampling with NT. First, the device should respond proportionally to the changing analyte concentration at the face of the needle[23,84]. Secondly, the concentration of the gas system must be equal to the analyte concentration at the face of the opening[23,84]. And third, the sorbent should be a zero sink for the target analytes[23,84]. Such conditions were evaluated by Gong *et al*., and their results demonstrated the suitability of NT for passive sampling [75].

Table 2.6. Equations that describe passive sampling analyte uptake in NT. n: mass of analyte loaded on the fibre or NT during the sampling time t; Dg: diffusion coefficient of the target analyte; A: area of the cross-section of the diffusion barrier; Cs: gas-phase analyte concentration at the coating position (sorbent bed); C_F: concentration of the analyte at the needle opening; SR: sampling rate; $SR_{(Z)}$: sampling rate at the position Z. $SR_{(Z')}$: sampling rate at the position Z'; D_g: Diffusion coefficient at 298 K; D_T: Diffusion coefficient at a different temperature, T (K); T: temperature

Applications of Fick's Law	$n = \frac{D_g A}{Z} \Delta C_{(S-F)} t$
Sampling rate	$SR = D_g \frac{A}{Z}$
TWA concentration determination	$\overline{C_F} = \frac{nZ}{ADt}$
Sampling rate at different path	$SR_{(Z')} = SR_{(Z)} \frac{Z'}{Z}$
Sampler response time	$R = \frac{Z^2}{2D_g}$
Diffusion coefficient correction	$D_T = D_g \left(\frac{T}{298}\right)^{3/2}$

Owing to the flexibility of selecting a wide range of sampling times in passive mode (from less than 1 min to days), several applications designed to test a broad range of analytes have been developed to date using SPME and NT devices[29,32,83,86,87]. However, up to date studies were only performed using blunt tip NTs [29,32,33]. In this work, we proposed for the first time the application of the extended tip NT packed with carboxen particles embedded into PDMS (see Fig.2.1) for sampling of volatile compounds in passive mode. It should be noted that this configuration is different from the one used for active sampling. First, the NT design with carboxen particles was not used for passive sampling; by adding a PDMS frit, Fick's law could not be applied in a straightforward manner towards the calculation of the concentration (as presented in Table 2.6). In such scenario, permeation of the analytes through the PDMS frit and diffusion through the open tubular path must be considered together with the aim of calculating the concentration on the sample. As expected, the initial configuration added more complexity to the calculations and higher inter-needle trap variability in passive mode. Conversely, by loading the particles onto the PDMS, it is assumed that PDMS acts only as glue, similar to SPME[1], and adsorption occurs mainly on Car particles. As such, the amount of sample collected would depend on the diffusion of the analytes from the entrance of the NT to the face of the sorbent (Z), the diffusion coefficient of the target analyte (D_g), the area of the cross-section of the diffusion barrier (A) and the concentration of the analyte at the needle opening (C_F).

In order to validate these assumptions, passive sampling was performed from a sampling chamber with a known concentration of benzene and toluene and with an electronic

control of temperature and humidity. Samples were collected at 15, 30 and 60 min, and all the experiments were performed in triplicate for each NT. As can be seen in Table 2.7, the inter-needle trap repeatability, expressed as RSD, was <15 % for both probes. Moreover, an average absolute deviation of 9% from the theoretical amount extracted was observed. Such differences can be due to different factors. First, when calculating the theoretical amount extracted, the diffusion path Z was assumed to be exactly 1.00 cm. Therefore, differences observed in relation to the theoretical value can be partially due to the inaccurate determination of the diffusion path.

Next, the diffusion coefficients of the analytes were estimated by the method proposed by Fuller, Schettler, and Giddings.[88] As can be found in the literature[88], such estimation is based on the number of atoms present on a given molecule rather than other physicochemical factors such as structure, conformation, or polarity. Expectedly, a common criticism of SPME/NT is a lack of published experimental sampling rate values[89].

Finally, an additional source of error could be related to the adsorption of analytes onto the needle walls. Several studies found that the likelihood of adsorption onto the needle walls is not easily predictable, and seems to depend on the concentration to which the device is exposed[23,90]. In addition, at long exposure times, the amount of analytes collected on the sorbent would be considerably higher than the amount adsorbed onto needle walls, and consequently, under these conditions, the needle adsorption effect on uptake rates would be negligible. It has also been observed that if the sampling temperature increases, the adsorption of the compound on the needle diminishes, and the experimental value of the sampling rates is closer to the theoretical value. Other authors

have also suggested that matter of adsorption onto the needle walls is not a major issue, as it is only observed in less volatile compounds[9,23]. Chen and Hsiech reported that the experimental sampling rates of dichloromethane at very short sampling times were higher than rates obtained with long sampling exposures[90]. However, similarly to observations reported by Chen and Pawliszyn, the values become constant as the sampling time increases[70]. In order to eliminate the effect of needle adsorption, Chen *et al*. proposed the use of deactivated needles for TWA samplers, such as Silicosteel-coated needles[15,23]. Further evaluation of needle deactivation would need to be carried-out for this prototype prior to its commercialization as a passive sampler.

In summary, the results herein presented demonstrate that the new extended tip needle trap packed with carboxen particles loaded on PDMS, and with a Z of approximately 1 cm, could be successfully used as a passive sampler if the diffusion path, diffusion coefficient, and needle deactivation are properly controlled/determined.

Table 2.7. Comparison of the amount of benzene collected in passive sampling mode (Z ~1.0 cm) by 2 different NTs packed with a PDMS frit of 0.2 cm and 1 cm of Car *versus* theoretical amounts determined using Fick's law.

Sample collection time (min)	Theoretical amount extracted (ng)	Experimental amount extracted (ng)		Inter-needle trap repeatability (%)		Experimental error (%)	
		NT_1	NT_2	RSD_1	RSD_2	CV_1	CV_2
15	6.6	6.0	6.3	10	8	9	5
30	13.2	12.2	14.5	15	14	7	9
60	26.5	23.0	30.0	13	5	12	13

2.3.4. Application of *PDMS-Car* NTs towards the evaluation of indoor air contaminants in active and passive sampling mode

Indoor air was analyzed at a polymer synthesis laboratory at the University of Waterloo. Several samples were collected in the span of a work day (8 h) to determine variations in the air contamination profile within this time limit. Active sampling through a 2 cm DVB NT was carried out every hour to observe intra-day variations. Passive sampling over a period of 8 hours, using two PDS-NT packed with 1 cm Car particles, were used to determine the average concentration of toluene to which workers were exposed. The sampling devices were located at approximately 2.5 meters from the rotary evaporator in order to account for the average exposure of a worker in the laboratory. As can be seen in Fig. 2.8, good agreement was observed between passive and active techniques. According to laboratory workers, the increase in the concentration of toluene, observed at two different times during the day, at 10:30 am and 2:30 pm, correlated to the use of a rotary evaporator.

The active-NT concentration can be considered a time-weighted average sample obtained over a short sampling period (approximately 20 min sampling), only allowing the analyst to obtain results for a specific fragment of the day rather than the entire day variation. This explains why the average of the concentrations calculated using the active NTD (0.025 ng/mL) was slightly lower than the one obtained with NT in passive sampling mode (0.030 ± 0.01 ng/mL, n=2). It is important to emphasize that toluene was not found to be present in concentrations higher than the regulatory quantities established by the National Institute for Occupational Safety and Health (NIOSH) at all times. For instance, the highest concentration of toluene found during the sampling was 0.078 ng/mL,

whereas the established 10-hour Threshold Limit Value (TLV) and the short-time exposure limit (STEL) of toluene are 377 and 565 ng/mL, respectively. The results presented in this study highlight the applicability of these techniques in the monitoring of more toxic compounds such as benzene, which have lower thresholds (0.32 ng/L TLV and 8 ng/L STEL)[23,33].

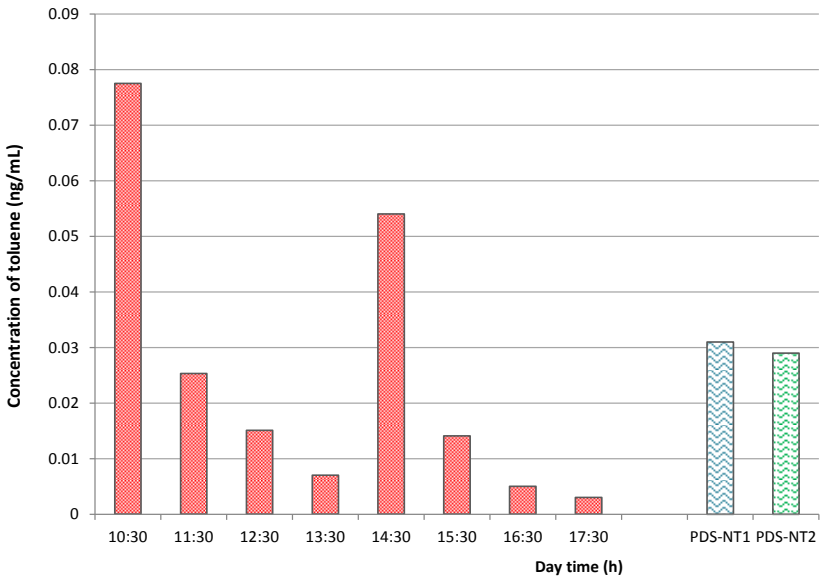

Figure 2.8. Concentration of toluene at different hours in a chemistry laboratory at University of Waterloo. TWA sampling was perform using PDS-NT using SGE NTs (Z=1 cm, t = 8 hours); Active sampling using a DVB (100 mL at 5mL/min).

2.4. Conclusion

Considering the increasing efforts made by the scientific community towards the development of new on-site sampling technologies, the present work seeks to showcase the most recent advances of NT technology. The first part of this chapter was undertaken to evaluate a new prototype of NT in terms of amount of amount of extracted analytes,

packing procedure, reproducibility of device after multiple uses, and desorption efficiency. As an active sampler, NTs performed well when applied towards the determination of biogenic emissions from pine trees. Subsequently, extended tip needles were packed in-lab with synthesized highly cross-linked PDMS as a frit to immobilize carboxen (Car) particles. Successively, the needles were packed with Car particles embedded in PDMS for passive sampling. The NT was installed in pen-device. The designed PDS-NT is meant to be paired with products from different manufacturers. As well, in-house or commercially available devices such those produced by SGE or Shinwa can be easily installed[20,21,33,74]. Results showed that the new prototype of NT functions as an effective passive sampling technique for air analysis. Application of NT passive sampling in combination with NT-spot sampling towards the analysis of indoor air in a polymer synthesis laboratory showed good agreement among both approaches.

Chapter 3 : Development and optimization of filters for needle trap devices (NTD) to enhance high efficiency atmospheric aerosol filtration

3.1. Introduction

Particles smaller than 100 nm in size are classified either as nanoparticles or ultrafine particles. The most common method for aerosol collection is filtration. There are two main kinds of filters used in aerosol sampling: fibrous filters and membrane filters. Fibrous filters consist of a mat of ultra fine fibers prepared in such a way that most are perpendicular to the particle flow.[57] In comparison, membrane filters are comprised high solid fractions and a complex pore structure, leading to high efficiency and a greater resistance to flow.[58,59,60]

Various factors, such as the structure of the filter, the properties of the particles of interest, as well as operational parameters, can affect the filtration process. As such, further research on the relationships between efficiency and particle size or between face velocity and efficiency can potentially aid in the development of better aerosol filtration methods.[61,62]

In past research, NT has been shown to be able to act as a suitable filter to collect particles; however, to date, the collection efficiency of the method towards particles in the nanometer range has yet to be studied. Consequently, the aim of the currently presented work involved the development and comparison of various frits for NT devices, which were then employed to investigate the feasibility of the NT device to capture particles smaller than 200 nm in high efficiency, in addition to determining under which conditions the method can be optimized. For this purpose, three different filters, fibrous, porous PDMS membrane, and Carboxene granular bed were selected for an investigation of filtration efficiency. Filters were first prepared with a large diameter so

as to be compatible with the scanning mobility particle sizer (SMPS), which was used to estimate the collection efficiency on a macroscopic scale. Next, a fibrous filtration model was proposed for calculation of needle trap filtration efficiency. Subsequently, a series of experiments were conducted to study the collection efficiency of the needle trap devices, which were packed with different sorbents such as porous PDMS, a nanofibrous filter, and Car particles. The NT device was first connected between the classifier and the condensation particle counter for sampling. After sampling the NT was injected in the GC/MS instrument for determination of particle concentration. It should be noted that the effect of different face velocities on the efficiency of the needle trap as a function of particle size was also investigated. Finally, to test the validity of the proposed model, the results obtained from theoretical calculations were compared with experimental findings.

3.1.1. Theoretical considerations

In order to compare the different filters, a parameter which defines filtration performance was required. Quality factor is a parameter to assessment for filter performance [57], which is defined as:

$$Q_f = \frac{-\ln p}{\Delta p} \tag{3.1}$$

where Δp is pressure drop and p is penetration.

The resistance airflow across a filter is called a pressure drop. In 1973, Davies presented the pressure drop as [63]:

$$\Delta p = \frac{\eta\, t\, U_0 f(\alpha)}{d_f^2} \tag{3.2}$$

where η is viscosity, t is thickness of filter, U_0 is face velocity, α is solidity or packing density and d_f^2 is diameter of filter.

Penetration is a fraction of particles, which exit the filter or penetrate the filter [57].

$$P = \frac{N}{N_0} = 1 - E \tag{3.3}$$

As discussed before, E is called collection efficiency, which is described as the fraction of entering particles retained by the filter (Equation.1.7). This equation shows the macroscopic property of filter efficiency [57].

$$E = \frac{N_0 - N}{N_0} \tag{3.4}$$

where the N_0 and N are the particle number concentrations at inlet and outlet of filter, respectively. The efficiency can be also defined in terms of Particles mass concentrations. In high efficiencies, the penetration is clearer indicator because small changes in collection efficiency are associated with large changes in penetration. For example, when E increases from 90 to 99%, P drops from 1 to 10 %.

As can be seen, the filtration performance can be assessed by collection efficiency and pressure drop. A good filter is expected to show high collection efficiency and low pressure drop.

The ability of NT to collect the particles can be also explained by classical filtration theory, which is based on the concept of single fiber efficiency. Therefore, the NT

efficiency is estimated by integration of single fiber efficiency of whole sorbent length L; a simplified equation is expressed below. The equation relates the macroscopic property of filter efficiency to the microscopic property of single-fiber efficiency [57].

$$E = 1 - \left(\frac{4\,\alpha\,E_{\Sigma}L}{\pi\,d_f}\right) \tag{3.5}$$

When the α refers to solidity or packing density of sorbent bed, d_f is fiber diameter or sorbent particles diameter and E_{Σ} is single sorbent collection efficiency, which is determined by deposition mechanisms.

The particles may be deposited on the fiber by simultaneous action of several mechanisms including, interception, diffusion (Brownian motion), inertial impaction and gravitational settling. These mechanisms are known as mechanical capture mechanisms and illustrated in Fig.3.1. Inertial impaction occurs when particle, by its inertia, is not able to adjust its direction and deviate from original gas streamline. Capture by interception occurs when a particle follows the gas stream and have insufficient inertia to departs from original gas stream. In such cases, a particle deposits when it comes within one particle radius of fiber surface. Collection of particles by interception is related to the ratio of particle diameter to sorbent diameter and packing density. Diffusion is caused by Brownian motion that can be sufficiently strong to move the particles from gas stream to a fiber. Typically, this mechanism is only significant for particle smaller than a few tenths of a micrometer. Contribution of gravitational settling is negligible compare to three mechanisms specifically for nanoparticles.

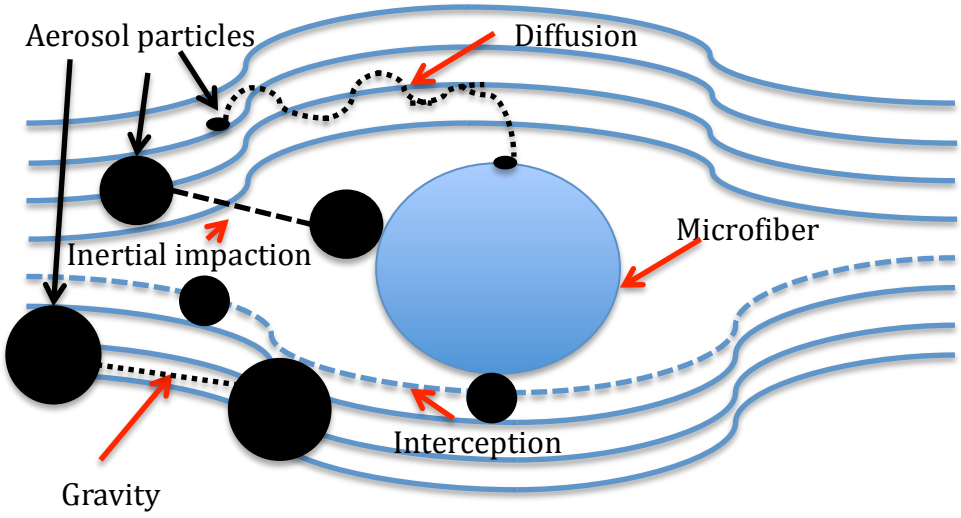

Figure 3.1. Particle trapping Mechanism

3.2. Experimental

3.2.1. Materials and reagents

All tested analytes, namely dioctyl phthalate (DOP), acetic acid, methanol, and cellulose acetate, were purchased from Sigma–Aldrich (Mississauga, ON, Canada). Helium of ultra-high purity was supplied by Praxair (Kitchener, ON, Canada). Carboxene 1000 (CAR) particles of 80/100 meshes were purchased from Sigma-Aldrich (Bellefonte, PA, USA). A bi-directional syringe pump, purchased from Kloehn (Las Vegas, NE, USA), was used for NTD sampling (ON, Canada). Stainless steel SGE needle traps were purchased from SGE (Melbourne, Australia). Polydimethylsiloxane (PDMS, Sylgard 184) was obtained from Dow Corning.

3.2.2. Instrumentation

An Agilent 6890 gas chromatograph coupled to a 5973 MSD quadrupole mass spectrometer (Agilent Technologies, Mississauga, ON, Canada) was used in this study. The oven temperature was initially held at 80 ^{0}C (2 min), gradually increased to 100 ^{0}C at

a rate of 20 ^{0}C min^{-1}, then ramped to 150 ^{0}C at 15 ^{0}C min^{-1}, with a final ramp to 250 ^{0}C (held 5 min) at 30 ^{0}C min^{-1}. A DB-5 (30 m x 0.25 mm x 0.25 μm) fused silica column with helium as the carrier gas at a flow rate of 1.0 mL/min was used for the chromatographic separation of fragrances. An aerosol generator (3076) from TSI (Shoreview, MN, USA) that included an atomizer was used to generate constant dioctyl phthalate DOP test aerosols ranging from 10 to 250 nm in diameter. A TSI (3080), employed as an electrostatic classifier, was used in conjunction with a condensation particle counter model (3787) from TSI to monitor number of produced particles by aerosol generator.

3.2.3. Synthesis of porous PDMS

PDMS pre-polymer was added to a curing agent in a ratio of (10:1) (w/w). The prepared 1% dodecyl sulfate sodium salt (SDS) solution was then added to the mixture of PDMS and curing agent with a ratio of (1:2), and stirred for 15 min. Glass capillaries with the same inner diameter as NTs were tilled with a homogenized milky mixture.[76] Polymerization was then allowed to proceed at 80 ^{0}C for 1 hour. The polymerized PDMS was then heated at 120 ^{0}C for 3 hours to evaporate remaining water droplets and also to remove any volatile impurities. It is important to note that the amount of water originally added to the mixture, as well as the temperature of the polymerization procedure could result in various porosities; as polymerization temperature is the most effective parameter in obtaining open pores, the temperature was increased to 20 degrees over the boiling point of water so as to obtain maximum porosity. It should be noted that speed of rotation, curing time and temperature, ratio of polymer-curing mixture and water droplets

(as porogen) could be affected the porosity of polymer. For example, at higher rotation speeds polymerization is formed faster and smaller pore size can be obtained. The smaller pore size was obtained when the higher temperature was applied. The polymerization process is slow when the applied temperature is low, which could allow to water droplet to coalesce, leading to larger pore size.

3.2.4. Synthesis of nanofibrous frits using the electrospinning method

The schematic of the electrospinning set-up is shown in Fig 3.2. For this configuration, the syringe is filled with a cellulose acetate/water/acetic acid solution. Its plunger is then placed in an actuator system to adjust the solution feed rate during the electrospinning process. The high voltage supply is connected to the needle syringe while the grounded metal mesh is used as a collector. Since an electric field is generated between the needle and collector, the solution flows out from the needle due to the electric force. The attached semicircular solution droplet at the outlet of the needle deforms into a conical shape, known as the Taylor cone. A jet of precursors is then formed after the electric force overcomes the surface tension of the cone. While the produced jets travel towards the collector, solvent evaporation continues until the surface area of sub-jets becomes sufficiently large. This process leads to the polymer nanofiber coating of the mesh surface. [62]

In this set-up, a Scanning Electron Microscope (SEM) was used to characterize the diameter of the fibers. A cellulose acetate solution was prepared by dissolving cellulose acetate in a solvent containing 75 vol % of acetic acid and 25 vol % of water.[91] The applied voltage was 15 kV, with a distance of 10 cm between the capillary and mesh surface. The solution feed rate remained constant at 8×10^{-3} mL/min. The density of the

nanofiber packing is dependent on the electrospinning period; longer electrospinning durations lead to larger nanofiber depositions on the substrate. In addition, the thickness of the nanofiber layer can also be altered.

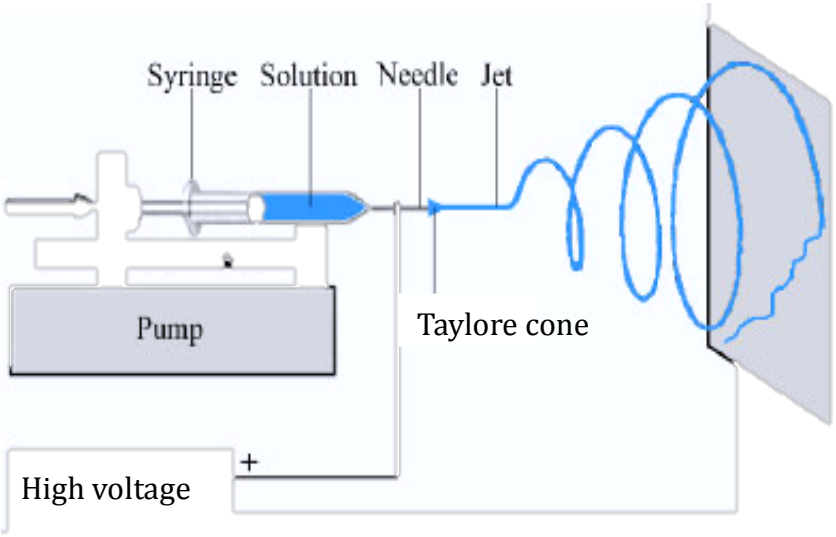

Figure 3.2. Schematic design of electrospinning set-up

3.2.5. Packing procedure of granular sorbent through the NT

For this series of needle trap preparations, the side hole of the needle trap was first sealed with Teflon slider, followed by a connection of the extended tip of the needle to the tap-water aspirator. Next, sorbent particles were drawn through the needle by aspirator. After packing the desired length of sorbent bed, a spring wire was used to immobilize the sorbent. The sorbent particles used in this work were 1 cm of 80/100 and 100/120 mesh Car. The packed needles were conditioned in the GC injector at 260 ^{0}C with helium as a carrier gas for 3 hours.

3.2.6. Experimental set-up

Fig. 3.3 illustrates the experimental set-up. An atomizer (TSI 3078) was used to generate the dioctyl phthalate aerosol particles. A differential mobility analyzer (DMA) was used for particle classification based on particle mobility sizes. A neutralizer was applied to prepare Boltzmann equilibrium charging status to the particles. The condensation particle counter (CPC) was used as a detector to measure the concentration number of particles. The filter holder was then placed between the DMA and CPC to trap monodispersed particles with the same mobility. A pressure gage was connected to the system to measure the pressure drop of the tested filters. The filtration face velocity was adjusted by the gas flow rate. Considering that the pressure drop and filtration efficiency of a given filter are two critical parameters used to estimate the quality factor of the filter, the pressure drops of the tested filters were recorded at different face velocities. Following, the filtration efficiencies of the filters were obtained for different particle sizes at face velocities of 16, 42, and 84 cm/s. For particle generation, a dioctyl phthalate solution was applied. Particles sized between 10 to 200 nm were selected for this study. The mean particle size was 50 nm, while sizes of 10, 20, 50, 100 and 200 nm were chosen for model calculations.

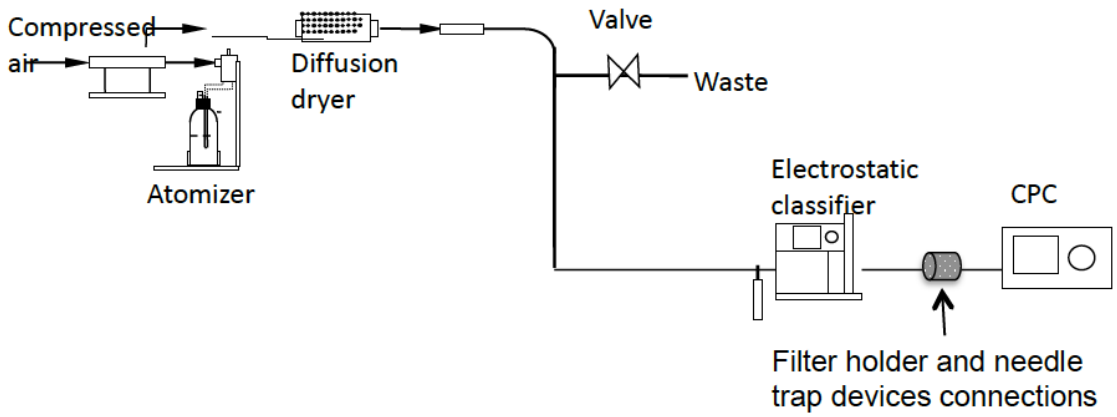

Figure 3.3. Schematic illustration of experimental set up

3.3. Results and discussions

3.3.1. Physical parameters of filters

The physical parameters of the porous PDMS and nanofibrous filters are summarized in Table 3.1. As previously mentioned in Section 3.2.3, porous PDMS was synthesized withdifferent water/polymer ratios so as to increase the porosity of the polymer (as can be seen in Fig. 3.4). The fibrous filter (Fig. 3.5 a and b) was produced with an electrospinning cellulose acetate solution (section 3.2.4). The mean fiber diameter (d_f) was estimated from scanning electron microscope (SEM) pictures. SEM pictures of the porous PDMS and nanofibrous filter can be seen in Fig. 3.6 (a) and (b), respectively. A pressure gauge was used for determinations of pressure drops (Δp). The thickness of the filters (t) was measured with the use of a digital thickness gauge. The solidity or packing density was estimated by equation 3.2, using known U_0, t, d_f and Δp.

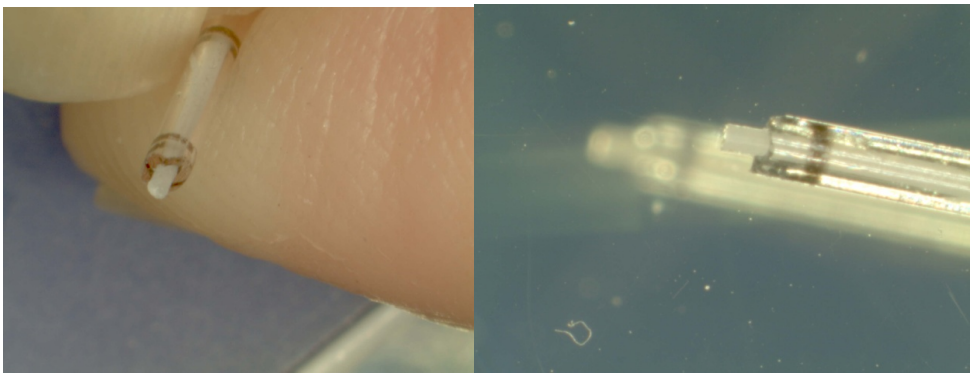

Figure 3.4. Images of a synthesized porous PDMS rod manufactured in laboratory

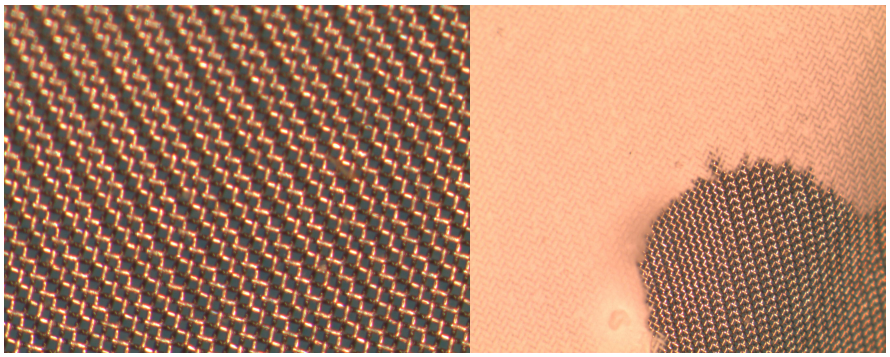

(a)

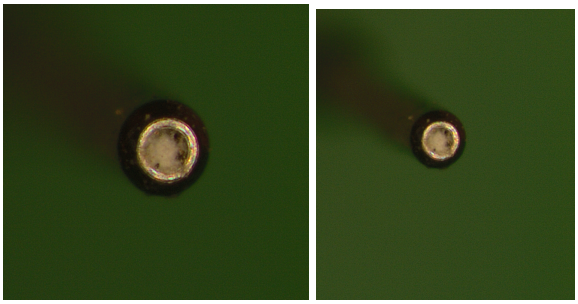

(b)

Figure 3.5. Images of a fibrous filter prepared by electrospinning; (a) metal mesh; (b) tip of the needle trap

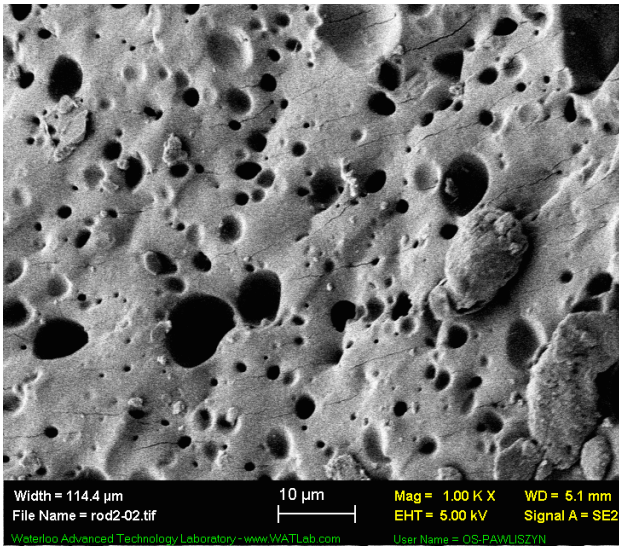

(a)

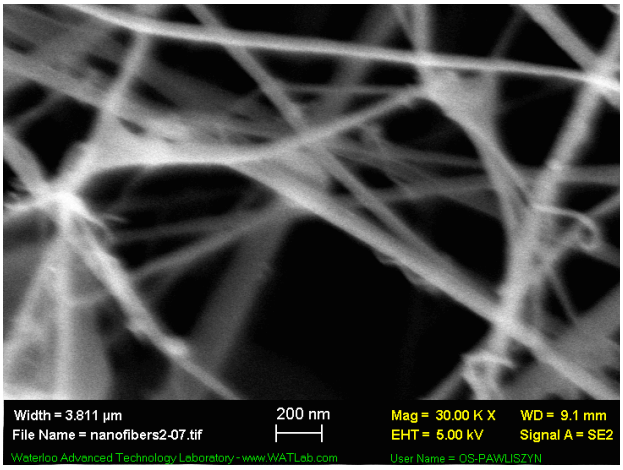

(b)

Figure 3.6. SEM images of (a) porous PDMS and (b) fibrous filter

Table 3.1. Physical parameter of filters

Filter types	Fibre diameter (d_f) (µm)	Thickness (t) (mm)	Solidity (α)
Porous PDMS	10.0	2.000	0.4
Nanofibrous	0.2	0.001	0.03
80/100 Car particles	150.0	10.000	0.37
100/120 Car particles	100.0	10.000	0.42

3.3.2. Theoretical calculation based on fibrous filtration model

The total filtration efficiency is the sum of efficiencies by the individual filtration mechanisms. The overall single fiber efficiency can be written as [57]:

$$E_{\Sigma} = E_{Int} + E_{Diff} + E_{Imp} + E_{Grv} + E_{Diff+Int} \quad (3.6)$$

The single fiber efficiency due to the interception is given bellow

$$E_{Int} = \frac{(1-\alpha)R^2}{Ku(1+R)} \quad (3.7)$$

More generally, the single fiber efficiency of diffusion is expressed as

$$E_{Diff} = 2\,Pe^{-(2/3)} \quad (3.8)$$

To estimate the overall single-sorbent collection efficiency specifically for smaller size particles, it is essential to include the interception of diffusing particles. It can be written as:

$$E_{Diff+Int} = \frac{1.24\,(R)^{2/3}}{(Ku\,Pe)^{1/2}} \quad (3.9)$$

The impaction and gravitational settling are negligible for nanometer size particles.

The only essential mechanism for the trapping of particles smaller than 200 nm is diffusion, while the contribution of interception is only significant for collection of particles larger than 200 nm. Impaction, on the other hand, contributes significantly to the capture of large particles. In the context of the present investigations, it should be noted that diffusion, which is predominantly dependent on particle diameter as well as the diameter of the filter sorbent particles, is the predominant mechanism for NT filtration efficiency. All other physical parameters used for theoretical calculations, namely face velocity, thickness of the filter, and fiber diameter, were assumed to be the same as the

empirical parameters obtained for the NT experiments. Based on model calculations (Tables 3.2 to 3.5), a particle size range of 40 - 60 nm would be collected with the lowest efficiency; this selected range would be too large for interception to be effective, and too small for diffusion. According to the obtained theoretical results, a smaller fiber diameter would likely collect more particles and present greater filtration efficiency. The effects of different sample particle sizes and face velocities on the efficiency of NT were also investigated (see Table 3.2 to 3.5). Based on theoretical calculation, the collection efficiency would be inversely proportional to the face velocity. The proposed model indicated that by optimizing empirical parameters such as fiber diameter, filter thickness, quality of packing, and sampling flow rate, the NT was able to trap a specific range of particles with high efficiency.

Table 3.2. Single-fiber efficiency and total efficiency for a filter with parameters t= 10 mm, α = 0.37 and U_0= 17 cm/s, d_f = 150 μm

Car particles (80/100 meshes)	Single-fiber efficiency			Overall filtration efficiency (%)
	E_D	E_{DR}	E_R	
10 nm	0.023	0.0006	-	90.5
20 nm	0.011	0.0005	-	76.0
50 nm	0.009	0.003	-	60.3
100 nm	0.004	0.0002	0.056	61.9
200 nm	0.001	0.0001	0.085	89.9

Table 3.3. Single-fiber efficiency and total efficiency for a filter with parameters t= 10 mm, α = 0.42 and U_0= 17 cm/s, d_f = 100 μm

Car particles (100/120 meshes)	Single-fiber efficiency			Overall filtration efficiency (%)
	E_D	E_{DR}	E_R	
10 nm	0.036	0.0003	-	92.6
20 nm	0.014	0.0002	-	79.4
50 nm	0.044	0.0002	-	65.4
100 nm	0.001	0.0001	0.062	63.8
200 nm	0.0008	0.0001	0.089	91.0

Table 3.4. Single-fiber efficiency and total efficiency for a PDMS filter with parameters t= 2 mm, α = 0.4 and U_0= 17 cm/s, d_f = 10 µm

(Porous PDMS)	Single-fiber efficiency			Overall filtration efficiency (%)
	E_D	E_{DR}	E_R	
10 nm	0.840	0.02	-	100
20 nm	0.106	0.013	0.001	90.2
50 nm	0.046	0.011	0.003	84.4
100 nm	0.021	0.010	0.01	97.5
200 nm	0.009	0.009	0.55	99.1

Table 3.5. Single-fiber efficiency and total efficiency for a nanofibrous filter with parameters t= 0.001 mm, α = 0.03 and U_0= 17 cm/s, d_f = 0.2µm

(Nanofibrous)	Single-fiber efficiency			Overall filtration efficiency (%)
	E_D	E_{DR}	E_R	
10 nm	0.934	0.003	-	100.0
20 nm	0.245	0.001	-	93.1
50 nm	0.083	0.082	0.001	83.6
100 nm	0.053	0.061	0.05	98.3
200 nm	0.004	0.006	0.67	99.5

3.3.3. Efficiency of different filters for different particle diameters by SMPS

The filtration efficiencies of the tested filters for different particle sizes were measured in experiments with the use of a scanning mobility particle sizer (SMPS). The efficiency data of nanofibrous, PDMS, and Car particles are shown in Fig.3.7; as the particle size increases from 10 nm to 200 nm, the efficiency curve forms a typical "v" shape for all samples. The lowest point of the v-shaped curve is the minimum efficiency, corresponding to 40 to 60 nm sized particles. At a 17cm/s face velocity, for Car particles, porous PDMS, and nanofibrous, the minimum obtained efficiencies were 40%, 62%, 80%, and 85%, respectively. Car particles with larger pore sizes allowed for more penetration of particles.

In addition, the findings are in a good agreement with the model calculations; the theoretical model indicated that efficiencies are expected to increase with decreasing effective fibre diameter. Thus, we have tested experimentally the efficiencies of three

types of filter samples. Similar trends were observed between theoretical calculations and experimental results. As can be visualized in Fig 3.7, Car particles were shown to yield the lowest efficiency results, followed by a significantly higher efficiency for PDMS, with the nanofibrous filter scoring slightly higher efficiency results than the PDMS.

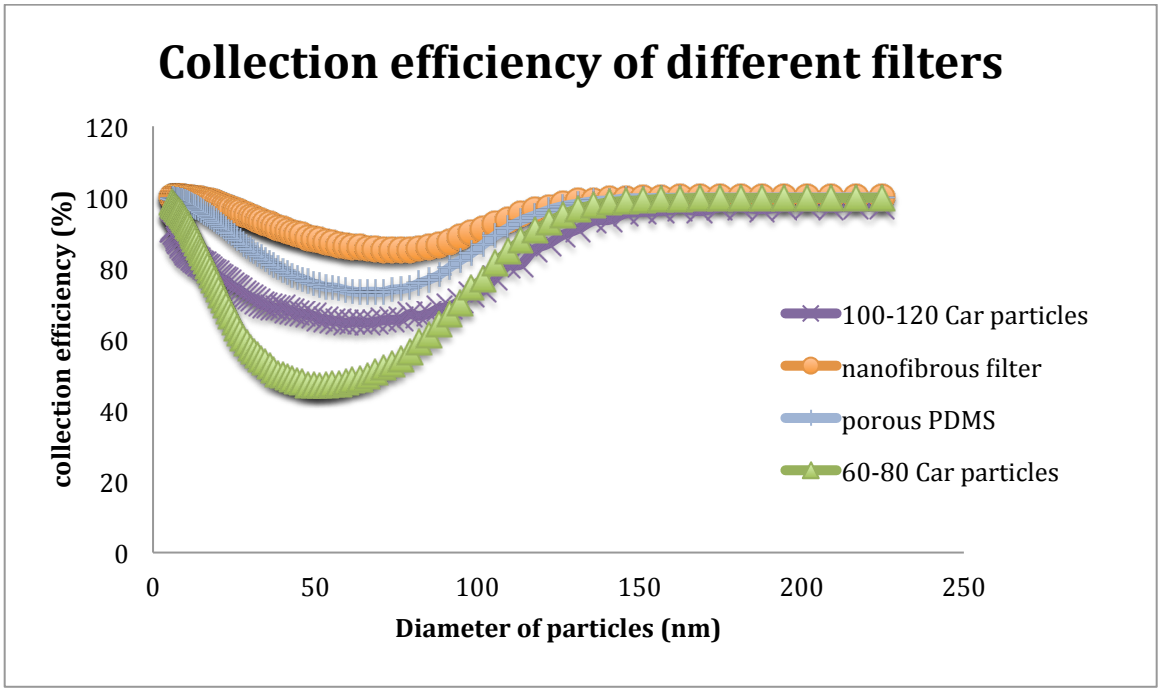

Figure 3.7. Collection efficiency of different filters for different particle sizes

3.3.4. Collection efficiency determination for filters by gas chromatography-mass spectrometry

To compare the theoretical calculations with experimental results, NTs were used to investigate the concentration of particles generated from a scanning mobility particle sizer set-up (see section 3.2.6). A series of needle trap devices packed with different sorbents such as carboxen sorbent, PDMS, and a fibrous filter polymer were used to collect the particles. The packed lengths (t) included 10 mm for Car particles, 2 mm for

porous PDMS and 0.001 mm for the fibrous filter. The calculated solidity values (α) were used across the investigation with consideration to small errors for different filters. The particle generator was set up to produce a constant concentration of particles, and the performance of the three proposed filters for NT devices were compared with data obtained by this particle-generator system. Before determinations of NT collection efficiency could be made however, the consistency of performance of the particle generator over the duration of the experiments had to be confirmed. For this purpose, a scanning mobility particle counter was used to monitor the overall number of particles generated within a specific period of time. Results demonstrated that the number of generated particles was constant over the experiment duration, with a slight increase observed by the end of each experiment due to evaporation of the solvent used in the original solution. According to Fig.3.8, there is no significant fluctuation in the generation of particles was observed. Next, to investigate the filtration efficiency and reproducibility of filters, concentration measurements of the target analytes were carried out by direct injection of NTs into a GC-MS system.

In order to evaluate potential differences in the collection capability of the NTs, extraction of a fixed concentration from the particle generator-sampling system was carried out at 2 mL/min. To reduce the effect of systematic errors, and statistically evaluate the results obtained only according to the factor of interest, namely the response in terms of mass extracted from different NTs, extractions were performed using a randomized block design. As can be seen in Tables 3.6, 3.7, and 3.8, no statistically significant differences in the amounts extracted for the probe analytes were found at a 95% level of confidence. The differences in the amounts extracted between the different

tested NTs can be explained by differences in the packing characteristics of each NT, as well as variations in the number of produced particles during the sampling. Finally, our results demonstrated that after three consecutive samplings with each NT device, relative standard deviations of less than 10 % were obtained.

Filtration efficiencies at different face velocities were also investigated. As can be seen in Tables 3.9 and 3.10, as face velocity increased from 17 to 84 cm/s, the efficiency of the fibers were observed to decrease. Both fibrous and PDMS filters showed a minimum collection efficiency at 84 cm/s. These results are in agreement with the theoretical model proposed by Lee and Liu, showing that particle trapping decreases with increasing face velocity.

A comparison of the experimentally obtained results with the calculated theoretical values based on the proposed model revealed a similar trend, despite the fibrous filter yielding slightly higher efficiency numbers based on the theoretical model. This can be explained by experimental and human errors incurred during the manual preparation of the NT devices. For instance, the obtained differences could be due to technical challenges, the manual preparation of the fibrous filter on the opening surface of NT, or discrepancies incurred during the electrospinning procedure; for example, the polymer solution could have travelled and adhered to the outer surface of NT, which would lead to variations in filter thickness. As a future work, the collection efficiency of the NT device could be increased with the use of a combination of the porous PDMS and fibrous filter, which may allow for an expansion into the applications of NT in various industries.

Table 3.6. Collection efficiency of PDMS membrane, Statistical comparison of 3 needle traps packed with porous PDMS. F_{NT} is the F-ratio for the evaluated treatments (different needle traps) and F_{crit} is the critical value of F for 9 experiments at a 95% level of confidence. RSD is the relative standard deviation for the inter-needle trap repeatability of NTs (n=3) at 5 mL/min.

Porous PDMS frit	**First trial**	**Second trial**	**Third trial**	**RSD (%)**	**Efficiency**
NT1	**3.10 ng/mL**	**3.53 ng/mL**	**3.00 ng/mL**	**8.26 %**	**86%**
NT2	**2.92 ng/mL**	**3.21 ng/mL**	**2.80 ng/mL**	**7.01 %**	**81%**
NT3	**3.45 ng/mL**	**3.00 ng/mL**	**3.22 ng/mL**	**6.25 %**	**85%**

Compounds	F_{NT}	F_{crit}
DOP	1.06	5.14

Table 3.7. Collection efficiency of granular Car particles, Statistical comparison of 3 needle traps packed with Car particles. F_{NT} is the F-ratio for the evaluated treatments (different needle traps) and F_{crit} is the critical value of F for 9 experiments at a 95% level of confidence. RSD is the relative standard deviation for the inter-needle trap repeatability of NTs (n=3) at 5 mL/min.

Car particles frit (80/100 meshes)	**First trial**	**Second trial**	**Third trial**	**RSD (%)**	**Efficiency**
NT1	**2.76 ng/mL**	**2.50 ng/mL**	**2.65 ng/mL**	**4.94 %**	**71%**
NT2	**2.40 ng/mL**	**2.72 ng/mL**	**2.79 ng/mL**	**7.88 %**	**70%**
NT3	**2.21 ng/mL**	**2.34 ng/mL**	**2.53 ng/mL**	**6.39 %**	**65%**

Compounds	F_{NT}	F_{crit}
DOP	3.04	5.14

Table 3.8. Collection efficiency of electrospinning fibrous polymer and statistical comparison of 3 needle traps. F_{NT} is the F-ratio for the evaluated treatments (different needle traps) and F_{crit} is the critical value of F for 9 experiments at a 95% level of confidence. RSD is the relative standard deviation for the inter-needle trap repeatability of NTs (n=3) at 5 mL/min.

Electrospin frit	First trial	Second trial	Third trial	RSD (%)	Efficiency
NT1	**3.11 ng/mL**	**3.39 ng/mL**	**3.41 ng/mL**	**5.07 %**	**89%**
NT2	**3.50 ng/mL**	**3.05 ng/mL**	**3.48 ng/mL**	**7.60 %**	**90%**
NT3	**3.33 ng/mL**	**3.18 ng/mL**	**3.60 ng/mL**	**6.31 %**	**91%**

Compounds	F_{NT}	F_{crit}
DOP	0.07	5.14

Table 3.9. Optimization of sampling flow rates by NT packed with porous PDMS; each experiment was repeated three times.

Porous PDMS frit	First trial	Second trial	Third trial	RSD (%)	Efficiency (%)
2 mL/min	**3.24 ng/mL**	**3.48 ng/mL**	**3.15 ng/mL**	**5.18 %**	**88%**
5 mL/min	**3.08 ng/mL**	**2.93ng/mL**	**3.30ng/mL**	**5.99 %**	**83%**
10 mL/min	**2.78ng/mL**	**3.15ng/mL**	**2.74ng/mL**	**7.17%**	**78%**

Table 3.10. Optimization of sampling flow rates by NT packed with electrospinning fibrous polymer; each experiment was repeated three times.

Electrospin frit	First trial	Second trial	Third trial	RSD (%)	Efficiency
2 mL/min	**3.42 ng/mL**	**3.56 ng/mL**	**3.10 ng/mL**	**7.01 %**	**88%**
5 mL/min	**3.24 ng/mL**	**2.90 ng/mL**	**3.43 ng/mL**	**8.41 %**	**86%**
10 mL/min	**2.96 ng/mL**	**3.32 ng/mL**	**2.87 ng/mL**	**7.80 %**	**82%**

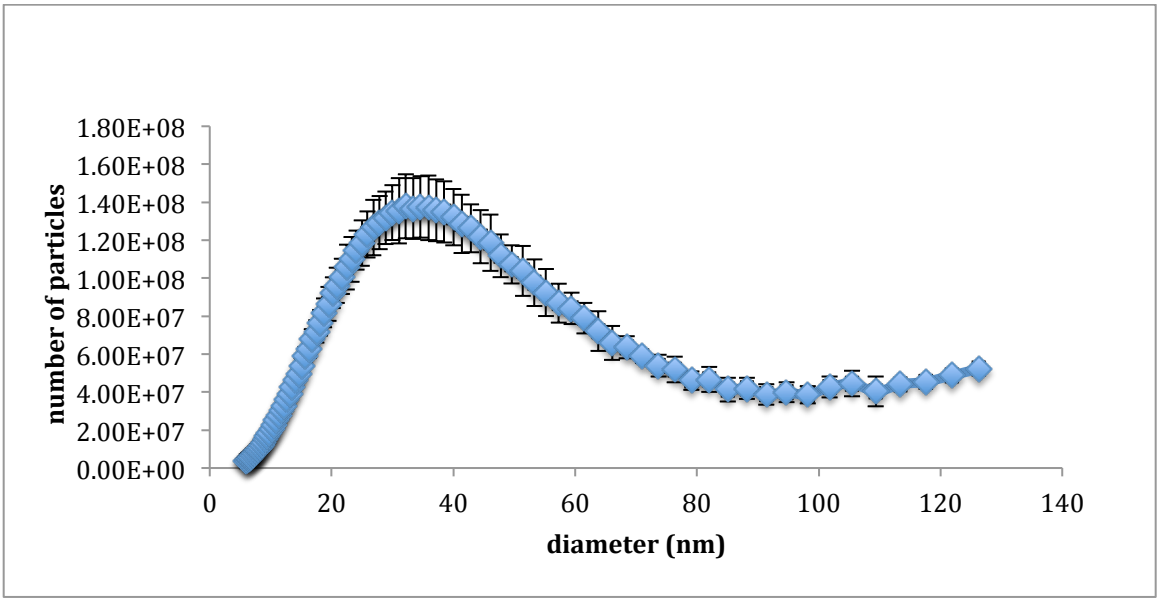

Figure 3.8. Number of generated particles during experimental periods

3.4. Conclusion

A combination of theoretical models and experimental data were used to investigate the filtration efficiency of three different filters. These structures, known as nanofibrous and membrane filters, possess potential applications in both molecular contamination and aerosol removal. A well-defined model for collection efficiency was used to study individual contributions of the fibers to the efficiency. An existing porous material model was modified and used to estimate the collection efficiency of the tested filters. According to the theoretical model, the nanofibrous filter, which was prepared by electrospinning, was shown to yield the greatest efficiency of all three tested filters. However, the efficiency obtained from experimental data showed deviation from the model due to experimental errors. This study has also demonstrated the high efficiency of the porous PDMS filter, although it yielded a higher pressure drop, consequently leading to a decline in the quality factor of this filter. Finally, it should be noted that the fibrous and porous PDMS filters have presented reasonable collection efficiencies in comparison to the granular Car particles. In addition, the manipulation of parameters such as fiber

diameter, face velocity, and solidity were shown to impact the efficiency of the devices under controlled conditions.

Chapter 4 : Determination of total and free concentration of fragrances from personal care products in breathing zone

4.1. Introduction

In recent years, the quality of the indoor air we breathe has become an important human health concern. Aerosols, which are emitted come form a variety of sources, including personal care products, air fresheners, and cosmetics, and they comprise the majority of indoor pollutants [8]. Inhalation of nanoparticles is a major exposure pathway for pollutants. Particles less than 7 μm in diameter are respirable into the alveolar and may contribute to infections, asthma, chronic cough, and lung cancer [92,93,94]. The perfume component of body sprays relies on volatile/ semi volatile compounds typically based on terpenoids while the particulate material will comes in part from the specific formulation of ingredients, such as aluminum chlorohydrate, encapsulates and other related ingredients [95,96]. Particulates and volatile compounds like fragrances are ubiquitous pollutants in indoor air [97]; however the measurement of released fragrances can be a challenging undertaking due to the distribution of the fragrances between the gas and particulate phases. Considering the potential negative health, a current exists in the industrial and health industries for analytical methods that can accurately determine free free and particle-bound concentrations of fragrances in indoor air.

In the past decade, many different sampling techniques, such as SPME fibers [98,42], solvent extraction [99], sorbents as traps [96] and filters [100] , have been introduced and used for analysis and quantification of fragrances in air. Despite theses advances, the simultaneous determination of free and total concentrations of fragrances has not yet been reported in literature to date. Of the above mentioned techniques, extraction of fragrances

is most commonly carried out by traps (sorbents) using solbent extraction. This method has a high detection limit and requires a large volume of solvent. Compared to these methods, SPME is more convenient one for extracting of volatile compounds in gas phase. The filtration technique, on the other hand, is effective only for analyzing total concentrations of fragrances in particulate phase. Generally, the direct measurements of free and particle-bounded fragrances are experimentally complicated with the currently available methods.

To overcome the drawbacks of these methods, Niri et al. [18] proposed the current use of NTDs for particulate analysis and SPME method for determination of free molecules simultaneously. The needle Trap Device (NTD) is an exhaustive, solvent less, and one-step sample preparation technique that can be easily calibrated. In addition, this approach eliminates errors associated with sample transport and storage, resulting more accurate, precise analytical data [16,101,29,30]. To further increase its deposition efficiency within the gas chromatograph injector, the new prototype of NT was constructed with a side hole above the sorbent and an extended tip which fits inside the restriction of the narrow neck liner to increase the desorption efficiency. The geometry of the extended tip needle trap is shown in Fig.4.1.

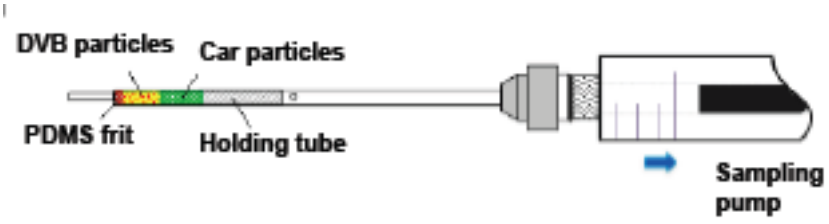

Figure 4.1. Extended tip needle trap configuration

As shown in Eq 4.1, the total concentrations of analyte can be easily obtained by controlling the sampled volume (V) and determining the amount extracted (n) in an analytical instrument.

$$C_0 = n/V_s \qquad (4.1)$$

Several factors, such as pore size and shape, surface area, and particle size, can affect the ability of a given analyte to access and interact with the surface of the adsorbent. Moreover, because of the special shape of the needle, the sorbents used for NT must have the appropriate physical characteristics in size, hardness, and shape as well as adequate mechanical and thermal stability [32].

One of the more interesting aspects of NT is its ability to act as a filter to trap particulate matter. When aerosols and particles pass through the sorbent bed, free molecules are adsorbed onto the surface of sorbent, whereas particles colloid and deposit onto sorbents bed based on mechanical collection mechanisms such as interception, diffusion, inertial impaction and gravitational settling [57]. The contribution of each mechanism varies with respect to sorbent porosity as well as particle samples size. By choosing appropriate sorbents and sampling flow rates, particles of different size ranges can be selectively trapped[18,42].

Recently, the needle trap technique was applied towards for sampling of polyaromatic hydrocarbons (PAHs) present in barbecue and cigarette smoke [42], the analysis of free and particle bound insecticides in mosquito coil smoke [18] and determination of biogenic volatile organic compounds from pine trees [17,102].

Solid phase microextraction (SPME) and needle trap devices both successfully combine sampling, sample preparation, and sample introduction. Analytical sampling by SPME has been employed for a variety of on-site environmental applications [36]. To quantify target analyte content, different calibration approaches can be performed such as external calibration, diffusion based calibration, and kinetic calibration [103]. The external calibration is the most commonly used method in this case, and being widely used for qualitative analysis of food [24], biological [25] and environmental samples [77], whereas gaseous samples are calibrated by means of a standard gas generating system. This method includes the preparation of several standard levels to achieve the relationship between the instrument response and target standard concentrations. The amount of unknown analyte can be calculated from the equation of the calibration curve. To ensure good quality quantitation it is important that the sampling procedure applies the same extraction conditions used for standard concentrations.

The aim of the currently presented work was to develop a simultaneous sampling method based on SPME and NTD for the determination of released fragrances from body sprays in both gaseous and particulate associated phases. The performances of the SPME and NT devices were evaluated in terms of extraction efficiency and reproducibility throughout a period of four hours by a standard particle generator system. In addition, the effect of the ventilation system on the depletion of body sprays particles was studied by a scanning mobility particle sizer (SMPS). In subsequent studies, determinations of free and total contents of fragrances were conducted with use of NTs and SPME fibers based on external calibration method in chamber. Application of this joint methodology to real

samples collected in a washroom environment allowed for a comparison of results with chamber studies.

4.2. Experimental

4.2.1. Materials and reagents

All tested analytes, namely; limonene, linalool, citral, citronellol, cinnamyl alcohol, benzyl benzoate, benzyl salicylate, butylated hydroxyltoluene, α-hexylcinnamaldehyde, 1-methyl-alpha-ionene and limonene were purchased from Sigma–Aldrich (Mississauga, ON, Canada). Helium of ultra-high purity was supplied by Praxair (Kitchener, ON, Canada). Carboxene 1000 (CAR) particles (surface area: 1200 m^2/g) of 60/80 mesh were purchased from Sigma-Aldrich (Bellefonte, PA, USA). Divinylbenzene (DVB) particles (surface area: 582 m^2/g) of 60/80 mesh were provided from Ohio Valley (Marietta, OH, USA). PDMS/CAR/DVB SPME fibers were obtained from Supelco (Oakville, ON, Canada). Fibers were conditioned according to the manufacturer instructions prior to their first use. A bi-directional syringe pump purchased from Kloehn (Las Vegas, NE, USA) was used for NTD sampling (ON, Canada). Stainless steel SGE needle traps were purchased from SGE (Melbourne, Australia). Polydimethylsiloxane (PDMS, Sylgard 184) was obtained from Dow Corning.

4.2.2. Instrumentation

An Agilent 6890 as gas chromatograph coupled to a 5973 MSD quadrupole mass spectrometer (Agilent Technologies, Mississauga, ON, Canada) was used in this study. The oven temperature was initially held at 80 ^0C (2 min), gradually increased to 100 ^0C at a rate of 3 $^0C\ min^{-1}$, further ramped to 150 ^0C at 20 $^0C\ min^{-1}$; to 200 ^0C (held 5 min) at 25 $^0C\ min^{-1}$; to 220 ^0C at 8 $^0C\ min^{-1}$; and final ramp to 290 ^0C (held 5 min) at 30 $^0C\ min^{-1}$. A

DB-5 (30 m x 0.25 mm x 0.25 μm) fused silica column with helium as the carrier gas at a flow rate of 1.0 mL/min was used for the chromatographic separation of fragrances.

4.2.3. Synthesis of highly porous PDMS

PDMS pre-polymer was added to a curing agent in a the ratio of (10:1) (w/w). The prepared 1% dodecyl sulfate sodium salt (SDS) solution was added to the mixture of PDMS and curing agent in a ratio (1:2), and stirred for 15 min. Glass capillaries with the same inner diameter as NTs were filled with homogenized milky mixture [76]. The capillaties were placed into an oven at 80 ^{0}C and allowed to polymerize for 1 hour. After curing the PDMS in oven, the oven temperature was increased so as to allow for evaporation of water droplets. The polymerized PDMS was then heated at 120 ^{0}C for 3 hours to allow remaining water to evaporate as well as to remove the volatile impurities. The amount of water added to the mixture as well as the temperature of polymerization were found to be key parameters for controlling the polymer porosity. As the temperature of the cured polymer was raised to 120 ^{0}C, the removal of water molecules left open structures with maximum porosity.

4.2.4. Preparation of homemade needle trap device

In the preparation of the needle trap, the side hole of the needle trap was first sealed with a Teflon slider, and then the extended tip of the needle was connected to the tap-water aspirator. The sorbent particles were drawn through the needle by aspirator. After packing the desired length of sorbent bed, a spring wire was used to immobilize the sorbent. The sorbent particles used for this work were 2mm of synthesized highly porous PDMS, plus 1 cm of 60/80 mesh DVB, and 1 cm of 60/80 mesh CAR. The synthesized porous PDMS was applied for immobilization of DVB and Car particles inside the tip of

the NT. In this set-up, the porous PDMS was assumed to act as a filter to trap the particles, increasing the collection efficiency of NT. Prior to use, DVB particles were washed 3 times with methanol to remove the any impurities of these particles. The prepared packed needles were conditioned in a GC injector at 260 ^{0}C with helium as carrier gas for 3 hour.

4.2.5. Sampling and desorption of needle traps

For sampling and verification of concentrations in the exposure chamber, the NTD was connected to the sampling pump while a volume of the gaseous sample was pumped from the chamber through the needle, at a flow rate of 5 mL/min. After sampling, the NTD was wrapped with aluminum foil and stored in a plastic bag on dry ice. Before injection, the NTD was removed from dry ice and allowed to reach room temperature. Once at room temperature, the cap of the tip was removed, and the NTD was introduced manually into a GC injector for desorption. NT sampling was conducted with the use of a bi-directional syringe pump purchased from Kloehn (Las Vegas, NE, USA).

4.2.6. Sampling chamber

Experiments were conducted in a 0.1m^3 cubic epoxy glass chamber designed at the University of Waterloo to simulate the desired washroom conditions (can be seen in Fig. 4.2). This chamber had 8 sampling ports to simultaneous insert of the sampling devices. The NTs and SPME fibers were then inserted through the holes in one side of the chamber, which were sealed with a Thermogreen LB-2 predrilled septa. The chamber also consisted of a port to introduce the sprays that was sealed with a Teflon cap after sampling. The chamber was also equipped with a mechanical fan and several ventilation holes to exchange air inside the chamber.

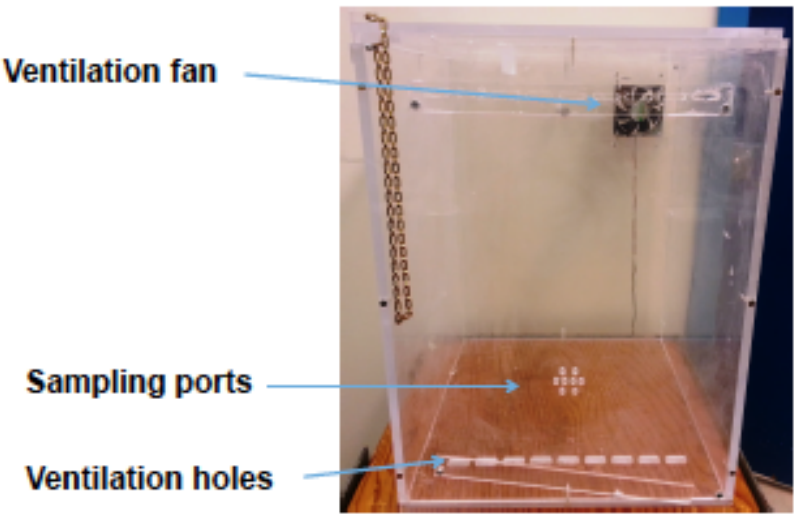

Figure 4.2.Schematic illustration of the designed sampling chamber at University of Waterloo

4.2.7. Performance evaluation of NT and SPME devices using the particle generator system

In this study, aerosol generator (3076) from TSI (Shoreview, MN, USA) including an atomizer was used to generate constant number of linalool and limonene aerosols. The produced aerosols had defined droplet sizes ranging from 10 to 150 nm in diameter. A TSI (3080) electrostatic classifier and a condensation particle counter model (3787) from TSI were used to monitor the particle size distribution in the chamber. Collection of target compounds was carried out from the chamber with NTs and SPME fibers simultaneously to allow discrimination between free and total concentration. In order to examine performance of the particle generation system and evaluate the collection capability of sampling devices, the aerosol output of the atomizer was connected to the sampling chamber. Meanwhile, the presented particles inside the chamber were drawn

into the electrostatic classifier and condensation counter to determine the number concentration of particles Background particle concentrations were measured from t =0−4 hour. The evaluation process was conducted using three SPME fibers and three NTs. All samples were taken from the chamber in a period of the four hours, and the sampling procedure was repeated for each device three times to study statistical variations. This approach was used to study potential differences in the collection capability of different devices, the particle size distribution in the chamber, and to monitor the number concentration of particles within the four hour period. The experimental set up was shown in Fig. 4.3.

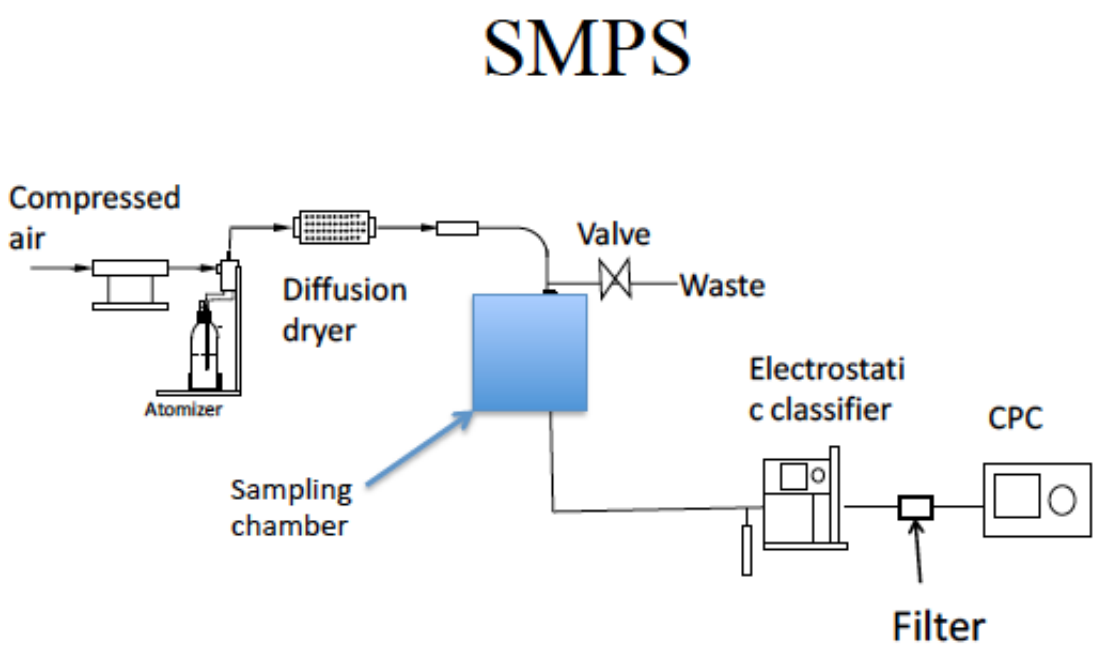

Figure 4.3. Schematic sketch of particle generator system

4.2.8. Monitoring the distribution of particles in sampling chamber

To identify the particle size distribution, the investigation was designed with two experimental cases. The first case studied the effect of body sprays on the distribution of particles in the chamber without a ventilation system. The second case was used to investigate the effect of a ventilation system on the depletion of particles and the distribution pattern. To mimic typical washroom condition, the air change rate was set. In all cases, the particle size distributions inside the chamber were monitored by a scanning mobility particle sizer (SMPS) system, which measured the number concentration of particles. The background particles in the chamber were determined each time before the injection of sprays. After every sampling, the chamber was cleaned, purged with pure nitrogen and covered by aluminum foil. In both cases, measurements were conducted immediately (t= 0) min, 15 min, 30 min and 45 min after spraying.

4.2.9. Standard gas generating system

Permeation tubes for the analytes under study were made by encapsulating pure analytes inside a 100 mm long (1/4 in.) Teflon™ tubing capped with 20 mm long solid Teflon™ plugs and (1/4) in Swagelok caps. Emission rates for each permeation tube were verified by periodic monitoring of weight loss of individual analyte tubes. A standard gas generator (model 491 MB, Kin-Tech Laboratories, La Marque, TX, USA) was used to generate standard gases with desired concentrations. The permeation tubes made in our laboratory were placed inside a glass chamber, held in a temperature-controlled oven and swept with a controllable constant flow of compressed air. Different concentrations of the analytes were obtained by adjusting both the permeation chamber temperature and the airflow rate. A gas sampling chamber, designed by Koziel et al. [77], was installed

downstream from the standard gas generators. This sampling chamber facilitated the steady-state mass flow of all the standards. The sampling chamber consisted of a custom made 1.5 L glass bulb with several sampling ports that were plugged with Thermogreen LB-2 predrilled septa. Omega 120 W heating tape was wrapped around the glass bulb to control the temperature inside the bulb. Air temperatures in the vicinity of the SPME fibers were maintained within ±1.2% of the adjusted temperature. Standard gas flow rates ranged from 50 to 3000 mL/min, resulting in mean air velocities similar to those encountered in indoor air environments.

4.2.10. Determination of free and total fragrance concentration

Extraction of free and particulate-bonded fragrances was performed using a PDMS/DVB/Car SPME fiber and a NTD being packed with 2mm porous PDMS, 1cm DVB and 1cm CAR, using the same composition as SPME fiber. The designed chamber was used to determine the free and total fragrances, which were released from perfume in a breathing zone. To stimulate the real conditions, the spray was introduced to the chamber for 2 seconds while the ventilation system was working. The NT was connected to the sampling pump and a 90 mL of the gaseous sample was pumped from the chamber through the needle, at a flow rate of 5 mL/min. After sampling, the NT was wrapped with aluminum foil and stored in a plastic bag on dry ice. Before injection the NT was removed from dry ice and let to reach the room temperature. The cap of the tip was then removed, and the device introduced into a GC injector for desorption. At the same time, the SPME fiber was placed in a sampling port for 16 minutes, then injected directly to the injector.

4.3. Results and Discussion

4.3.1. Optimization of sampling procedure

Standard gases for all target fragrances with various level of concentration were produced as described in section 4.2.9.

The mixed bed Car/PDMS/DVB fibre was chosen to the analysis of fragrances due to its well-known properties for extraction of volatile and semi-volatile compounds [103104]. During extraction by solid coating due to a limited surface area available for adsorption, after long extraction times and at a high analyte/interference concentration, compounds with poor affinity towards the coating are frequently displaced by analytes with stronger binding, or those present in the sample at high concentrations. If the saturation occurs, due to competition the equilibrium amount extracted can vary with the concentrations of both the target and other analytes [103]. Hence, for SPME quantitative analysis, the selection of optimum extraction time is a critical step. Fig. 4.4 presents the extraction time profile of five selected target fragrances. As can be seen, the equilibria for the analytes under study were reached after 30 min. At this time was considered to be too long for extraction and no significant increases were observed in the amount of extracted analytes, an extraction time of 25 min was chosen for all subsequent analyses. It is important to emphasize that no displacement effects were observed between these compounds. When the extraction time was selected, the calibration curve for SPME was constructed. The limits of detection and quantification were calculated from calibration curves (Table 4.1). The amount of extracted by use of NT as an exhaustive method is proportional to the sampling volume as long as breakthrough does not occur. For breakthrough investigation, two NT connected in series. To this purpose, if the rear NT

was desorbed and no no analyte was found, the breakthrough was considered insignificant. All data on linearity, limit of detection (LOD) and limit of quantification (LOQ) are summarized in table 4.1.

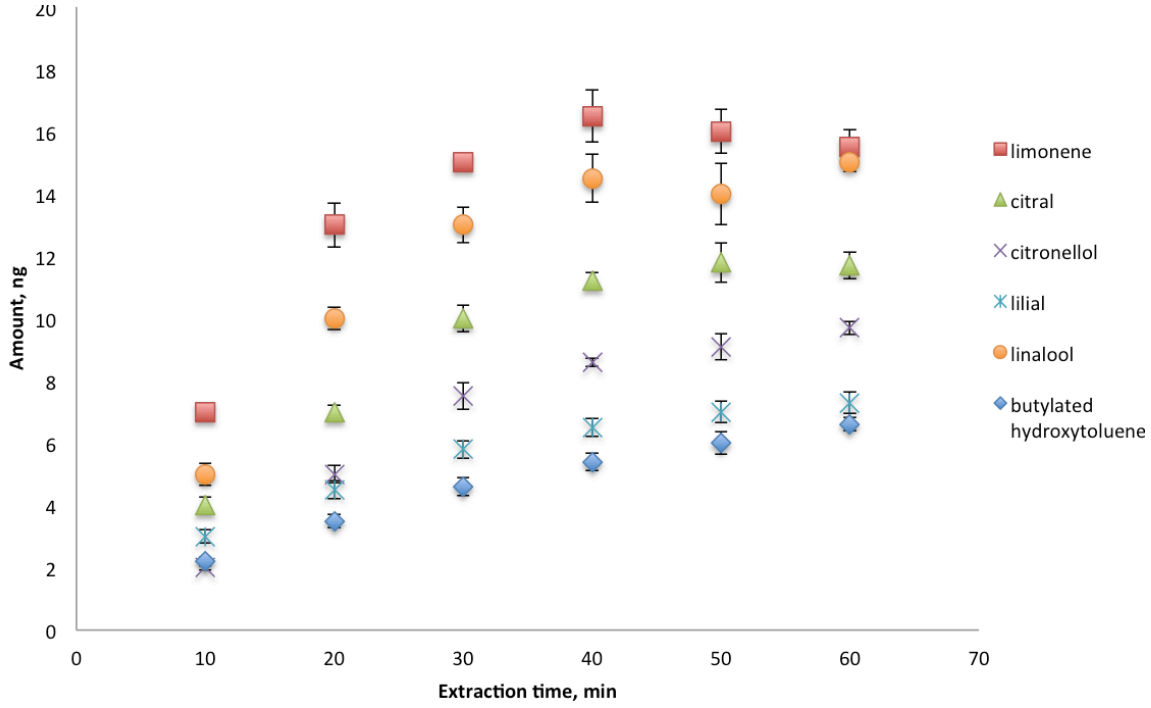

Figure 4.4. Extraction time profile for different fragrances using a DVB/Car/PDMS SPME fiber

Table 4.1. Calibration results for SPME and NT

Sampling approaches	Compounds	LOD (ng/mL)	LOQ (ng/mL)	RSD (%)	R^2
SPME	Limonene	0.04	0.09	6.1	0.9969

(n = 3)	Linalool	0.05	0.12	4.6	0.9905
	Citral	0.06	0.15	5.5	0.9954
	Citronellol	0.05	0.17	4.0	0.9924
	Lilial	0.05	0.17	5.8	0.9932
	Butylated hydroxyl toluene	0.07	0.18	5.1	0.9921
NTD (n = 3)	Limonene	0.05	0.15	5.3	0.9989
	Linalool	0.06	0.21	3.7	0.9970
	Citral	0.06	0.20	4.3	0.9934
	Citronellol	0.05	0.17	4.1	0.9965
	Lilial	0.07	0.22	5.0	0.9941
	Butylated hydroxyl toluene	0.06	0.21	4.7	0.9956

4.3.2. Evaluation of NT and SPME by particle generator system

The particle generator was set up to produce a constant concentration of particles; the performances of three different NTDs and SPME fibers were studied by this particle-generator system. However, before an evaluation of the NT and SPME methods could take place, it was necessary to confirm the performance of the particle generator over a four hour period. A scanning mobility particle counter was used to monitor the number

concentrations of particles within a specific period of time. Differences between the ubiquitous particles in the air of the chamber ('blank' particles), and the actual number of generated particles by the system are shown in Fig. 4.5. The number of generated particles was constant over the four hour period, with a slight increases noted to occur by the end of experiment; this observed phenomenon was determined to be due to solvent evaporation occurring in the original solution as shown in Fig. 4.6. and Fig. 4.7. illustrates the average size distribution of the generated particles from beginning to end. An investigation into the figures of merit from Fig. 4.7 did not reveal a significant fluctuation in the generation of particles. To investigate the extraction efficiency and reproducibility of NT and SPME, concentration measurements of the target analytes were carried out simultaneously with both techniques.

NT was used to sample limonene and linalool in both gaseous and particulate phases, while SPME was applied towards the extraction of target analytes in gaseous phases. In order to evaluate potential differences in the collection capability of the NTs and SPMEs, extraction of a fixed concentration from the particle generator-sampling system was carried out at 5 mL/min. To reduce the effect of systematic errors, and statistically evaluate the results obtained only according to the factor of interest, namely the response in terms of mass extracted of the different NT and SPME devices, extractions were performed using a randomized block design. As can be seen in Table 4.2 and Table 4.3, no statistically significant differences were found in the amount extracted for the probe analytes was found at a 95% level of confidence. The differences in the amounts extracted between individual tested NTDs and SPME fibers can be explained by differences in the packing characteristics of each NT, and variations in the number of

produced particles throughout the the sampling period. For example, the number of particles was observed to increase at the end of sampling due to solvent evaporation, which slowly increased the concentration of solution, and consequently, the number of particles. Finally, it was observed that after three samplings with each NTDs and SPMEs the relative standard deviations were less than 15% and 13 %, respectively.

Table 4.2. Statistical comparison of 3 needle traps packed with synthesized PDMS and Car/DVB particles. $F_{NT}$is the F-ratio for the different treatments evaluated (different needle traps) and F_{crit} is the critical value of F for 9 experiments at a 95% level of confidence. RSD is the relative standard deviation for the inter-needle trap repeatability of 3 NTs (n=3) at 5 mL/min.

Compounds	NT1 RSD (%) (n=3)	NT2 RSD (%) (n=3)	NT3 RSD (%) (n=3)	Total RSD (%) Inter- NT	F_{NT}	F_{crit}
Limonene	7 %	8 %	10 %	12 %	3.7	6.9
Linalool	3 %	14 %	10 %	15%	5.1	

Table 4.3. Statistical comparison of 3 SMPE fibers with PDMS/Car/DVB sandwich coating. F_{SPME} is the F-ratio for the different treatments evaluated (different SPMEs) and F_{crit} is the critical value of F for 9 experiments at a 95% level of confidence. RSD is the relative standard deviation for the inter-needle trap repeatability of 3 SPMEs (n=3).

Compounds	SPME1 RSD (%) (n=3)	SPME2 RSD (%) (n=3)	SPME3 RSD (%) (n=3)	Total RSD (%) Inter- SPME	F_{SPME}	F_{crit}
Limonene	5 %	6 %	8 %	7 %	0.2	5.7
Linalool	4 %	11 %	10 %	13%	0.3	

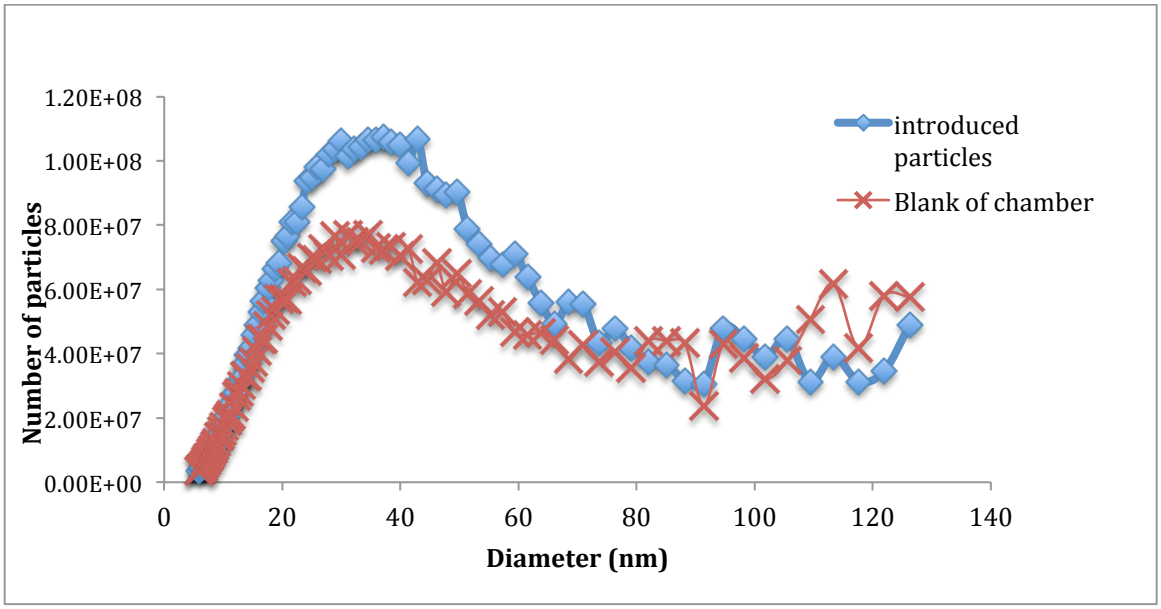

Figure 4.5. Particle distribution in sampling chamber

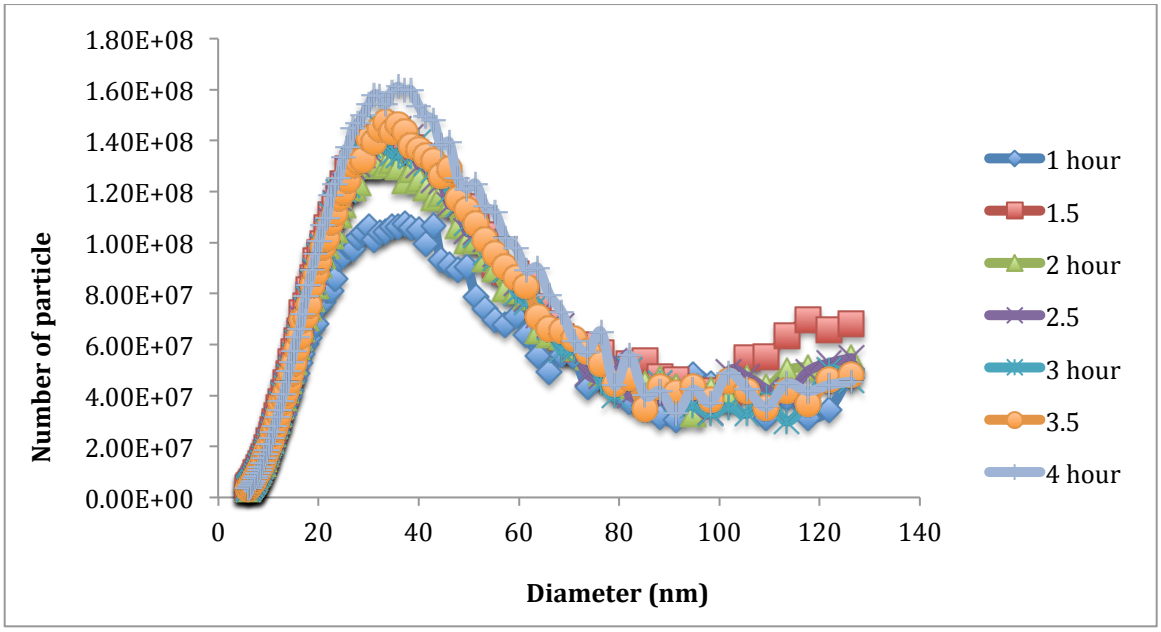

Figure 4.6. Number of particles during a 4 hour period of introduction of particles in the chamber

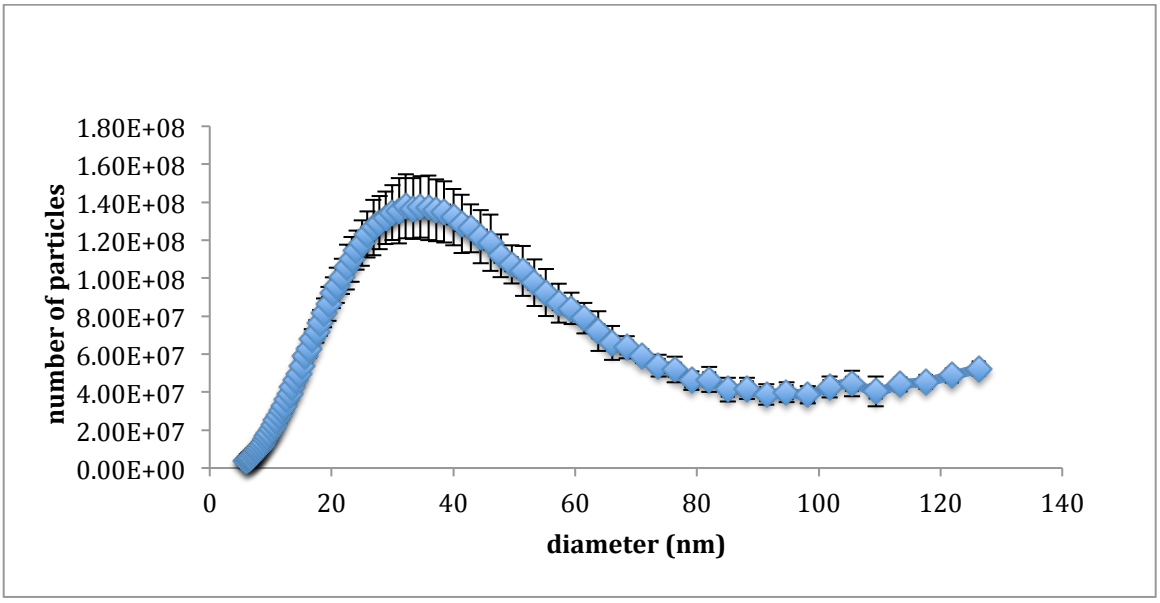

Figure 4.7. Average number of particles in the chamber within a four hour period

4.3.3. Distribution of spray and perfume particles in sampling chamber

To study the effect of a ventilation system in the depletion rate of particles, a series of different experiments were performed. First, the size distribution of spray particles was studied without any ventilation as shown in Fig. 4.8 and Fig 4.10. Antiperspirant sprays containing powder actives generated a significantly higher number of particles compared to regular liquid body sprays. Liquid body sprays are made from oily compounds specifically formulated to allow superior application to the skin surfaces; however, these sprays have an affinity to stick to walls and different surfaces. In the second experiment, the effect of ventilation on the distribution of particles was investigated. The torturous air flow created inside the chamber increased the level of ubiquitous particles in the chamber blanks, yielding a substantial increase in the depletion rate of particles as shown in Fig. 4.9 and Fig 4.11. Considering these results, it is likely that in real life applications, particles are quickly passed through the ventilation system or deposited on the different

surfaces such as walls. The results are in a qualitative agreement with a study by Weschler and Shields (2003), who studied the effect of air change rates on the distribution of particles within a chamber [105].

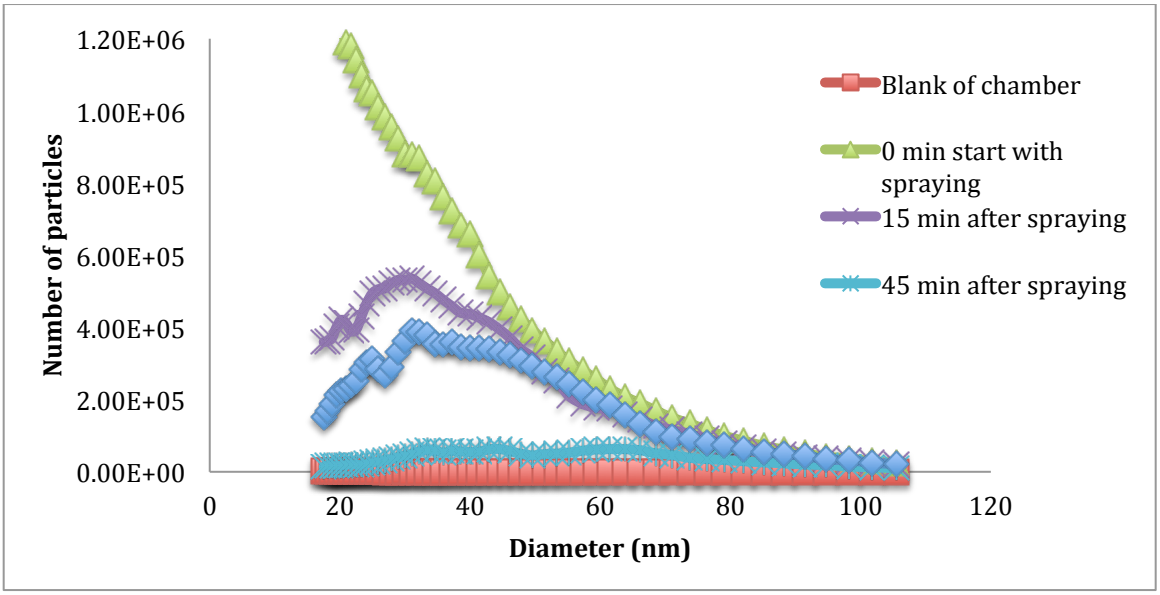

Figure 4.8. Distribution of powdery spray particles in a chamber without a ventilation fan

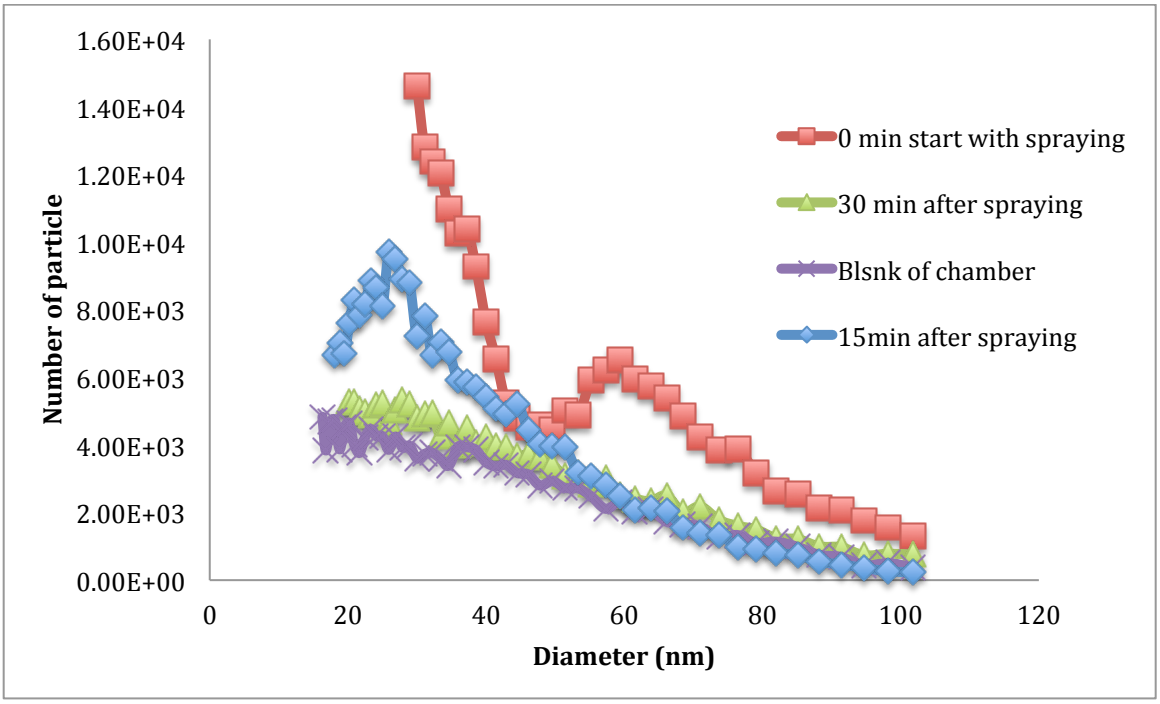

Figure 4.9. Distribution of powdery spray particles in a chamber with a ventilation fan

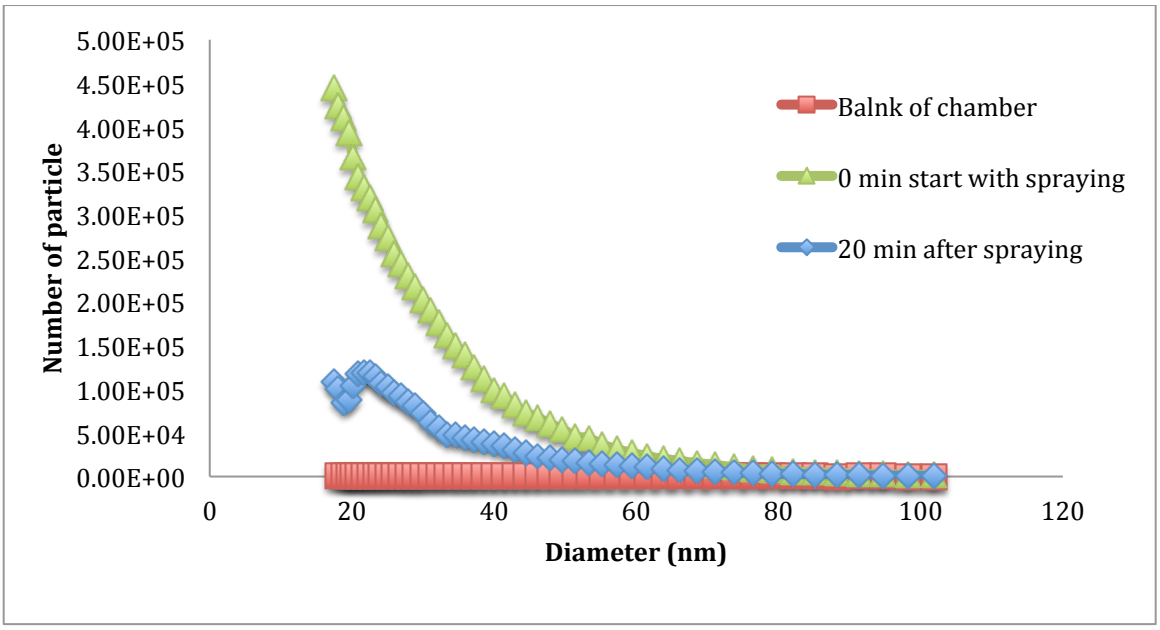

Figure 4.10. Distribution of regular liquid spray particles in a chamber without a ventilation fan

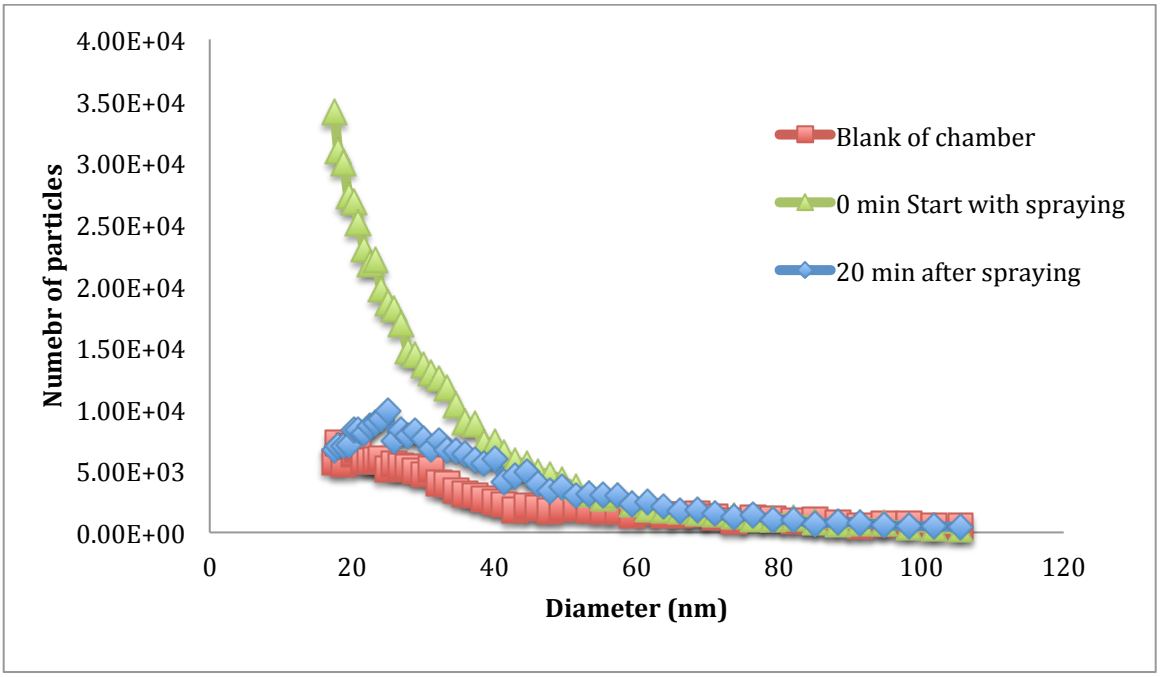

Figure 4.11. Distribution of regular liquid spray particles in a chamber with a ventilation fan

4.3.4. Determination of free and total amount of fragrances (chamber studies)

The obtained data may help refine risk assessments of fragrances emitted from sprays; in this case, the amounts of released (breathable) fragrance allergens are of foremost interest. The released gaseous and particle-bound fragrances from a variety of test specimens into chamber were determined by NT and SPME in parallel. Two different personal care products such as powdery body spray and regular body spray, were analyzed with the proposed method. Integrated samples were collected over the periods of 0-30 min (t = 0 parallel with introducing sprays, t = 30 min after spraying). Fig. 4.12 and Fig 4.13 illustrate the concentration distributions of the emitted fragrances from body sprays between gaseous and particulate phases. It is important to emphasize that NT can collect both free and particulate-bound fragrances, while SPME can extract only free chemicals. For this reason, NT was found to collect a higher amount of chemicals, even

for short spray periods. As can be seen (t = 0), the SPME fiber presented lower extraction amounts for semi volatile compounds such as citral and butylated hydroxytolunene. This can be explained by the greater distribution coefficient of semi volatile compounds between the gaseous and particulate phase in comparison with the low distribution coefficient of volatile compounds. As volatile compounds tend to release as gaseous compounds, they can easily diffuse to the boundary layer of the SPME fiber, while the diffusion capability of particles through the boundary layer is much lower. After 30 minutes, the chamber air was sampled to quantify the concentration of the remaining fragrances. A similar concentration was observed with both sampling approaches. These results might be explained based on the reported findings in section 4.3.3, the depletion of particles increases with time due to losses of particles through the ventilation system and their deposition onto the walls. Therefore, since the number of particles is significantly low, most of the fragrances are expected to be found in gas phase. As already mentioned, based on its configuration, SPME is a particle-free sample preparation technique, based on its configuration. However, NT determines total analyte concentrations (free + particulate-bound). Thus, concentrations obtained using SPME and NT were equivalent to each other for the investigated analytes in the absent of particles.

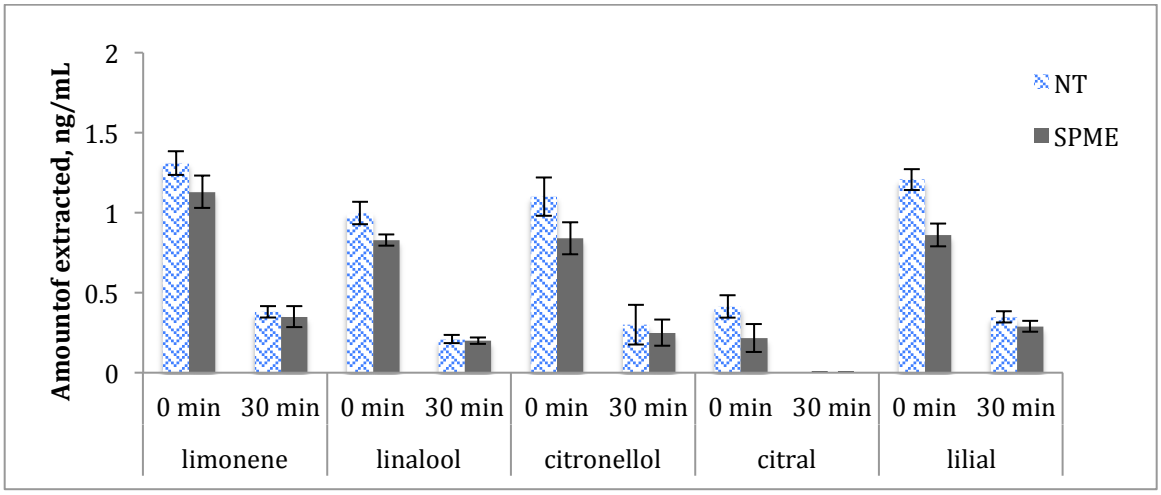

Figure 4.12. Free and total concentrations of fragrances from a powdery spray present in chamber in the vicinity of the 'breathing zone area', mimicking the consumer use.

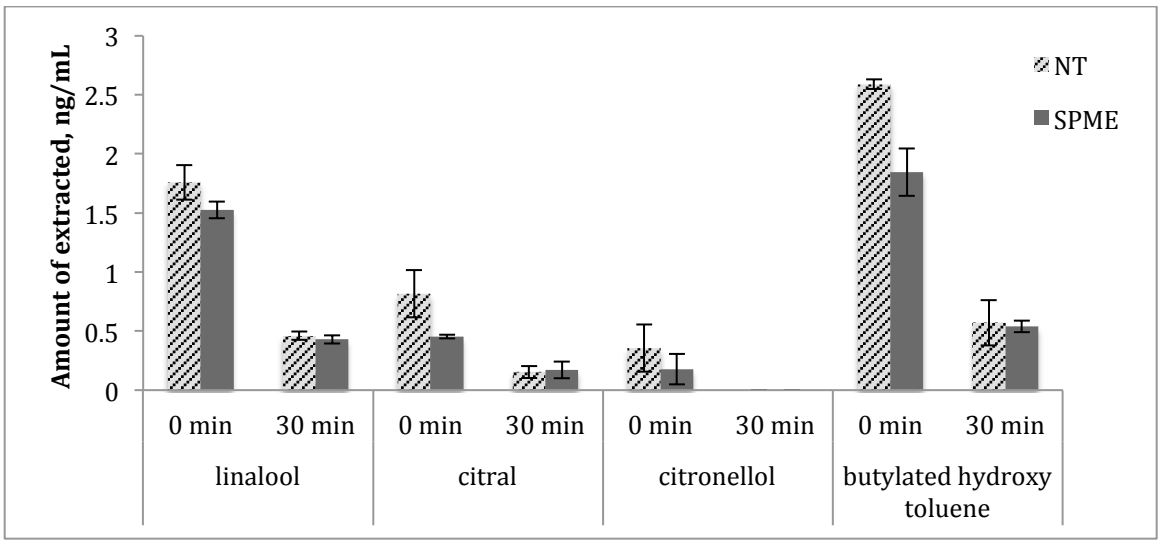

Figure 4.13. Free and total concentrations of fragrances from a liquid spray present in chamber in the vicinity of the breathing zone area, mimicking the consumer use.

4.3.5. Application to real washroom sampling

Finally, the proposed method was applied to real samples collected in a 10-m^3 washroom and in the vicinity of the breathing zone. Washroom samples were taken after the

application of different products such as powdery and regular liquid sprays. All samples were collected in duplicate. To determine whether these compounds were residues from sprays and not contaminants from washroom detergents, an analysis of the ambient air of the sampled washroom was conducted before each spraying. The profiles of the free and total concentrations of target analytes are summarized in Table 4.4 and Table 4.5. As can be seen, the highest concentrations were found for limonene (0.53 ng/mL) and linalool (0.48 ng/mL). The observed trends were showed a good agreement with results obtained for the chamber studies. However, inside the chamber, the concentration of analytes was higher than inside a real washroom. This deviation likely stems from the close environment nature of the chamber; there are less dilution effects from the atmosphere, which can affect the distribution of analytes.

Table 4.4. Compounds found in washroom air samples by NT and SPME after the application of powdery spray

Powdery Spray (Washroom study)	**Amount of extracted by NTD (ng/mL), N = 2**		**Amount of extracted by SPME (ng/mL) N=2**	
Limonene	0.32	0.35	0.26	0.25
Linalool	0.44	0.48	0.25	0.29
Citral	0.32	0.31	0.19	N.Q
Citronellol	0.24	0.27	N.Q	N.Q
Lilial	0.39	0.42	0.20	0.22

Table 4.5. Compounds found in washroom air samples by NT and SPME after the application of liquid spray

Regular liquid Spray (Washroom study)	Amount of extracted by NTD (ng/mL), N = 2		Amount of extracted by SPME (ng/mL) N=2	
Linalool	0.50	0.53	0.37	0.40
Citral	0.33	0.30	N.Q	0.17
Citronellol	N.Q	N.Q	N.Q	N.Q
Butylated hydroxyl toluene	0.43	0.46	0.24	0.28

4.4. Conclusion:

A method for direct detemination of the fragrances in both gaseous and particulate phases has been developed. An evaluation of the NTDs and SPME fibers has showed good extraction efficiency and reproducibility. An ANOVA test showed that at the 95% level of confidence, there were no statistical differences observed among the results from application of the SPME fibers and NTDs. Moreover, the particle generator system was examined, and indicating a robust and reliable system for the generating of particles. The study of method performance demonstrated the precision of combined method (RSD < 15 %), and good sensitivity, with LODs ≤ 0.12 ng/mL. A method performance evaluation carried out in real samples showed the same trends as the designed experimental chamber. It should be noted that the ventilation system was observed to increase the depletion rate of particles. Currently, further research is in progress to improve the collection efficiency of the NTDs for particle smaller than 100 nm, to investigate the distribution coefficient of target analytes between two gaseous and particle phase in

various temperatures, to determine the effect of humidity level on sampling, and to expand the applications of NT to other areas of research.

Chapter 5 : Summary

The theoretical and technical aspects of NT have been investigated since the 1970s. Several studies have reported applications of NT as an active and passive sampler for on-site analysis of environmental samples. However, to date, NT technology has yet to be employed as a conventional analytical device in different industries due to the limited commercial supply of devices and inadequate technical solutions to practical requirements. Inspite of the current lack of commercial availability, the simplicity and rapid desorption capabilities of the method are attractive factors that can potentially broaden the applications of NT. To overcome the technical limitations of current NT devices, this thesis aims to further the development of NT for on-site environmental applications. In addition, the current work includes comprehensive studies on the filtration processes of NTs, and addresses the application of NT for analysis of free and total concentrations in combination with SPME.

Initial research was first undertaken to evaluate a new prototype of NT in terms of amount of extracted analytes, packing procedure, reproducibility of device after multiple uses, and desorption efficiency. To further increase the desorption efficiency of the method, a new NT design was then designed with a side hole above the sorbent and an extended tip that fits inside the restriction of the narrow neck liner. Next, commercially packed needles with divinylbenzene particles were selected to investigate the extraction performance of NTs after multiple uses. No statistical differences were observed between extracted amounts of different NTs. On-site applications, NTs were shown to also perform well when applied towards the determination of biogenic emissions from pine trees. Subsequently, extended tip needles were packed in-lab with synthesized highly

cross-linked PDMS as a frit to immobilize carboxen (Car) particles. The performances of needles were then compared in terms of extraction efficiency at different flow rates. The obtained results showed a 95 % level of confidence based on the ANOVA test. Successively, the needles were packed with Car particles embedded in PDMS for passive sampling. Results showed that the new prototype of NT functions as an effective passive sampling technique for air analysis. Application of NT passive sampling in combination with NT-spot sampling towards the analysis of indoor air in a polymer synthesis laboratory showed good agreement among both approaches. The obtained experimental findings showed that a satisfactory performance was obtained using NT devices as spot samplers, as well as a passive sampler.

Next, the filtration efficiency of NT associated with nanometer-sized particles was addressed in both theoretical and experimental levels. A comparison of theoretical values calculated from the theoretical model with experimental findings yielded similar trends. The highest observed efficiency was obtained for the tested filter containing the lowest fiber diameter. Although the nanofibrous filter was observed to display the greatest collection efficiency values, the filter was shown to yield low reproducibility values due to technical issues related to the preparation of the tip of the needle; consequently, the porous PDMS was selected as a more efficient filter. As a future perspective, a combination of porous PDMS and Car particles might make for a suitable filter.

Finally, quantitative analysis of released fragrances from personal care products in both gaseous and particulate matter phases was performed using NT and SPME simultaneously. The total concentration of fragrances was obtained by NT sampling, while the free molecule concentration was obtained by SPME sampling. The obtained

results revealed that volatile compounds tend to release as gaseous compounds, which can easily diffuse to the boundary layer of the SPME fiber, while for semi-volatile compounds, differences were found between the free and total concentrations, demonstrating a higher amount of particulate binding. Consequently, NT is a practical device for sampling of complex gaseous matrices, including particulates.

Future studies

Remarkable future works of investigation for the NT technique are proposed in the area of sorbent technologies, automation for high-throughput analysis, filtration methodology, as well as biological applications such as breath analysis, proteomics, and metabolomics studies.

To date, various commercial sorbents have been used to extract volatile compounds from complex matrices. However, the modification and improvement of sorbents to extract a broader range of chemicals is a challenging, albeit exciting area of focus. Briefly, the development of general sorbents (or mixed-bed sorbents) could provide better extraction efficiencies of compounds with low affinity, greater sensitivity for analytes found in trace levels of concentration. In addition, the development of new sorbents could expand the use of NT in proteomics and metabolomics investigations where the distribution of extracted analytes is similar to the distribution found in the original sample matrix.

Due to technical challenges related to manual in-lab preparation of NT devices, the mechanization of the packing, sampling, and desorption processes is a critical aspect in further development of NT technology. Although the manually packed extended tip NT devices presented in this thesis displayed excellent reproducibility and precision, the automation of the packing procedure would considerably improve the intra- and inter-

reproducibility of the NT method. In addition, the lack of commercial availability of NT has prevented its applications in several industries. Therefore, future efforts should be undertaken towards the widespread distribution of commercial devices, automation of the packing procedure, as well as mechanization of the sampling and desorption processes using a specific NT auto-sampler, which would consequently lead to convenient and easy handling devices.

Future works on the NT device would include investigations into filtration efficiency under different environmental conditions, such as high humidity and a wide range of temperatures. Further investigations could also involve the monitoring of atmospheric contaminants and the mechanics of their distribution in gaseous and particulate matter phases.

Copyright permission for the materials of Chapter 2

RightsLink®

Home | Create Account | Help | Live Chat

Title:	Development of Needle Trap Technology for On-Site Determinations: Active and Passive Sampling
Author:	Saba Asl-Hariri, German A. Gómez-Ríos, Emanuela Gionfriddo, et al
Publication:	Analytical Chemistry
Publisher:	American Chemical Society
Date:	Jun 1, 2014

LOGIN

If you're a copyright.com user, you can login to RightsLink using your copyright.com credentials. Already a RightsLink user or want to learn more?

PERMISSION/LICENSE IS GRANTED FOR YOUR ORDER AT NO CHARGE

This type of permission/license, instead of the standard Terms & Conditions, is sent to you because no fee is being charged for your order. Please note the following:

- Permission is granted for your request in both print and electronic formats, and translations.
- If figures and/or tables were requested, they may be adapted or used in part.
- Please print this page for your records and send a copy of it to your publisher/graduate school.
- Appropriate credit for the requested material should be given as follows: "Reprinted (adapted) with permission from (COMPLETE REFERENCE CITATION). Copyright (YEAR) American Chemical Society." Insert appropriate information in place of the capitalized words.
- One-time permission is granted only for the use specified in your request. No additional uses are granted (such as derivative works or other editions). For any other uses, please submit a new request.

References:

(1) Naigaga, I.; Kaiser, H.; Muller, W. J.; Ojok, L.; Mbabazi, D.; Magezi, G.; Muhumuza, E. *Phys. Chem. Earth, Parts A/B/C* **2011**, *36* (14-15), 918–928.

(2) Oliva, M.; José Vicente, J.; Gravato, C.; Guilhermino, L.; Dolores Galindo-Riaño, M. *Ecotoxicol. Environ. Saf.* **2012**, *75* (1), 151–162.

(3) Maes, G. E.; Raeymaekers, J. A. M.; Hellemans, B.; Geeraerts, C.; Parmentier, K.; De Temmerman, L.; Volckaert, F. A. M.; Belpaire, C. *Aquat. Toxicol.* **2013**, *126*, 242–255.

(4) Zhao, H.; Li, X. *Environ. Pollut.* **2013**, *174*, 297–304.

(5) Wille, K.; De Brabander, H. F.; Vanhaecke, L.; De Wulf, E.; Van Caeter, P.; Janssen, C. R. *TrAC Trends Anal. Chem.* **2012**, *35*, 87–108.

(6) Zaatari, M.; Novoselac, A.; Siegel, J. *Build. Environ.* **2014**, *73*, 151–161.

(7) Barro, R.; Regueiro, J.; Llompart, M.; Garcia-Jares, C. *J. Chromatogr. A* **2009**, *1216* (3), 540–566.

(8) Molhave, L.; Clausen, G.; Berglund, B.; Ceaurriz, J.; Kettrup, A.; Lindvall, T.; Maroni, M.; Pickering, A. C.; Risse, U.; Rothweiler, H.; Seifert, B.; Younes, M. *Indoor Air* **1997**, *7* (4), 225–240.

(9) Seethapathy, S.; Górecki, T.; Li, X. *J. Chromatogr. A* **2008**, *1184* (1-2), 234–253.

(10) Djozan, D.; Sorouraddin, M. H.; Norouzi, J.; Farajzadeh, M. A. *Microchim. Acta* **2012**, *177* (1-2), 81–88.

(11) Albaseer, S. S.; Mukkanti, K.; Rao, R. N.; Swamy, Y. V. *TrAC Trends Anal. Chem.* **2011**, *30* (11), 1771–1780.

(12) Bendicho, C.; De La Calle, I.; Pena, F.; Costas, M.; Cabaleiro, N.; Lavilla, I. *TrAC Trends Anal. Chem.* **2012**, *31*, 50–60.

(13) Farré, M.; Pérez, S.; Gonçalves, C.; Alpendurada, M. F.; Barceló, D. *TrAC Trends Anal. Chem.* **2010**, *29* (11), 1347–1362.

(14) Wang, D. K. W.; Austin, C. C. *Anal. Bioanal. Chem.* **2006**, *386* (4), 1089–1098.

(15) Pawliszyn, J. *Handbook of Solid Phase Microextraction*; Chemical Industry Press: Beijing, 2009.

(16) Lord, H. L.; Zhan, W.; Pawliszyn, J. *Anal. Chim. Acta* **2010**, *677* (1), 3–18.

(17) Asl-Hariri, S.; Gómez-Ríos, G. A.; Gionfriddo, E.; Dawes, P.; Pawliszyn, J. *Anal. Chem.* **2014**, *86* (12), 5889–5897.

(18) Niri, V. H.; Eom, I.-Y.; Kermani, F. R.; Pawliszyn, J. *J. Sep. Sci.* **2009**, *32* (7), 1075–1080.

(19) Wang, A.; Fang, F.; Pawliszyn, J. *J. Chromatogr. A* **2005**, *1072* (1), 127–135.

(20) Mieth, M.; Kischkel, S.; Schubert, J. K.; Hein, D.; Miekisch, W. *Anal. Chem.* **2009**, *81* (14), 5851–5857.

(21) Reyes-Garcés, N.; Gómez-Ríos, G. A.; Souza Silva, É. A.; Pawliszyn, J. *J. Chromatogr. A* **2013**, *1300*, 193–198.

(22) Pawliszyn, J. **2003**, *75* (11), 2543–2558.

(23) Chen, Y.; Koziel, J. A.; Pawliszyn, J. *Anal. Chem.* **2003**, *75* (23), 6485–6493.

(24) Mousavi, F.; Pawliszyn, J. *Anal. Chim. Acta* **2013**, *803*, 66–74.

(25) Mirnaghi, F. S.; Pawliszyn, J. *J. Chromatogr. A* **2012**, *1261*, 91–98.

(26) Qin, T. *Talanta* **1997**, *44* (9), 1683–1690.

(27) Koziel, J. A.; Odziemkowski, M.; Pawliszyn, J. *Anal. Chem.* **2001**, *73* (1), 47–54.

(28) Eom, I.-Y.; Tugulea, A.-M.; Pawliszyn, J. *J. Chromatogr. A* **2008**, *1196-1197*, 3–9.

(29) Warren, J. M.; Pawliszyn, J. *J. Chromatogr. A* **2011**, *1218* (50), 8982–8988.

(30) Eom, I.; Tugulea, A.; Pawliszyn, *J. Chromatogr. A* **2008**, *1197*, 3–9.

(31) Přikryl, P.; Kubinec, R.; Jurdáková, H.; Ševčík, J.; Ostrovský, I.; Soják, L.; Berezkin, V. *Chromatographia* **2006**, *64* (1-2), 65–70.

(32) Zhan, W.; Pawliszyn, J. *J. Chromatogr. A* **2012**, *1260*, 54–60.

(33) Lord, H. L.; Zhan, W.; Pawliszyn, J. *Anal. Chim. Acta* **2010**, *677* (1), 3–18.

(34) Warren, J. M.; Parkinson, D.-R.; Pawliszyn, J. *J. Agric. Food Chem.* **2013**, *61* (3), 492–500.

(35) Gong, Y.; Eom, I.-Y.; Lou, D.-W.; Hein, D.; Pawliszyn, J. *Anal. Chem.* **2008**, *80* (19), 7275–7282.

(36) Gómez-Ríos, G. A.; Reyes-Garcés, N.; Pawliszyn, J. *J. Sep. Sci.* **2013**, *36* (17), 2939–2945.

(37) Eom, I.; Niri, V. H.; Pawliszyn, J. *J. Chromatogr. A* **2008**, *1197*, 10–14.

(38) Chai, M.; Pawliszyn, J. *Environ. Sci. Technol.* **1995**, *29* (3), 693–701.

(39) Vrana, B.; Schüürmann, G. *Environ. Sci. Technol.* **2002**, *36* (2), 290–296.

(40) Wang, A.; Fang, F.; Pawliszyn, J. *J. Chromatogr. A* **2005**, *1072*, 127–135.

(41) Ueta, I.; Mizuguchi, A.; Okamoto, M.; Sakamaki, H.; Hosoe, M.; Ishiguro, M.; Saito, Y. *Clin. Chim. Acta* **2014**, *430*, 156–159.

(42) Li, X.; Ouyang, G.; Lord, H.; Pawliszyn, J. *Anal. Chem.* **2010**, *82* (22), 9521–9527.

(43) Berezkin, V. G.; Makarov, E. D.; Stolyarov, B. V. *J. Chromatogr. A* **2003**, *985* (1-2), 63–65.

(44) Kubinec, R.; Berezkin, V. G.; Górová, R.; Addová, G.; Mračnová, H.; Soják, L. *J. Chromatogr. B* **2004**, *800* (1-2), 295–301.

(45) Saito, Y.; Ueta, I.; Kotera, K.; Ogawa, M.; Wada, H.; Jinno, K. *J. Chromatogr. A* **2006**, *1106* (1-2), 190–195.

(46) Johnson, B. J.; Huang, S. C.; Wong, A.; Yao, L. *Microchem. J.* **1994**, *49* (1), 78–84.

(47) Ogawa, M.; Saito, Y.; Ueta, I.; Jinno, K. *Anal. Bioanal. Chem.* **2007**, *388* (3), 619–625.

(48) Ueta, I.; Saito, Y.; Hosoe, M.; Okamoto, M.; Ohkita, H.; Shirai, S.; Tamura, H.; Jinno, K. *J. Chromatogr. B. Analyt. Technol. Biomed. Life Sci.* **2009**, *877* (24), 2551–2556.

(49) Mieth, M.; Schubert, J. K.; Gro, T.; Sabel, B.; Kischkel, S.; Fuchs, P.; Hein, D.; Zimmermann, R.; Miekisch, W. *Anal. Chem.* **2010**, *82* (6), 2541–2551.

(50) Mieth, M.; Kischkel, S.; Schubert, J. K.; Hein, D.; Miekisch, W. *Anal. Chem.* **2009**, *81* (14), 5851–5857.

(51) Trefz, P.; Kischkel, S.; Hein, D.; James, E. S.; Schubert, J. K.; Miekisch, W. *J. Chromatogr. A* **2012**, *1219*, 29–38.

(52) Ueta, I.; Saito, Y.; Hosoe, M.; Okamoto, M.; Ohkita, H.; Shirai, S.; Tamura, H.; Jinno, K. **2009**, *877*, 2551–2556.

(53) Wang, J.; Kim, S. C.; Pui, D. Y. H. *Aerosol Sci. Technol.* **2011**, *45* (3), 443–452.

(54) Borm, P. J. A.; Kreyling, W. *J. Nanosci. Nanotechnol.* **2004**, *4* (5), 521–531.

(55) Kreyling, W. G.; Semmler, M.; Möller, W. *J. Aerosol Med.* **2004**, *17* (2), 140–152.

(56) Mills, N. L.; Donaldson, K.; Hadoke, P. W.; Boon, N. A.; MacNee, W.; Cassee, F. R.; Sandström, T.; Blomberg, A.; Newby, D. E. *Nat. Clin. Pract. Cardiovasc. Med.* **2009**, *6* (1), 36–44.

(57) Wiley: Aerosol Technology: Properties, Behavior, and Measurement of Airborne Particles, 2nd Edition - William C. Hinds http://ca.wiley.com/WileyCDA/WileyTitle/productCd-0471194107.html (accessed Jul 13, 2015).

(58) Spurny, K.; Lodge, J. P.; Frank, E. R.; Sheesley, D. C. *Environ. Sci. Technol.* **1969**, *3* (5), 453–464.

(59) Kuo, Y.-M.; Huang, S.-H.; Lin, W.-Y.; Hsiao, M.-F.; Chen, C.-C. *J. Aerosol Sci.* **2010**, *41* (2), 223–229.

(60) Galka, N.; Saxena, A. *Filtr. Sep.* **2009**, *46* (4), 22–25.

(61) Cyrs, W. D.; Boysen, D. A.; Casuccio, G.; Lersch, T.; Peters, T. M. *J. Aerosol Sci.* **2010**, *41* (7), 655–664.

(62) Leung, W. W. F.; Hung, C. H.; Yuen, P. T. *Sep. Purif. Technol.* **2010**, *71* (1), 30–37.

(63) L□ffler, F. *Chemie Ing. Tech. - CIT* **1974**, *46* (8), 364–364.

(64) Brown, R.C. Air Filtration: An Integrated Approach to the Theory and Applications of Fibrous Filters; Pergamon Press: Oxford, UK, 1993. jourlib.org http://www.jourlib.org/references/9022729 (accessed Aug 10, 2015).

(65) Lee, K. W.; Liu, B. Y. H. *J. Air Pollut. Control Assoc.* **1980**, *30* (4), 377–381.

(66) Manton, M. J. *Atmos. Environ.* **1979**, *13* (4), 525–531.

(67) Marre, S.; Palmeri, J. *J. Colloid Interface Sci.* **2001**, *237* (2), 230–238.

(68) Wang, J.; Pui, D. Y. H. *J. Nanoparticle Res.* **2008**, *11* (1), 185–196.

(69) Müller, L.; Górecki, T.; Pawliszyn, J. *Fresenius. J. Anal. Chem.* **1999**, *364* (7), 610–616.

(70) Chen, Y.; Pawliszyn, J. *Anal. Chem.* **2004**, *76* (19), 5807–5815.

(71) Ouyang, G.; Chen, Y.; Pawliszyn, J. *Anal. Chem.* **2005**, *77* (22), 7319–7325.

(72) Górecki, T.; Namieśnik, J. *TrAC Trends Anal. Chem.* **2002**, *21* (4), 276–291.

(73) Partyka, M.; Zabiegała, B.; Namiésnik, J.; Przyjazny, A. *Crit. Rev. Anal. Chem.* **2007**, *37* (1), 51–78.

(74) Mieth, M.; Schubert, J. K.; Gröger, T.; Sabel, B.; Kischkel, S.; Fuchs, P.; Hein, D.; Zimmermann, R.; Miekisch, W. *Anal. Chem.* **2010**, *82* (6), 2541–2551.

(75) Gong, Y.; Eom, I.-Y.; Lou, D.-W.; Hein, D.; Pawliszyn, J. *Anal. Chem.* **2008**, *80* (19), 7275–7282.

(76) Juchniewicz, M.; Stadnik, D.; Biesiada, K.; Olszyna, A.; Chudy, M.; Brzózka, Z.; Dybko, A. *Sensors Actuators, B Chem.* **2007**, *126* (1), 68–72.

(77) Koziel, J. A.; Martos, P. A.; Pawliszyn, J. *J. Chromatogr. A* **2004**, *1025* (1), 3–9.

(78) Zini, C. A.; Augusto, F.; Christensen, E.; Smith, B. P.; Caramão, E. B.; Pawliszyn, J. *Anal. Chem.* **2001**, *73* (19), 4729–4735.

(79) Lord, H. L.; Möder, M.; Popp, P.; Pawliszyn, J. B. *Analyst* **2004**, *129* (2), 107–108.

(80) Stashenko, E. E.; Martínez, J. R. *J. Sep. Sci.* **2008**, No. 31, 2022.

(81) Vuckovic, D.; Shirey, R.; Chen, Y.; Sidisky, L.; Aurand, C.; Stenerson, K.; Pawliszyn, J. *Anal. Chim. Acta* **2009**, *638* (2), 175–185.

(82) Liu, X.; Pawliszyn, R.; Wang, L.; Pawliszyn, J. *Analyst* **2004**, *129* (1), 55–62.

(83) Sheehan, E. M.; Limmer, M. a; Mayer, P.; Karlson, U. G.; Burken, J. G. *Environ. Sci. Technol.* **2012**, *46* (6), 3319–3325.

(84) Martos, P. A.; Pawliszyn, J. *Anal. Chem.* **1999**, *71* (8), 1513–1520.

(85) Pawliszyn, J. *Anal. Chem.* **2003**, *75* (11), 2543–2558.

(86) Lord, H. L.; Zhang, X.; Musteata, F. M.; Vuckovic, D.; Pawliszyn, J. In vivo solid-phase microextraction for monitoring intravenous concentrations of drugs and metabolites. *Nature protocols*, 2011, *6*, 896–924.

(87) Zare Sakhvidi, M. J.; Bahrami, A.; Ghiasvand, A.; Mahjub, H.; Tuduri, L. *Environ. Monit. Assess.* **2012**, *184* (11), 6483–6490.

(88) Fuller, E. N.; Schettler, P. D.; Giddings, J. C. *Ind. Eng. Chem.* **1966**, *58*, 18.

(89) Tumbiolo, S.; Gal, J.-F.; Maria, P.-C.; Zerbinati, O. *Anal. Bioanal. Chem.* **2004**, *380* (5-6), 824–830.

(90) Chen, C.-Y.; Hsiech, C.; Lin, J.-M. *J. Chromatogr. A* **2006**, *1137* (2), 138–144.

(91) Han, S. O.; Youk, J. H.; Min, K. D.; Kang, Y. O.; Park, W. H. *Mater. Lett.* **2008**, *62* (4-5), 759–762.

(92) Johansen, J. D. *Am. J. Clin. Dermatol.* **2003**, *4* (11), 789–798.

(93) Bridges, B. *Flavour Fragr. J.* **2002**, *17* (5), 361–371.

(94) Schnuch, a.; Oppel, E.; Oppel, T.; Römmelt, H.; Kramer, M.; Riu, E.; Darsow, U.; Przybilla, B.; Nowak, D.; Jörres, R. a. *Br. J. Dermatol.* **2010**, *162* (3), 598–606.

(95) Sanchez-Prado, L.; Lamas, J. P.; Alvarez-Rivera, G.; Lores, M.; Garcia-Jares, C.; Llompart, M. *J. Chromatogr. A* **2011**, *1218* (31), 5055–5062.

(96) Lamas, J. P.; Sanchez-Prado, L.; Lores, M.; Garcia-Jares, C.; Llompart, M. *J. Chromatogr. A* **2010**, *1217* (33), 5307–5316.

(97) Rothe, H.; Fautz, R.; Gerber, E.; Neumann, L.; Rettinger, K.; Schuh, W.; Gronewold, C. *Toxicol. Lett.* **2011**, *205* (2), 97–104.

(98) Koziel, J. A.; Noah, J.; Pawliszyn, J. *Environ. Sci. Technol.* **2001**, *35* (7), 1481–1486.

(99) Ladji, R.; Yassaa, N.; Balducci, C.; Cecinato, A.; Meklati, B. Y. *Sci. Total Environ.* **2009**, *408* (2), 415–424.

(100) Singer, B. C.; Coleman, B. K.; Destaillats, H.; Hodgson, A. T.; Lunden, M. M.; Weschler, C. J.; Nazaroff, W. W. *Atmos. Environ.* **2006**, *40* (35), 6696–6710.

(101) Gong, Y. Eom, I.; Lou, D.; Hein, D.; Pawliszyn, J. *Anal. Chem.***2008**.

(102) Reyes-Garcés, N.; Gómez-Ríos, G. A.; Souza Silva, E. A.; Pawliszyn, J. *J. Chromatogr. A* **2013**, *1300*, 193–198.

(103) Pawliszyn, J. *Handbook of Solid Phase Microextraction*; Elsevier, 2011.

(104) Masuck, I.; Hutzler, C.; Luch, A. *J. Chromatogr. A* **2010**, *1217* (18), 3136–3143.

(105) Weschler, C. J.; Shields, H. C. *Atmos. Environ.* **2003**, *37* (39-40), 5621–5631.